UNIVERSITÀ DEGLI STUDI DI MILANO

SCUOLA DI DOTTORATO TERRA, AMBIENTE E BIODIVERSITA'
DIPARTIMENTO DI BIOLOGIA

DOTTORATO DI RICERCA IN BIOLOGIA ANIMALE – XXIV CICLO

Zebrafish (*Danio rerio*) as a model for studying cardiovascular system development. Characterization of new markers: *ve-ptp*, *numb* and *numblike*

settore scientifico disciplinare BIO/05

Tesi di Dottorato di:
Efrem Alessandro FOGLIA
Matr. n. R08065

Tutor: **Prof. Carla LORA LAMIA**

Anno Accademico 2010-2011

Index

Introduction

Formation of a functional vascular system is essential for the proper development of Vertebrate embryos, as well for the survival of adults. In fact, blood vessels have various critical functions: they transport oxygenated blood to tissues throughout the body, and carry out catabolites and waste products. In addition, the circulatory system serves as a conduit for communication between distant tissues through the transport of hormones and allows the rapid deployment of immune responses to distal sites in the body (Lawson and Weinstein, 2002; Jin *et al*., 2005).

The development of the vascular system in Vertebrate embryos has been extensively studied, due to the fact that it has a significant clinical importance. Indeed a wide range of congenital and acquired human diseases are associated with pathological blood vessels formation. Previous works uncovered many genes crucial for the development, growth and differentiation of vessels, including three genes we are characterizing in our laboratory: *ve-ptp*, *numb* and *numblike*. Unfortunately these genes, in addition to a lot of others, have not been well studied *in vivo* (Weinstein, 2002; Isogai *et al*., 2003; Jin *et al*., 2005).

So, with the aim to improve the knowledge of the mechanisms and of the genes involved in vascular development we used zebrafish (*Danio rerio*) as model system to study *ve-ptp*, *numb* and *numblike* in an *in vivo* contest.

FORMATION AND DEVELOPMENT OF VERTEBRATE VASCULAR SYSTEM

Embryonic blood vessels formation requires several cell surface receptors and adhesion proteins. Several signaling molecules and transcription factor genes have been implicated in the development of Vertebrate vasculature: *vegf*, *vegfr1*, *vegfr2*, *vegfr3*, *tie1*, *tie2*, *angiopoietin1*, *angiopoietin2*, *efnb2*, *ephB4*, *scl*, *fli1*, *runx*, *gridlock*, *dab2* and many more. A lot of them has been analyzed in zebrafish, amphibians, birds and mammals and displays similar temporal and spatial expression patterns (Fouquet *et al*., 1997; Liao *et al*., 1997; Gering *et al*., 1998; Chin *et al*., 1998; Liang *et al*., 1998; Liao *et al*., 1998; Lyons *et al*., 2000; Kataoka *et al*., 2000; Oleinikov *et al*., 2000; Lawson *et al*., 2001; Pham *et al*., 2001; Habeck *et al*., 2002; Torres-Vazquez *et al*., 2004). Furthermore the function of these genes appears to be conserved in all Vertebrates (fig.1; Carmeliet *et al*., 1996; Ferrara *et al*., 1996; Cleaver and Krieg, 1998; Lawson *et*

al., 2002; Jin *et al* 2005).

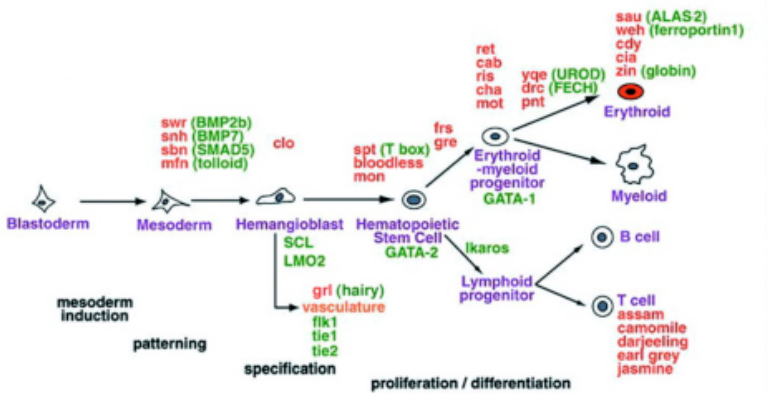

Fig. 1: Differentiation scheme of zebrafish vascular/hematopoietic system. Genes involved in the differentiation scheme are highlighted in green. Mutant zebrafish that affect this particular stage of development are highlighted in red. When the gene for the mutant has been isolated, it is written in parentheses (adapted from Thisse and Zon, 2002).

In Vertebrates there are two major morphogenetic processes that lead to a correct vascular development: vasculogenesis and angiogenesis (Risau, 1998).

Vasculogenesis

The cardiovascular system is the first organ system to develop in the embryo. The hemangioblast is the common progenitor of angioblasts and of hematopoietic stem cells (predecessors of endothelial and of blood cells, respectively) and differentiate in the lateral mesoderm where condense into aggregations called blood islands. These clusters show an inner layer made of hematopoietic stem cells and an external layer made of angioblasts (Risau, 1995; Rumpold *et al*., 2004; Gilbert, 2006).

In zebrafish angioblasts arise in the posterior lateral mesoderm, close to progenitor of blood stem cells and between 18 somites stage and 24 Hours Post Fertilization (hpf) they migrate to the midline of the trunk to form the Intermediate Cell Mass (ICM; fig.2). The ICM is ventral to the notochord and is flanked laterally by the somites (Risau and Flamme, 1995; Lawson and Weinstein, 2002; Herbert *et al*., 2009; Swift and Weinstein, 2009).

ICM angioblasts assemble into a longitudinally aligned trunk axial vessel: the Dorsal Aorta (DA), which lies ventral to the notochord (fig.2). Subsequently, a subpopulation of angioblasts sprouts ventrally from the DA and connects with adjacent cells to form the Posterior Cardinal Vein (PCV), founding just below and immediately juxtaposed to

the DA (fig.2).

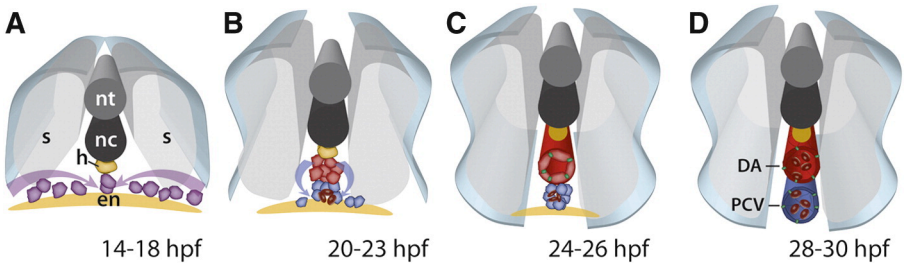

Fig. 2: Phases of vasculogenesis in the zebrafish embryo. Schematic cross sections of the trunk region at representative stages of development. (A) From 14 hpf onward, angioblasts (purple) that originate in the lateral plate mesoderm migrate over the endoderm towards the midline just below the hypochord, where they aggregate to form a vascular cord. (B) At around 17 hpf, angioblasts start to express arterial markers in arterial cells (red). These cells are located in the dorsal portion of the vascular rod and will give rise to the DA, whereas venous markers expressing cells are located more ventrally (blue) and will contribute to the PCV and CV. At 21 hpf, angioblasts located in the ventral part of the vascular cord start migrating ventrally and accumulate below the forming DA. (C) The DA forms and lumenizes prior to the PCV and CV in the absence of blood cells (brown) by cord hollowing. Venous angioblasts aggregate and coalesce around the blood cells to ultimately form a tube. (D) At 30 hpf, both vessels are fully formed and carry blood flow. Endothelial cell junctions (green); nt, neural tube; nc, notochord; h, hypochord; s, somites; en, endoderm (Ellertsdottir *et al*., 2010).

In zebrafish there is only a single unpaired DA and PCV (fig.3), but in many other Vertebrates one or the other of these vessels are initially bilaterally paired on either side of the midline and fuse together to form a single tube at later stages of development (in mammals DA and PCV are initially both paired, whereas in Xenopus, the PCVs are initially paired but the DA assembles as a single tube; Zhong *et al*., 2001; Herbert *et al*., 2009; Swift and Weinstein, 2009).

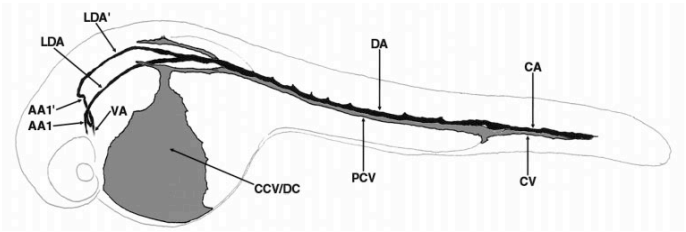

Fig. 3: Circulation in the developing zebrafish at 24 hpf. Diagram of active vessels in the zebrafish embryo just before initiation of circulation, at approximately 24 hpf. This pattern is representative of those seen in angiograms. AA1-AA1', mandibular arches; VA, ventral aorta; LDA-LDA', lateral dorsal aortas; CCV/DC, common cardinal vein/duct of Cuvier; CA, caudal artery; CV, caudal vein (Isogai *et al*., 2001).

The *de novo* formation of main axial vessels described right now is called vasculogenesis.

Successively takes place angiogenesis, the second crucial phase of vascular

development.

Angiogenesis

In the trunk angiogenesis leads to the establishment of a primordial network of Intersegmental Vessels (ISVs) subsequently modified to give rise to the definitive vascular tree (Risau, 1997; Roman and Weinstein, 2000).

During a first sprouting (20-28 hpf; fig.4A) primary vessels emerge bilaterally from the DA, adjacent to the vertical boundaries between myotomes, and grow dorsally toward the nervous system. As they approach the dorsolateral roof of the neural tube, they divide into two major branches that turn caudally and rostrally and fuse together to form two bilateral Dorsal Longitudinal Anastomotic Vessels (DLAVs; fig.4B-D; Isogai *et al.*, 2003). Once the formation of the primary vascular network completes, a secondary set of sprouts begins to arise bilaterally from the PCV and grow dorsally, as did the primaries (1.5-2.5 Days Post Fertilization, dpf; fig.4C-E). Approximately half of the secondary ISVs make a connection with primaries substituting them, while the residuals simply regress and disappear or contribute to form other separate set of vessels (Isogai *et al.*, 2003).

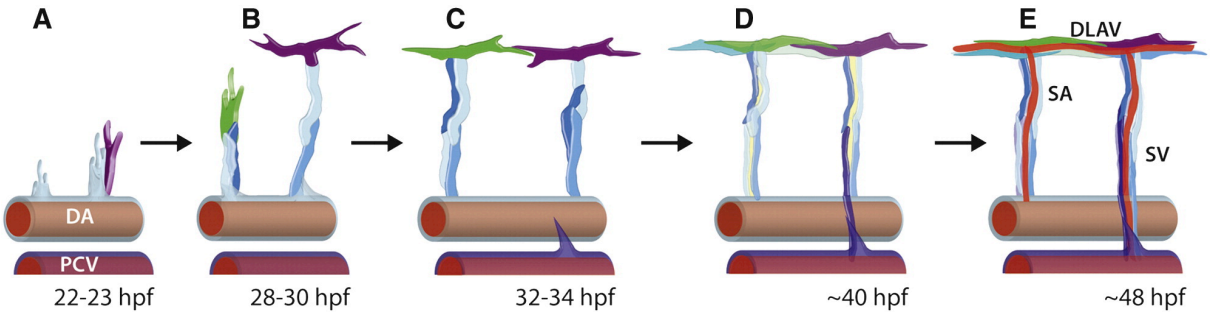

Fig. 4: A model for the morphogenetic events that lead to the formation of ISV and DLAV in the trunk. Two neighboring sprouts are depicted as representative examples. The leading cells are indicated in green and purple, respectively. (A) At 22 hpf ECs of the DA form sprouts that grow along the somite boundaries up to the dorsal roof of the neural tube. (B, C) At the dorsal side of the embryo, the ECs cells send extensions toward their anterior and posterior neighbors to establish connections. (D) At around 32 hpf, a secondary wave of angiogenic sprouts emerges from the PCV. These sprouts connect with the adjacent primary vessel (D, on the right), which will become a segmental vein. (E) Blood flow in ISVs commences after segmental arteries, segmental veins and DLAV have been established (Ellertsdottir *et al.*, 2010).

At 2 dpf other important vessels, the SupraIntestinal Arteries (SIAs) and the SubIntestinal Veins (SIVs), begin to develop near the yolk through angiogenic sprouts. SIAs branch out from the DA, just caudal to the pronephric glomera, while SIVs drain

directly into the PCV and the Common Cardinal Vein (CCV); both will provide blood supply to the digestive system (Isogai *et al*., 2001).

Angiogenesis is not only characterized by sprouting and branching events. In the tail region of embryos the main axial vessels are the DA and the Caudal Vein (CV), which is organized in a plexus till 4.5 dpf. Starting from 2 dpf the CV plexus is drastically modified up to a complete re-absorption of the network of vessels. At the end of this angiogenic process tail will show only one venous vessel (fig.5; Isogai *et al*., 2001).

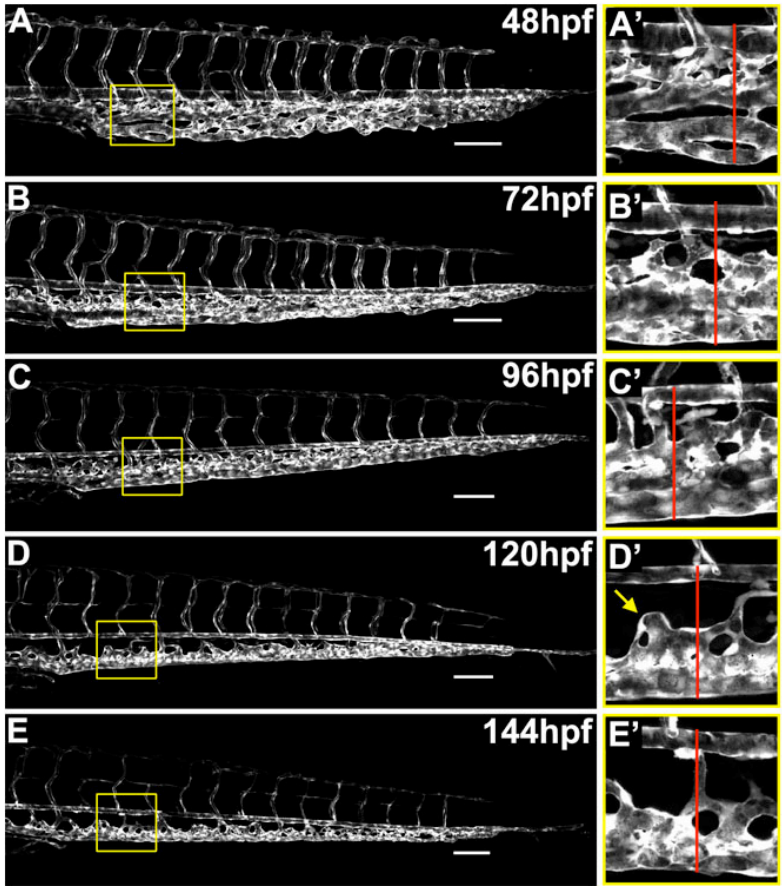

Fig.5: Development of zebrafish CV plexus. (A-E') Confocal images of CV at different developmental stages. (A-E) images of CV from 2 dpf to 6 dpf; (A′-E′) higher magnification images of the boxed regions shown in A-E. Red bars indicate the distance between the axial artery and vein (adapted from Choi *et al*., 2011).

Arterial-venous differentiation

Early studies about Vertebrate circulatory system showed that the difference between arteries and veins was based on physiological factors, such as the direction and the pressure of blood flow (Keele, 1957).

Nevertheless evidence from later lineage-tracing studies indicates that some angioblasts might be restricted to an arterial or venous fate before the blood vessels formation or the onset of circulation, involving a complex interaction of several signalling pathways (Lawson and Weinstein, 2002).

Some studies demonstrate that the expression of a specific arterial or venous marker, pertaining to the Eph-ephrin pathway, results in the acquisition of a definite endothelial identity. In detail ephrin-B2 (efnb2), an Eph family transmembrane ligand, marks arterial but not venous endothelial cells from the onset of angiogenesis. Conversely, Eph-B4, the receptor for ephrin-B2, marks veins but not arteries (fig.6; Wang *et al.*, 1998).

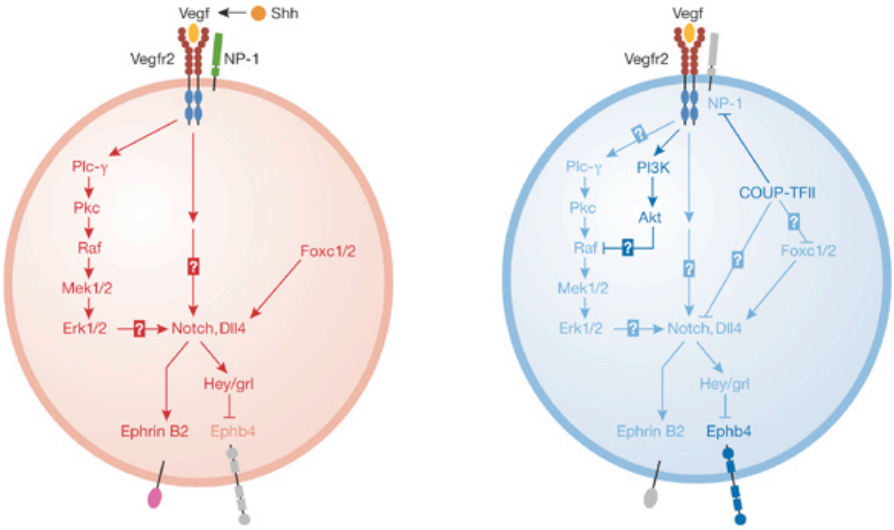

Fig.6. Model of ephrinB2-EphB4 expression in arterial and venous endothelium. ephrinB2 is exclusively expressed in arterial endothelial cells, whereas EphB4 in venous endothelial cells. Both are under control of the same pathways (Shh and Notch; adapted from Lin *et al.*, 2007).

The expression of these markers is predominantly under control of two factors working upstream (fig.6, fig.7): Notch and Sonic Hedgehog Homolog (SHH; Smithers *et al.*, 2000; Lawson *et al.*, 2001; Villa *et al.*, 2001).

SHH induces somitic tissue to express *vegf* playing an important role for determination of cell types that lie adjacent to the notochord (fig.7; Odenthal *et al.*, 1996; Lawson *et al.*, 2002). The exposure of angioblasts to Vegf induces the Notch signaling which results in the expression of arterial-specific genes in the presumptive arterial cells, while in venous territory leads to the repression of arterial cell fate (fig.7; Odenthal *et al.*, 1996; Lawson *et al.*, 2002; Lawson and Weinstein, 2002).

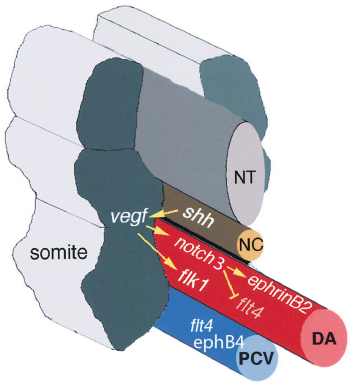

Fig.7. Model of signalling pathways responsible for arterial-venous differentiation. Diagram of a cross-section through a zebrafish trunk at approximately 24 hpf. NT, neural tube; NC, notochord (adapted from Lawson *et al*., 2002).

ZEBRAFISH AS A DEVELOPMENTAL MODEL SYSTEM

Zebrafish (*Danio rerio*) is a tropical fish native to Southeast Asia. It possesses a unique combination of features that makes it particularly well suited for experimental and genetic analysis of early vertebrate development.

Zebrafish adults are small, so many fishes can be housed in a small space. They have a relatively short generation time, an adult female reaches the sexual maturity in about three months and it lays hundreds of eggs per mating every few weeks, generating many progeny for genetic or experimental analysis. The zebrafish eggs are fertilized and develop externally to the mother, providing ready access to the developing animal at all stages of its development. The fertilized embryos develop rapidly, making it possible to observe the entire course of early development in a short time. Somitogenesis begins at about 9 hpf and at 24 hpf the zebrafish embryo has already formed all the major tissues and many organ precursors, such as a beating heart, circulating blood, nervous system, eyes and ears, all of which can be readily observed under a simple dissecting microscope. Larvae hatch by about 2.5 dpf and they are swimming and feeding by 5–6 dpf (Sumanas and Lin, 2004; Weinstein, 2002).

A variety of tools and methodologies have been developed to exploit the advantages of the zebrafish system. Zebrafish embryos and early larvae are optically clear, allowing for direct, non-invasive observation or experimental manipulation at all stages of their development such as Whole-mount *In Situ* Hybridisation (WISH) analysis of gene expression patterns with extraordinarily high resolution (Vogel and Weinstein, 2000). The externally developing embryos are readily accessible to experimental manipulation by techniques such as microinjection of biologically active molecules (RNA, DNA or antisense oligonucleotides), cell transplantation, fate mapping and cell lineage tracing

(Holder and Xu, 1999; Kozlowski and Weinberg, 2000; Mizuno *et al*., 1999; Reifers *et al*., 2000; Stainier *et al*., 1993).

The genetic methods available in the fish have been complemented in the last few years by a full array of genomic and molecular genetic tools. Relatively dense meiotic and radiation hybrid maps now allow for the rapid genetic and physical localization of mutations and genes (http://zfish.uoregon.edu). Large-insert clones of genomic DNA are available from Yeast Artificial Chromosome (YAC), Bacterial Artificial Chromosome (BAC) and P1 Artificial Chromosome (PAC) libraries. Extensive Expressed Sequence Tag (EST) sequencing and mapping projects are underway (http://zfish.wustl.edu). Efforts have also been initiated to obtain the complete sequence of the zebrafish genome, a feat that will undoubtedly dramatically increase the usefulness of the mutants and genetic tools available in the fish (Vogel and Weinstein, 2000).

ZEBRAFISH AS A MODEL SYSTEM TO STUDY VASCULOGENESIS AND ANGIOGENESIS *IN VIVO*

The development of the vasculature has been extensively examined in a variety of Vertebrates, but *in vivo* studies of vasculogenesis/angiogenesis have been traditionally difficult.

In Vertebrates to observe blood vessels directly in living embryos is often difficult, it dues to their opacity or development internal to the mother. Shortly after 24 hpf zebrafish embryos present blood circulation and most adult organs are forming; moreover zebrafish embryos are readily observable under a simple dissecting microscope (Vogel and Weinstein, 2000; Amatruda and Zon, 1999). The optical clarity and accessibility of the zebrafish embryo also permit efficient application of experimental embryologic methods for *in vivo* analysis of vascular development, notably confocal microangiography. In fact it's possible to inject fluorescent beads into the blood flow in order to visualise the entire vascular tree *in vivo* (Weinstein *et al*., 1995).

Because of their small size, zebrafish embryos also receive enough oxygen by passive diffusion from external medium to survive and continue to develop in reasonably normal fashion for several days even in the complete absence of blood circulation,

facilitating phenotypic analysis of animals with circulatory defects (Stainier, 2001). This combination of features has made it possible to perform large-scale forward-genetic mutant screens to isolate embryonic and early larval lethal mutations in the zebrafish (Driever *et al*., 1996; Haffter *et al*., 1996), including many that specifically affect the cardiovascular system (Chen *et al*., 1996; Stainier *et al*., 1996; Weinstein *et al*., 1995). Zebrafish embryos and larvae are raised in an aqueous environment and are readily permeable to many different compounds in their culture media. By simply adding the chemicals or drugs to the zebrafish embryo culture water, potential pro or antiangiogenic activities of these substances can be rapidly and easily evaluated along with the assessment of additional unwanted teratogenic or toxic side effects on other developing organs. This method has already been successfully used to treat zebrafish with known inhibitors of specific growth factors like Vegf to study angiogenic signalling (Chan *et al*., 2002), or to study the effects of toxins on vascular development (Cheng *et al*., 2001).

In addition transgenic zebrafish, with green fluorescent vessels, have been generated. The application of transgenic technology to the zebrafish (Jowett, 1999) has resulted in the ability to create or enhance *in vivo* imaging capabilities and spatially and temporally control gene expression. Transgenic zebrafish lines expressing Green Fluorescent Protein (GFP) within vascular endothelial cells have been particularly useful for studying the formation of the vasculature *in vivo* (Lawson and Weinstein, 2002a; Kidd and Weinstein, 2003).

Zebrafish is a good model for comparative studies of vascular development. Comparison between the blood vessels of zebrafish and other vertebrates also reveals a striking degree of anatomical and functional conservation of vascular pattern. For example, most of the cranial vessels in 2.5–3.5 dpf zebrafish are also found in other developing Vertebrates. These vessels include the aortic arches, lateral dorsal aorta, internal carotid arteries, primordial hindbrain channel, anterior cardinal vein and basilar artery. This conservation of vascular anatomy suggests that vascular development is directed by genetically programmed and evolutionarily conserved control mechanisms and that the information obtained from zebrafish should be readily transferable to other Vertebrates. Indeed, the analysis of various vascular-specific genes first identified and described in other species confirms a high degree of evolutionary conservation between

orthologous (Roman and Weinstein, 2000; Weinstein, 2002; Kidd and Weinstein, 2003).

VE-PTP

The regulation of endothelial cell contacts is of central importance for the physiological role of the endothelium as a barrier between blood and tissue and for the formation and maintenance of blood vessels; in fact the formation and outgrowth of blood vessels, as well as the control of vascular permeability, are dependent on dissociation, rearrangement and re-closure of inter-endothelial cell junctions (Schnittler, 1998; Dejana *et al*., 2000; Vestweber, 2000).

Ve-ptp is a trans-membrane protein that constitutes endothelial junctions and, interacting with VE-cadherin (Vascular Endothelial cadherin), may play parts in the regulation of molecular interactions between proteins of cell-to-cell junctions. Consequently Ve-ptp may result crucial for cell migration and proliferation, cellular signalling and changes in para-endothelial permeability (Fachinger *et al*., 1999).

Molecular organisation of endothelial junctions

Endothelial cells have specialized junctional regions, which are comparable to TJs (Tight Junctions) and AJs (Adherens Junctions) that characterize epithelial tissues. The distribution and the organisation of these junctions change along the vascular tree in regard to different requirement of permeability. The several molecules forming AJs and TJs share common features despite they differ in structure; for instance in both junction types the adhesion is mediated by trans-membrane proteins: VE-cadherin in AJs and the members of the Claudin family, Occludin, JAMs (Junctional Adhesion Molecules) and ESAM (Endothelial cell Selective Adhesion Molecule) in TJs (fig.8). All these junctional adhesion proteins bind intracellular proteins with their cytoplasmic domain, such as Catenins, a-actinin, ZO-1, ZO-2 and Plakoglobin, that anchor them to cytoskeletal filaments, important for the junction stability and for the dynamic regulation of junction opening and closure (fig.8; Schnittler, 1998; Dejana, 2004).

Some intracellular and transmembrane proteins at AJs are kinases and phosphatases, such as SHP2 (Src-homology-2 (SH2)-domain-containing protein tyrosine phosphatase-2) and DEP1 (Density Enhanced Protein-1), also known as CD148. The only known

phosphatase whose expression appears to be restricted to vascular endothelial cells is Ve-ptp, a specific Vascular Endothelial-Protein Tyrosine Phosphatase (Fachinger *et al*., 1999).

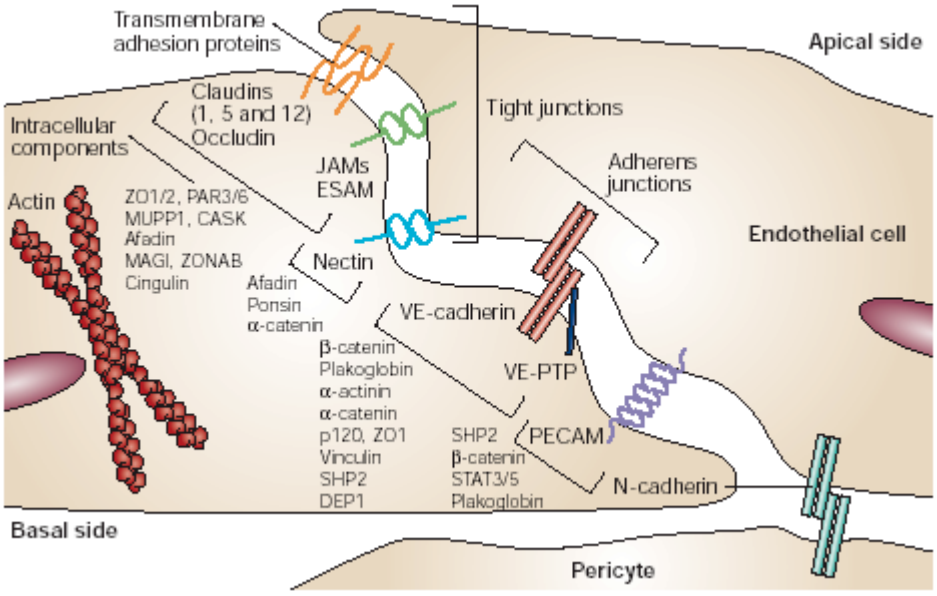

Fig. 8: A schematic representation of the molecular organisation of endothelial junctions (Dejana, 2004).

Protein tyrosine phosphatase super-family

Protein tyrosine phosphorylation is an critical role in a lot of events during cell growth and differentiation (Ullrich and Schlessinger, 1990). The level of tyrosine phosphorylation is determined by the opposing actions of PTKs (Protein Tyrosine Kinases) and PTPs (Protein Tyrosine Phosphatases). In contrast with the extensive analysis and information on the role of PTKs, studies on the physiological importance of PTPs are limited (Tonks *et al*., 1988; Kuramochi *et al*., 1996). All PTPs have an 11 amino acids conserved consensus motif (I/V)HCXAGXGR(S/T)G (X can be any amino acid); the cysteine and arginine residues within the consensus motif are essential for the PTP activity (Kuramochi *et al*., 1996; Guan and Dixon, 1991).

Members of the PTP super-family can be divided in classical PTPs or Dual-Specificity Phosphatases (DSPs, fig.9). Classical PTPs contain one or two catalytic domains that surround the signature motif, called PTP domain, and their catalytic action is principally direct to pTyr residues. Classical enzymes are further subdivided into transmembrane receptor-like (RPTPs) and non-transmembrane (non-TM) forms, on the basis of the

sequences that flank their PTP domains. Flanking domains offers a potential binding site for regulatory ligands, thus permitting regulation of RPTP activity, either directly or indirectly, in response to specific stimuli. Most RPTPs have two intracellular PTP domains but the reason for this remains unclear. In almost all cases, the more carboxy-terminal PTP domain has little or no catalytic activity but may function as a site of interaction with regulatory/targeting proteins (Tonks *et al*., 1988; Kuramochi *et al*., 1996; Guan and Dixon, 1991). Similarity between classical PTPs and DSPs is restricted to the signature motif, although there is conservation in the fold of the catalytic domain (Yuvaniyama *et al*., 1996; Fauman *et al*., 1998). As their name implies, DSPs typically dephosphorylate both pTyr and pSer/pThr residues (Tonks and Neel, 2001).

Ve-ptp belongs to the unique subclass of receptor-type PTPs bearing exclusively fibronectin type III-like repeats in the extracellular domain and a single catalytic domain in the cytoplasmic tail (Brady-Kalnay and Tonks, 1995; Nawroth *et al*., 2002).

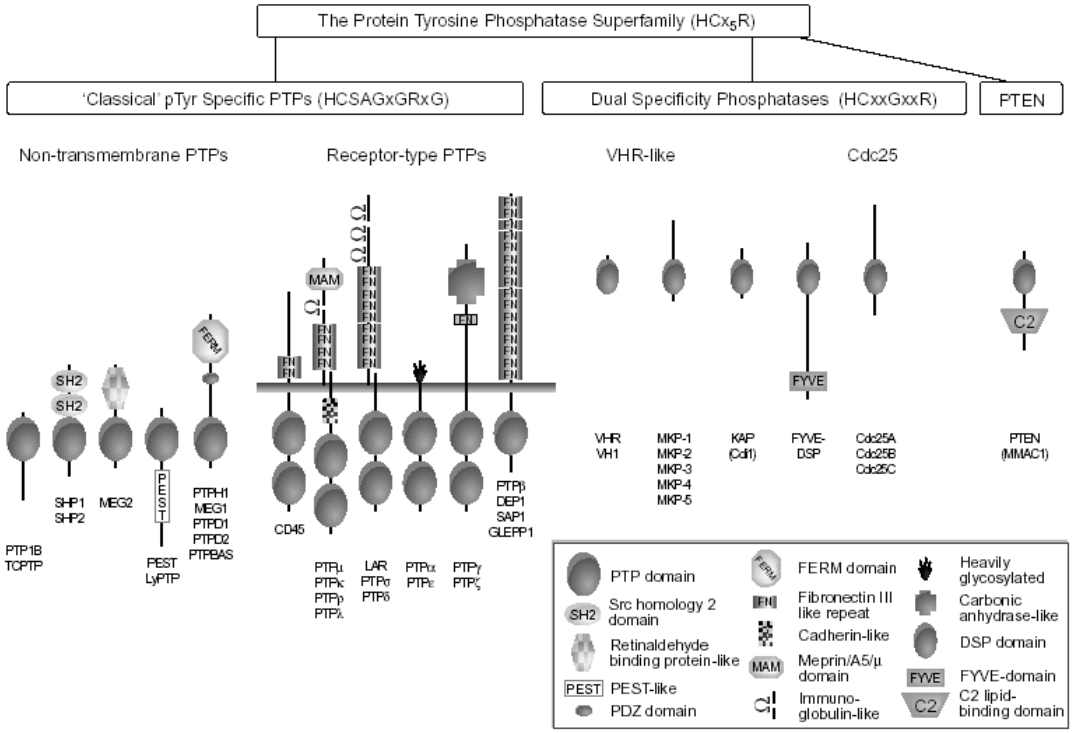

Fig. 9: A schematic representation of different types of the tyrosine phosphatase super-family members. The classical (phosphotyrosine-specific) PTPs are shown on the left hand side. These can be subdivided further into non-transmembrane and receptor-like PTPs. On the right are the dual-specificity phosphatases (DSPs). PTP (catalytic) domains are shown as large or small ovals for classical PTPs and DSPs respectively. Structural features of PTP regulatory (i.e. non-catalytic) domains are shown in the boxed inset (Tonks and Neel, 2001).

Identification and expression pattern analysis of mouse *Ve-ptp*

The RTK (Receptor Tyrosine Kinase) activity in endothelial cells is essential for vasculogenesis and angiogenesis, so reasonably endothelial cells-specific PTPs play an important role in the balancing signals with RTKs (Hanahan, 1997; Risau, 1997).

In order to detect endothelial specific members of the protein-tyrosine phosphatase family a murine brain capillary cDNA library has been screened identifying a PTP specifically expressed in vascular endothelial cells called Ve-ptp (Krueger *et al*., 1990; Fachinger *et al*., 1999).

The *Ve-ptp* cDNA contained a 5' UTR (UnTranslated Region) of 130 bp, a 3' UTR of 32 bp and an open reading frame of 5994 bp encoding a polypeptide of 1998 aminoacids. Structural prediction programs identified 17 extracellular fibronectin type III-like repeats (FNIII repeats), one putative transmembrane domain and one intracellular phosphatase domain (PTP domain). Sequence comparison revealed 83% identity of the full-length amino acids sequence with the human homologue HPTPβ, while the intracellular part of the protein sequence was 94% identical to the corresponding part of HPTPβ (Nawroth *et al*., 2002).

The structure of the Ve-ptp extracellular domain suggests a role of this protein as an adhesion receptor. VE-cadherin is the essential adhesion molecule in endothelial adherens junctions and is directly involved in the maintenance of endothelial cell contacts *in vitro* and *in vivo* (Lampugnani *et al*., 1992; Gotsch *et al*., 1997; Corada *et al*., 1999). Surprisingly, VE-cadherin is dispensable for initial vessel formation, but it is required for their maintenance (Crosby *et al*., 2005). The interaction between VE-cadherin and Ve-ptp is the first demonstrated interaction that involves exclusively the membrane-proximal extracellular domains of these junctional proteins. It is possible that the direct binding between these domains affects the conformation or the clustering of VE-cadherin, thus influencing its adhesive activity. Moreover, it is supposed that Ve-ptp recruits and/or activates an unidentified phosphatase that directly dephosphorylates VE-cadherin so affecting cell layer permeability. As both the enzymatically inactive and enzymatically active form of Ve-ptp inhibits VE-cadherin phosphorylation, it also suggests that phosphatase activity of Ve-ptp is not required for cadherin phopsphorylation (Nawroth *et al*., 2002).

Northern blot, RT-PCR analysis and *in situ* hybridisation have been later performed to analyse the expression pattern during the embryonic development and in the adult tissues.

Northern blot assays revealed a strong expression of *Ve-ptp* mRNA in lung, heart and brain and a weaker expression in kidney and liver of adult mice. Semi-quantitative RT-PCR performed with RNA obtained from mouse organs confirmed these data while RT-PCR analysis on RNA extracted at different developmental stages showed that during embryonic development *Ve-ptp* expression was weak at E11 (Embryonic day 11), increased at E15 and reached the maximum at E17 (Fachinger *at al*., 1999).

The expression pattern analysis of *Ve-ptp* mRNA was also performed by *in situ* hybridisations on frozen sections of mouse embryonic tissues. At the earliest stage analysed (E9.5), expression was detectable in the endothelial cell layer lining the dorsal aorta and during the subsequent developmental stages it was increased throughout the developing vascular system (fig.10a-d). Moreover, strong hybridisation signals were visible in endothelial cells forming blood vessels, whereas no specific signals were detected in blood cells or smooth muscle cells surrounding the vessels (fig.10b-c). At E15.5 specific signals were detectable in all organs with highest expression in the lung. Comparison to serial sections hybridised with an antisense probe of *Vegfr-2* (Vascular Endothelial Growth Factor Receptor 2, *Flk-1*), an endothelial cell marker (Millauer *et al*., 1993), confirmed the vascular endothelial specific expression pattern of *Ve-ptp*. In contrast to the uniform expression levels of *Vegfr-2* in different types of embryonic endothelial cells, *Ve-ptp* is more strongly expressed in endothelial cells lining larger vessels than those of small capillaries and veins. On brain sections of newborn mice, specific expression of *Ve-ptp* was detectable in brain capillaries as well as in larger vessels, and no specific signals were visible in neuronal or glial cells (Fachinger *at al*., 1999).

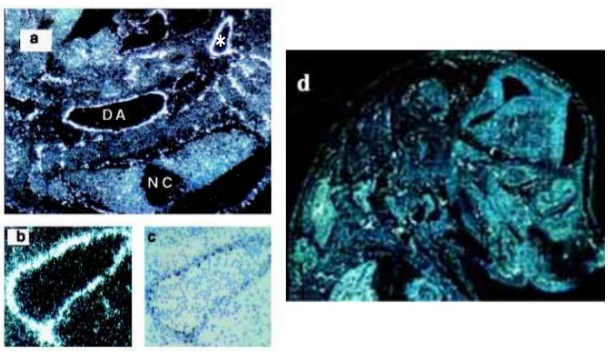

Fig.10: Expression analysis of *Ve-ptp* by *in situ* hybridisation on embryonic tissues sections. (a) Dark field image of an E12.5 embryo section hybridised with a *Ve-ptp* antisense probe. NC: neural crest, DA: dorsal aorta, (b) dark field and (c) bright field image of a higher magnification of the vessel indicated in a (asterisk), (d) sagittal sections of E15.5 embryos head region (Fachinger *at al*., 1999).

Ve-ptp mutants and null-mice

In order to analyse Ve-ptp function in the vascular system development have been generated mice carrying a gene disruption leading to the expression of a truncated, secreted form of Ve-ptp lacking the complete intracellular and transmembrane domains and the most membrane proximal extracellular fibronectin type III-like repeat. This strategy led to the expression of nuclear β-galactosidase under the control of the endogenous *Ve-ptp* promoter (Bäumer *et al*., 2006).

Homozygous mutant embryos (mt/mt) died at E10 and before E8.5 no phenotypic alterations are visible. Between E8.5 and E9.5 homozygous mutant embryos show growth retarded, displayed an enlarged pericardial cavity and an incomplete heart turning (fig.11C-D). At this developmental stage, embryos showed vascular pattern disorganization, in particular in cerebral and intersomitic vessels (fig.11E-H). In fact *de novo* blood vessels formed normally in mutant mice, whereas intraembryonic and extraembryonic vasculature showed dramatic defects in remodelling (fig.11A-B), suggesting an important role of Ve-ptp in blood vessel remodelling and angiogenesis. On the other hand heterozygous mutants mice (+/mt) were phenotypically indistinguishable from the wild-type (wt; fig.12A-B), and presented comparable rates of viability and fertility.

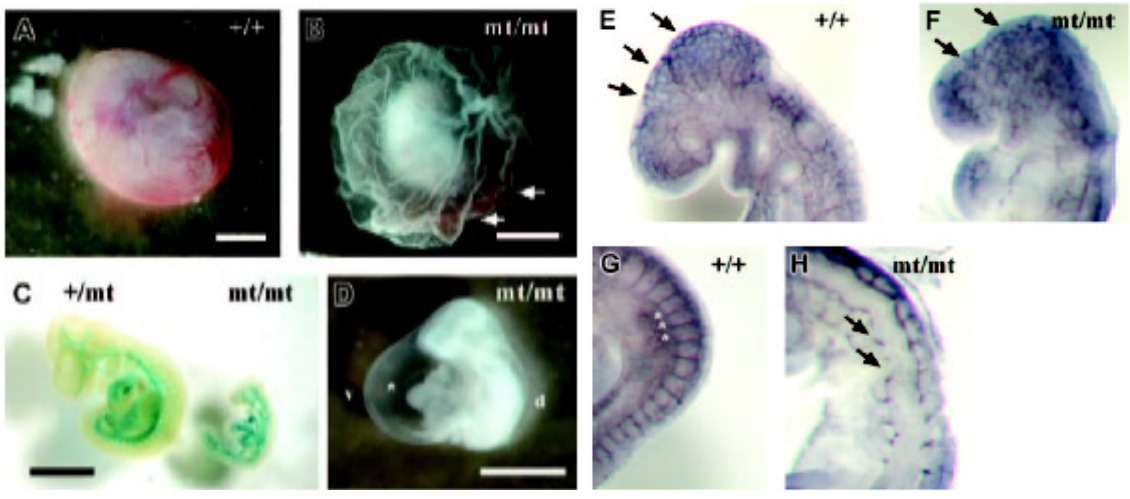

Fig. 11: Developmental and vascular defects in Ve-ptp-lacZ mutant embryos. (A) Normal vascularisation in an E9.5 wt yolk sac, (B) pale yolk sac of a Ve-ptp$^{mt/mt}$ embryo with blood islands (white arrows), (C) growth retardation in a rare E10.0 homozygous Ve-ptp mutant, stained for β-galactosidase. The Ve-ptp$^{+/mt}$ embryo on the left had 25 somite pairs, whereas its Ve-ptp$^{mt/mt}$ littermate on the right was less than half the size and had only 10 somite pairs. (D) Pale-looking E9.5 Ve-ptp homozygous mutant embryo with severely enlarged pericardium (asterisk). d: dorsal; v, ventral. (E-H) E9.0 embryos immunostained for PECAM-1. (E) Well-organized cerebral vascular network (arrows) in an E9.0 wild-

type embryo brain, (F) disconnected clusters of endothelial cells (arrows) in a Ve-ptp$^{mt/mt}$ littermate, (G) well-defined intersomitic sprouts (asterisks) in an E9.0 wild-type embryo, whereas intersomitic vessels (black arrows) failed to develop in a homozygous mutant embryo (H) (Baumer *et al*., 2006).

Ve-ptp expression pattern was analysed both during embryonic development and in different tissues from adult heterozygous mice by β-galactosidase staining and by immunohistochemistry. It revealed a distinct vascular pattern of *Ve-ptp* expression with a remarkable preference for arterial endhotelium (fig.12C-D). Furthermore immunohistochemistry analysis of (+/mt) adult organs cryosections with an antiboby against Ve-ptp and PECAM-1 (Platelet/Endothelial Cell Adhesion Molecule-1) showed that arterial endothelium was stained much more strongly than the venous (fig.12C, D). All these data revealed that Ve-ptp protein and transcriptional expression were more prominent in arterial than in venous endothelium (Bäumer *et al*., 2006).

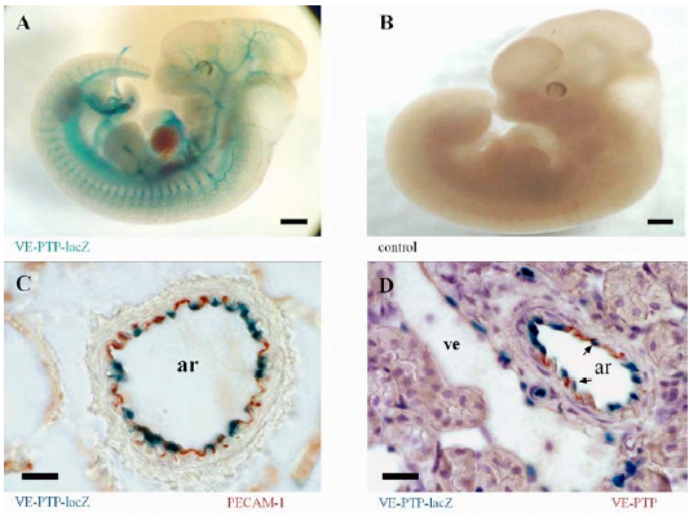

Fig.12: Ve-ptp is predominantly expressed in arterial endothelium. (A) Whole mount β-galactosidase staining of an E12.5 Ve-ptp$^{+/mt}$ embryo showing a distinct vascular pattern of *Ve-ptp* transcriptional activity (represented by the lacZ expression pattern), whereas the same staining of a wild type littermate (B) was negative. C-D Cryosections of an adult Ve-ptp$^{+/mt}$ heterozygous kidney. (C) An arterial vessel (ar) is immunolabeled for PECAM-1 (red) and endothelial nuclei are β-galactosidase stained (blue), recording *Ve-ptp* transcriptional activity, (D) immunolabeling for Ve-ptp with mAb 109.3 (red) and β-galactosidase staining (arrow depicts endothelial nuclei). Ar: arterial endothelium; ve: venous endothelium (Bäumer *et al*., 2006).

Afterwards have been generated *Ve-ptp* null mice in which *Ve-ptp* was replaced by *lacZ* to elucidate the functional role of Ve-ptp in vascular development (Dominguez *et al*., 2007). By this way it has been confirmed the *Ve-ptp* expression in both arterial and venous endothelial cells, with a preferential expression in arterial vessels and it has been demonstrated that Ve-ptp is essential for a correct cardiovascular development. In fact, *Ve-ptp* KO (Knock-Out) embryos appeared developmentally delayed starting at E9.0 and smaller than the controls (fig.13A-B), also showing vascular defects in areas where the remodelling should take place (fig.13C-F). In these embryos, the cephalic plexus

failed to remodel into a hierarchical branched vascular network and it remained as a plexus with only minor pruning (fig.13C-D). Moreover cross sections of PECAM-1 immunostained E9.0 embryos revealed abnormalities also in the main vessels; dorsal aortas were smaller and had a narrowed lumen than in control embryos, while cardinal veins appeared poorly defined and incompletely reshaped (fig.13G-H).

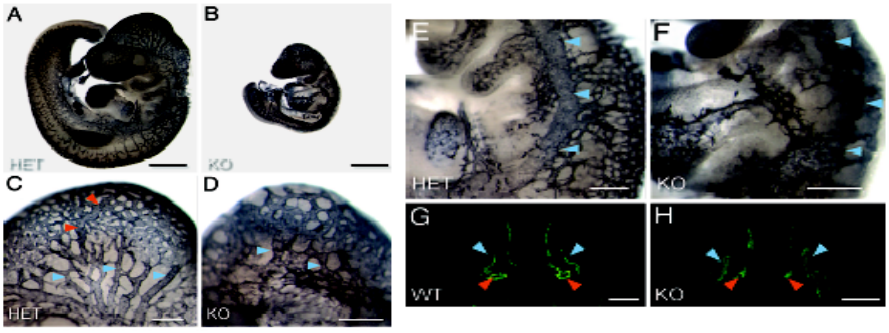

Fig.13: Defects in vascular remodelling in Ve-ptp$^{Lz/Lz}$ null-mice embryos. (*A–F*) Whole mount PECAM-1-stained E9.5 embryos. Ve-ptp$^{Lz/+}$(*A*, *C*, and *E*) compared with a Ve-ptp$^{Lz/Lz}$ littermate (*B*, *D*, and *F*). (*C* and *D*) A close up of the head vasculature shows the normal remodelling pattern of veins (blue arrows) and arteries (red arrows) in Ve-ptp$^{Lz/+}$ embryos (*C*). In Ve-ptp$^{Lz/Lz}$ embryos, the venous plexus (blue arrows) undergoes only minor remodelling (*D*). (*E* and *F*) Close up of the cardinal vein (blue arrows), which does not form correctly in Ve-ptp$^{Lz/Lz}$ embryos (*F*). (*G* and *H*) PECAM-1 immunostaining of E9.0 embryo cross sections at heart level. The dorsal aortas (red arrows) are small and collapsed in Ve-ptp$^{Lz/Lz}$ embryos (*H*) compared with wt (*G*), and the cardinal veins (blue arrows) are diffuse and not clearly delineated (blue arrow) (Dominguez *et al*., 2007).

Identification and expression pattern of *ve-ptp* in zebrafish.

ve-ptp in zebrafish has been identified in our lab and encode for a 1892 aa polypeptide, showing the same domains previously described in mouse: a cytoplasmic catalytic domain, called PTP domain, a trans-membrane region and an extracellular domain organized in 15 Fibronectin type III (FNIII) like repeats (fig.14).

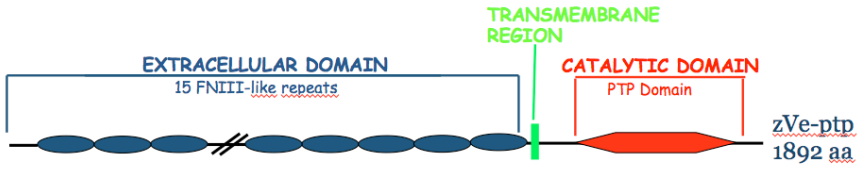

Fig.14: Homolog of Ve-ptp in zebrafish. zVe-ptp exhibit three characteristic regions: an extracellular domain (blue), a catalytic domain (red) and a transmembrane region (green).

In order to evaluate the spatial expression pattern, WISH has been conducted on embryos fixed at different developmental and larval stages (26 hpf, 40 hpf, 2 dpf and 3 dpf; fig.15A-D). This analysis revealed that *ve-ptp* in zebrafish is expressed in developing vascular system, highlighting a strong similarity with murine expression pattern. At 26 hpf the mRNA was detectable in the DA and in CV plexus (fig.15A-B) and later in the cephalic vessels, in the aortic arches, in the CCV, in the ISVs, in the DLAVs, in the bulbus arteriosus and in the atrium of the heart (fig.15C-D). Afterwards RT-PCR analysis has been conducted on total RNAs extracted from different embryonic and larval stages and from various adult organs to determine temporal and spatial expression of *zve-ptp*. In embryos the transcript was observed since the first developmental stages, while in adult was detected in each organ analysed (fig.15E-F; Carra *et al*., manuscript under revision).

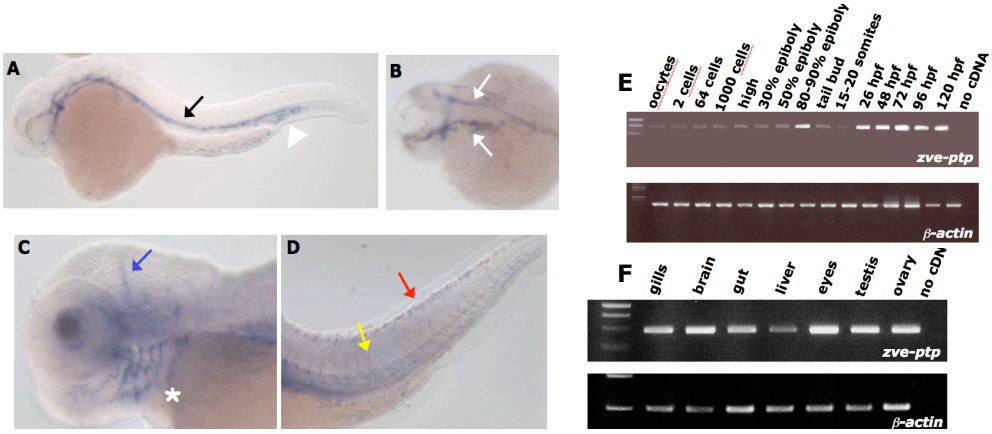

Fig.15: Expression pattern of *zve-ptp*. On the left: WISH analysis. (A) Lateral and (B) dorsal picture of a 26 hpf embryo; the transcript is expressed in DA (black and white arrows) and in CV plexus (white arrowhead). Lateral vision of (C) cephalic and (D) tail region of a 3 dpf embryo. Hybridization signal is detectable in cranial vessels (blue arrow), aortic arches (white asterisk), ISVs (yellow arrow) and DLAVs (red arrow). All the embryos are shown with head on the left. On the right: RT-PCR assays. Temporal expression analysis on total RNAs extracted from (E) different embryonic and larval stages and from (F) adult organs. β-actin serves as internal control (Carra *et al*., manuscript under revision).

Loss of function analysis of zVe-ptp.

To clarify the role of Ve-ptp during vascular development, knockdown assays have been conducted microinjecting *in vivo* a specific morpholino (*ve-ptp*MO).

A morpholino (MO) is a synthetic antisense oligonucleotide 25 bp long, which is complementary to a specific sequence of the mRNA target (Nasevicius and Ekker, 2000). Morpholinos have been successfully used in *Xenopus laevis* and zebrafish to

knockdown gene function by preventing the translation (fig.16; Ekker, 2000) or by modifying the splicing of pre-mRNA of the target gene. Alteration of the splicing events may cause a specific exon skipping or the retention of an intron and its insertion in the mature mRNA (fig.16; Kole and Sazani, 2001).

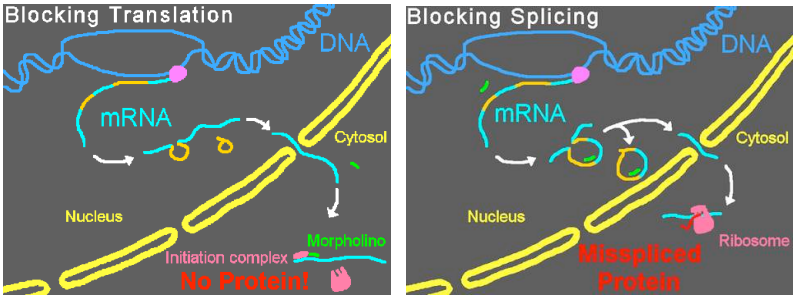

Fig.16. Mechanisms of function of morpholinos. Created by Jon D. Moulton of Gene Tools, LLC, made available under the GNU Free Documentation License {{GFDL-self}}.

Embryos may be injected since 1 cell stage to 4 cells stage; so microtubule-mediated movement spreads MO in all the blastomeres (Nasevicius and Ekker, 2000).

During loss of function experiments it is crucial to identify the working dose of MO to inject, testing precautionarily different dosages of MO. Indeed the seriousness of the defects/phenotypes obtained is dose-dependent: higher doses correspond to severe defects and high mortality and vice versa. Therefore working dose must keep down mortality and maintain the body plan, producing detectable defects (Nasevicius and Ekker, 2000). In order to exclude that the obtained phenotypes are unspecific consequences of a microinjection and to validate their specificity, parallel experiments have been conducted, injecting a std-ctrlMO that hasn't got any target in zebrafish.

Embryos, microinjected with 0.5 pmol/embryo of *ve-ptp*MO (called morphants), have been first observed *in vivo* evaluating vascular defects and then subdivided into four phenotypic classes. Subsequently, plastic sections of the members of these classes have been made, to characterize in detail the observed alteration (fig.17; Carra *et al.*, manuscript under revision).

- CL.I, 19%; the embryos belonging to this class were totally comparable with controls.
- CL.II, 62%; these morphants showed cephalic micro-haemorrhage and clots of blood cells in the tail, especially in the CV plexus, which anyway don't obstruct the blood circulation (fig.17C-D). Analysis of sections revealed that all the blood cells making the clots were crammed inside the vessels (fig.17E).

- CL.III, 11%; the embryos making up this phenotypic class displayed pericardial oedema, an accumulation of blood cells in the sinus venosus and a complete absence of blood circulation, despite the heart beat was unaltered (fig.17F). Transverse sections showed an increased calibre of CV (fig.17G).
- Cl.IV, 8%; these morphants had a damaged body plan and didn't display blood circulation. Moreover these embryos exhibited a considerable accumulation of blood cells in CV plexus and, analysing plastic sections, extravasation of cells was detectable in the tail region (fig.17H-L). Additionally this region showed a severe enlargement of the CV (fig.17L).

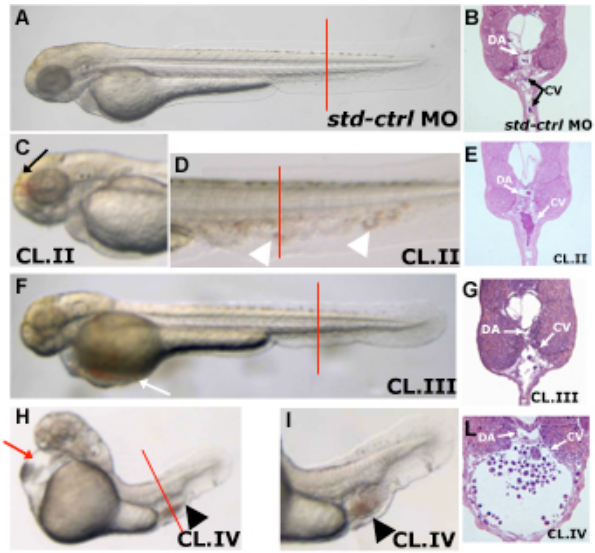

Fig. 17: Loss of function analysis. (A, B) std-ctrl MO injected embryo, (C-L) *ve-ptp*MO injected embryos belonging to CL.II, CL.III and CL.IV. (A, C, D, F, H, I) *in vivo* images of (A, F, H) whole mount embryos and of close up of (C) head and of (D, I) tail. (B, E, G, L) transverse sections of the embryos previously analysed in whole mount. Micro-haemorrhage (black arrow), clots in the CV plexus (white arrowhead), blood cells accumulation in pericardial region (white arrow), pericardial oedema (red arrow), blood cells accumulation in the CV region (black arrowheads). Sections are collected at the levels showed from the red line. All the embryos are shown with head on the left (adapted from Carra *et al*., manuscript under revision).

NUMB AND NUMBLIKE

Cell fate decisions are crucial events during embryonic development and take place by complex mechanisms of asymmetric segregation of several mRNA and proteins during cell division (fig.18; Cayouette and Raff, 2002).

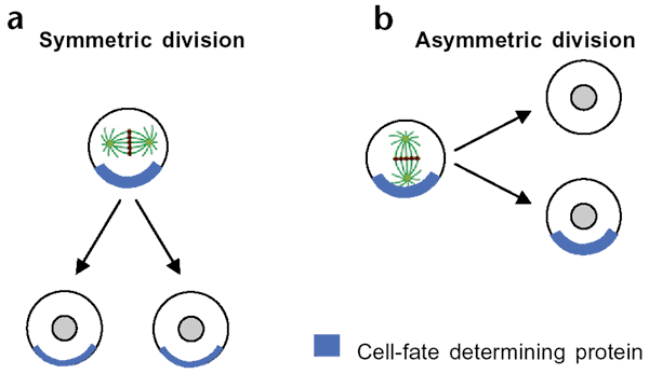

Fig.18: Symmetric and asymmetric segregation of a cell-fate determining protein that is localized to the apical cortex in vertebrate neuroepithelial cells. (a) In a cell division with a horizontal mitotic spindle (oriented parallel to the plane of the neuroepithelium), the cell fate protein (blue) is inherited by both daughter cells. (b) In a cell division with a vertical mitotic spindle, it is inherited by only one daughter cell (Cayouette and Raff, 2002).

Numb is a membrane-associated protein first identified in *Drosophila melanogaster* where may be asymmetrically located at one pole of the cell. Hence during mitosis this protein can be inherited unequally by the two daughter cells, directing them to different fates (Rhyu *et al*., 1994; Spana *et al*., 1995; Zhong *et al*., 2000). Therefore it is plain that the correct distribution of this protein is essential to promote differentiation toward a specific cell fate (Guo *et* al., 1996; Verdi *et al*., 1996; Zhong *et al*., 1996; Zhong *et al*., 2000).

Functions of Numb and Numblike

Genes homologous to d*numb* have been identified in different Vertebrates (mouse, rat, chicken and human) showing that similar structure is conserved through evolution. A homolog of *Numb*, called *Numblike*, has also been characterized in mouse (Verdi *et al*., 1996; Zhong *et al*., 1996; Zhong *et al*., 1997; Wakamtsu *et al*., 1999).

Mammalian Numb and Numblike act as adaptor protein interacting with several molecules and regulating multiple cell functions (fig.19). A number of pathways, which control cell development, have been described to interact with Numb and/or Numblike (Androutsellis-Theotokis *et al*., 2006; Jiang and Hui, 2008). Furthermore in mammals their roles seem to be overlapped, although recent studies suggest they may maintain some distinct functions (Gulino *et al*., 2010).

A critical region for determining Numb and Numblike functions is the amino terminal PhosphoTyrosine-Binding domain (PTB), characteristic region of these proteins in all

Vertebrates. PTB domain binds diverse proteins, as the ubiquitin ligase Itch (fig.19), which causes degradation and function inhibition of Notch and Gli1 (a SHH pathway transducer; McGill and McGlade, 2003; Di Marcotullio *et al*., 2006).

PTB domain is also partially involved in cell membrane localization (fig.19), contributing to the role of Numb and Numblike in the regulation of Notch receptor pathway (Santolini *et al*., 2000).

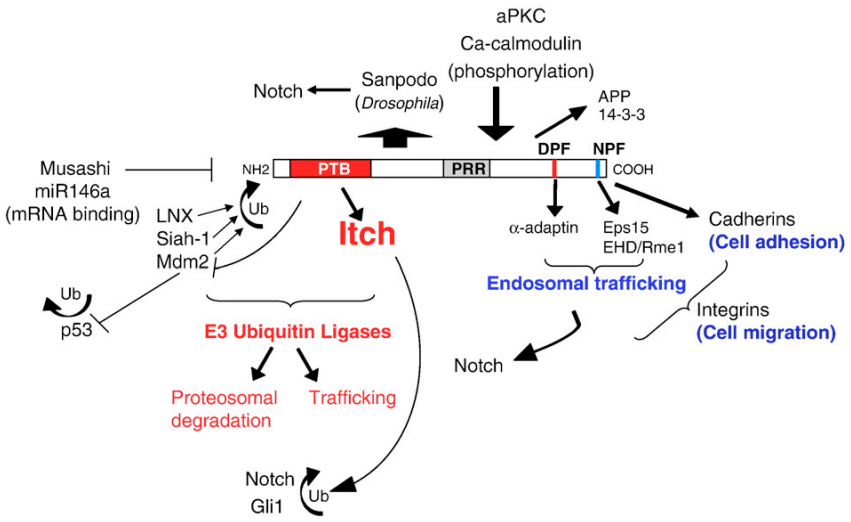

Fig.19: Structure–activity relationships of Numb. Numb levels are regulated by Musashi and miR146a, ubiquitination by LNX, Siah-1 and Mdm2 and phosphorylation by aPKC and calcium-calmodulin. Numb interacts with Itch to ubiquitinate Notch and Gli1, with Mdm2 to hamper ubiquitination of p53, with endocytic machinery to control Notch trafficking and with cadherin and integrins to control cell adhesion and migration. APP: amyloid precursor protein (Gulino *et al*., 2010).

Numb was originally identified as an inhibitor of Notch signaling in *D. melanogaster*; in fact, recruiting Itch, an E3-ubiquitin ligase belonging to Nedd4 family, leads to polyubiquitination and degradation of Notch Inter Cellular Domain (ICD; McGill and McGlade, 2003; McGill *et al*., 2009).

Furthermore Numb may also control the intracellular trafficking of Notch, causing endocytosis and sequestration of full-length Notch or Notch ICD, thereby suppressing their function (Knoblich, 2008; Gulino *et al*., 2010).

Role of Notch during vascular development

Notch has been first characterized in *D. melanogaster* and encodes for a trans-membrane receptor, which plays a critical role in cell fate determination (Kidd *et al*., 1986; Weinmaster, 1997; Artavanis-Tsakonas *et al*., 1999).

Successive studies in mammals revealed the presence of four different Nocht receptors and six ligands: Jagged (1 and 2) and Delta (1, 2, 3 and 4; Weinmaster *et al*., 1991; Weinmaster *et al*., 1992; Lardelli *et al*., 1994; Lindsell *et al*., 1995; Uyttendaele *et al*., 1996; Dunwoodie *et al*., 1997; Jen *et al*., 1997; Luo *et al*., 1997; Shutter *et al*., 2000).

The bond between Notch and its ligand produce two proteolytic cuts of the receptor activating the ICD (fig.20; Mumm and Kopan, 2000). Then this dominium translocate in the nucleus where bind a C promoter binding factor 1, Suppressor of hairless, Lag1 (CSL) thus interact with DNA (fig.20). This interaction switches CSL from suppressor to transcriptional factor (Ong *et al*., 2006).

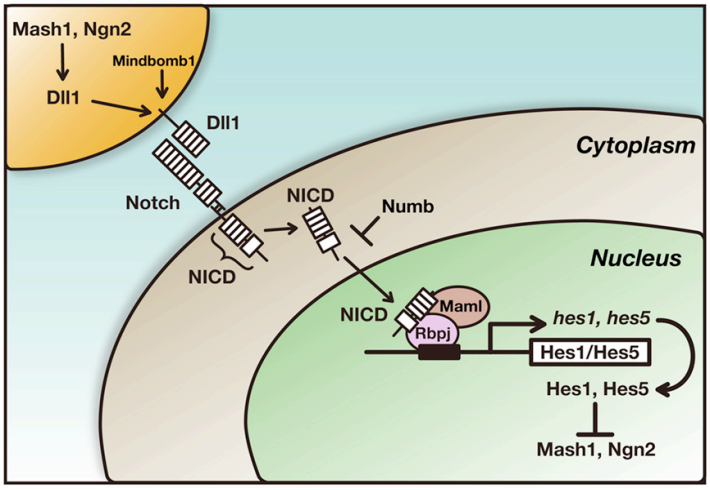

Fig.20. The core pathway of Notch signaling. Proneural genes such as *Mash1* and *Ngn2* promote neuronal differentiation and induce the expression of Dll1, which in turn activates Notch in neighboring cells. Upon activation of Notch, the Notch intracellular domain (NICD) is released from the transmembrane portion and transferred to the nucleus, where it forms a complex with the DNA-binding protein Rbpj and the transcriptional co-activator Maml. The NICD–Rbpj–Maml complex induces the expression of transcriptional repressor genes such as *Hes1* and *Hes5*. Hes1 and Hes5 then repress the expression of proneural genes and Dll1, thereby leading to the maintenance of neural stem/progenitor cells. Numb inhibits Notch signaling and induces neuronal differentiation (Shimojo *et al*., 2011).

Notch signaling is an evolutionarily conserved regulatory circuitry implicated in cell fate determination in various developmental processes including neurogenesis, myogenesis, oogenesis, development of the eye, hematopoietic stem cell self-renewal and differentiation of blood lineages (Greenwald, 1998; Bray, 1998; Bresciani *et al*., 2010).

Moreover it has been shown that Notch pathway plays a key role during vasculogenesis and angiogenesis and that it is required for arterial-venous differentiation of endothelial cells during embryonic development (Xue *et al*., 1999; Krebs *et al*., 2000; Thirston and

Yancopoulos, 2001; Raya *et al*., 2003; Krebs *et al*., 2004).

As a rule Notch pathway acts by a mechanisms called lateral inhibition. Two cells exhibiting receptors and ligands transmit and receive signals; a modification in this exchange of information cause a transcriptional feedback response that produce an amplification of the alteration. So one cell will express predominantly Notch and otherwise the adjacent cell express the ligands (Artavanis-Tsakonas *et al*., 1999).

Several studies demonstrated that Notch is implicated in vascular development of Vertebrates. In zebrafish, chicken and mice angioblasts and differentiated endothelial cells express *Notch* (1-4) and a number of its ligands, as *Dll4*, *Jag1* and *Jag2* (Shirayoshi *et al*., 1997; Vargesson *et al*., 1998; Krebs *et al*., 2000; Lawson *et al*., 2001; Villa *et al*., 2001). However Notch signaling member's expression is restricted to arterial endothelium and it is completely absent in veins, suggesting a role of Notch in acquisition of arterial identity of the vessels. To verify this hypothesis in zebrafish it has been generated *mindbomb dll4*$^{-/-}$ mutants (*mib*) who failed to activate Notch receptors causing a complete lost of functionality of its pathway (fig. 21 A-F; Jiang *et al*., 1996). *mib* mutants didn't express *notch3* and the arterial markers *efnb2* and showed an ectopic expression of venous markers in arterial territory (fig. 21 A-F; Lawson *et al*., 2001).

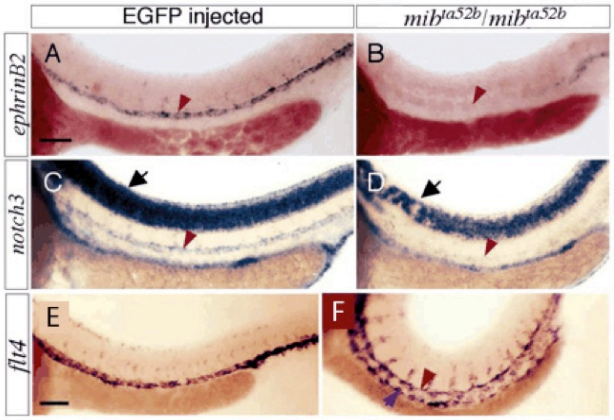

Fig. 21: Expression of arterial and venous markers in *mib* mutants. WISH of arterial (*ephrinb2*, *notch3*) and venous (*flt4*) markers. A, C, E control embryos; B, D, F mutants. In mutants arterial markers are down regulated and inversely venous are up regulated. Arrows and arrowheads highlight the hybridization signals. All the embryos are shown with head on the left. (adapted from Lawson *et al*., 2001).

Contrariwise ubiquitary expression of Notch ICD caused ectopic expression of arterial markers to the detriment of venous (fig. 22 A-F; Lawson *et al*., 2001).

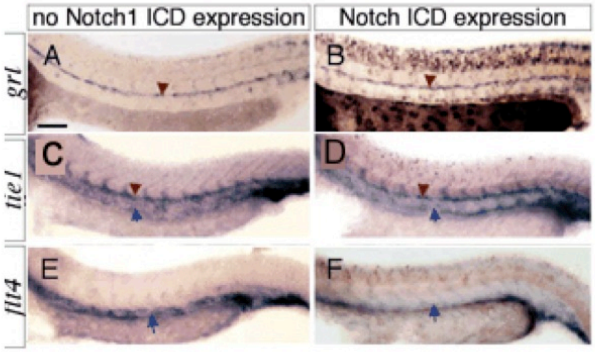

Fig. 22: Expression of arterial and venous markers in embryos in which Notch ICD expression is ubiquitous. WISH of arterial (*grl*) and venous (*tie1*, *flt4*) markers. A, C, E control embryos; B, D, F constitutive expression of NICD. When Notch ICD is over-expressed venous markers are clearly down regulated. Arrows and arrowheads highlight the hybridization signals. All the embryos are shown with head on the left. (adapted from Lawson *et al*., 2001).

Identification and expression pattern of *Numb* in mouse

The gene *Numb* has been identified in mouse, where encodes four alternatively spliced transcripts, which generate four proteins containing the N-terminal PTB domain and a C-terminal Proline-Rich Region (PRR, containing putative Src homology 3-binding sites; fig. 23). The N-terminus of mNumb shows a similarity with dNumb of 63%, while C-terminus shows a lower similarity with the respective region of dNumb (23%; Zhong *et al*., 1996).

Alternative splicing affects both PTB and PRR domains. A large 48 aa insert in the PRR distinguishes Numb1 (653 aa) and Numb3 (642 aa) isoforms (Numb-PRRL) from Numb2 (604 aa) and Numb4 (593 aa), which miss it (Numb-PRRS). A smaller 11 aa insert in PTB region also distinguishes Numb1 and Numb2 from Numb3 and Numb4 (fig. 23; Zhong *et al*., 1996; Dho *et al*., 1999). This small region of 11 aa seems to permit the tethering of the protein to the cell membrane (Dho *et al*., 1999).

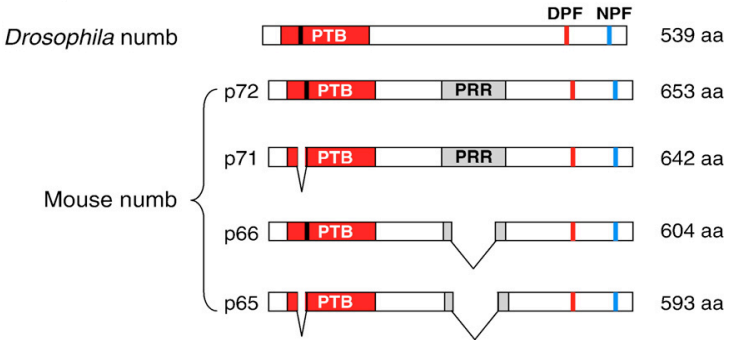

Fig. 23: Structure of Numb isoforms. In mouse, due to alternative splicing, Numb show four isoforms. They differ for the presence/absence of an 11 aa insert in the PTB domain and of a 48 aa insert in the PRR (adapted from Gulino *et al*., 2010).

Moreover the different isoforms have specific localization. By western blot conducted on embryos and on adults tissues it has been observed that Numb3 and 4 are ubiquitously diffuse in all adult's tissues while Numb1 and 2 are detectable only in embryos and in adult's brain, thymus and lung. All these data, taken together, suggested a specific role for the different isoforms of the protein (Dho *et al*., 1999).

Numb mRNA has been clearly identified both in embryos and in adult. WISH demonstrated that m*Numb* is expressed in all tissues and organ during embryological development; especially in Nervous Central and Periferic Systems (NCS and NPS), while immuno-histochemistry showed an intense signal of localization of the protein in the sites of generation of hemangioblasts and of primitive hematopoiesis (Zhong *et al*., 1996; Cheng *et al*., 2008).

To complete the expression pattern analysis of m*Numb* Northern Blot and RT-PCR have been conducted on adult tissues; these analyses demonstrated the expression of the gene in liver, gut, kidney, brain, lung, spleen, thymus, lymph nodes, bone marrow and heart (Zhong *et al*., 1996; Wilson *et al*., 2007).

<u>*Numb* mutant mice: analysis of vascular function</u>

m*Numb* function in vascular development has been analyzed by characterization of homozygous ($Numb^{-/-}$) and heterozygous ($Numb^{+/-}$) mutant mice (Zilian *et al*., 2001).

$Numb^{+/-}$ mutants showed the same phenotype of wild type embryos (fig. 24 A,C), while $Numb^{-/-}$ mutants died before E11.5 stage cause defect in vascular development (fig. 24 B,D; Zilian *et al*., 2001).

Indeed all the observed homozygous mutants presented defects in the vascular system. In those mutants vasculogenesis took place normally but defects in angiogenesis were detectable from E10 stage. In detail, capillaries and vessels of cardinal venous plexus showed a drastic reduction in number and a clear incorrect shape and failed to connect with cranial capillaries; intersomitic vessels seemed to be altered, too (Zilian *et al*., 2001).

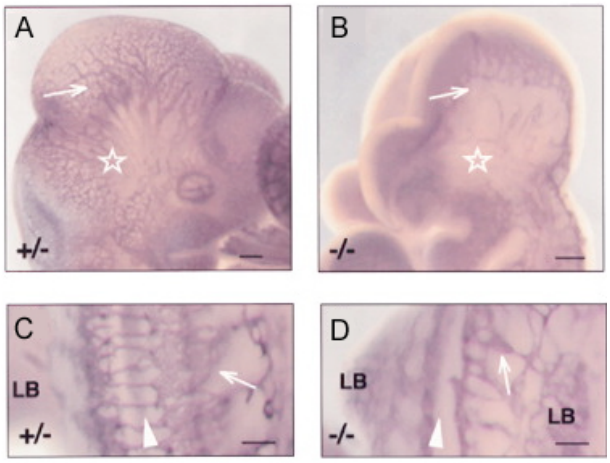

Fig. 24: Requirement of Numb for angiogenic remodeling. Normal and mutant embryos (left and right panels, respectively) from timed pregnancies were analyzed for phenotypes at E10.5. Whole-mount anti-PECAM1 antibody staining of blood vessels (A, B) in the head, and (C, D) in the trunk region. (A, B) In mutant embryos, vessels forming the cardinal vein plexus were reduced in number, of irregular diameter, and failed to connect with cranial capillaries. (C,D) Anti-PECAM1 antibody staining of intersomitic capillaries at the level of the anterior LB. In mutant embryos, intersomitic capillaries were reduced in number, dysmorphic, and failed to sprout across the dorsal midline. Instead, occasional endothelial blisters were observed. Cardinal vein plexus, asterisk; cranial capillaries and endothelial blister in the trunk, arrow; intersomitic capillaries, arrowhead; LB, limb bud. (Zilian *et al*., 2001).

Moreover at a later stage they also presented pericardial edema and rarely they displayed cardiac malformation and developmental delay (Zilian *et al*., 2001).

Identification and expression pattern of *Numblike* in mouse

In mouse *Numblike* has been cloned and it encodes for a cytoplasmic protein (603 aa) that doesn't show any splicing isoform (fig. 25). mNumblike displays extensive aminoacidic sequence homology to mNumb (76%) and to a lesser extent to dNumb (63.7%); it contains a PTB domain (N-terminus) as well as a specific poly-glutamine repeat (C-terminus) and a typical region made of 41 aa (N-terminus) which are absent in mNumb. Inversely mNumblike fails to presents the PRR characteristic of all the isoforms of mNumb (fig. 25; Zhong *et al*., 1997).

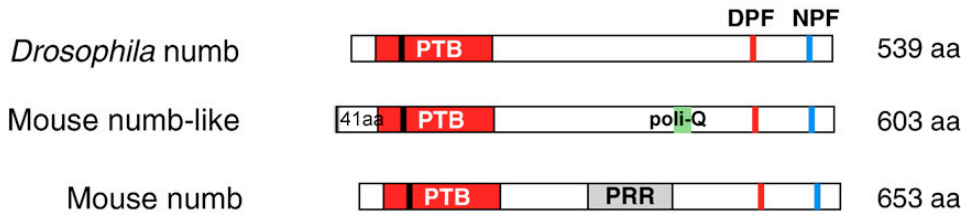

Fig. 25: Structure of Numblike isoform. In mouse, Numblike show only one isoform. It differs from mNumb in the typical N-terminal region of 41 aa and in the poly-glutamine repeat, both absent in Numb (adapted from Gulino *et al*., 2010).

Numblike expression has been analyzed by immuno-hystochemistry assays and WISH (Zhong *et al*., 1997). At E9.5 stage it is expressed predominantly in the trigeminal ganglia while later (E12.5) in all the nervous system. Remarkably m*Numblike* in the neural tube is detectable only in ventricles, where mitosis is modest; nervous tissues characterized by intense cell division express principally *Numb* (Zhong *et al*., 1997).
Recently, RT-PCR analyses demonstrated that the mRNA of m*Numblike* is also detectable in hematopoietic organs, as thymus, spleen and lymph nodes (Wilson *et al*., 2007).

<u>*Numblike* mutant mice: analysis of vascular function</u>

To clarify the function of Numblike in vascular development, mutant mice *Numblike*$^{-/-}$ have been generated. Those mice were viable, fertile and they didn't show any defect, nor embryonically nor in adult organisms (Petersen *et al*., 2002). It seemed to show that Numblike hasn't any important role during the development of vascular system in mice.

<u>Double mutant mice: analysis of vascular function</u>

Successively it has been generated double mutant, too (<u>D</u>ouble <u>K</u>nock <u>O</u>ut, DKO). Deleting both *Numb* and *Numblike,* the resulting mice died prematurely (E9) and at early stages they showed more serious defects than in singles mutants. To prevent this trouble Petersen and co-worker generated conditional double mutant mice. In a *Numblike*$^{-/-}$ background the gene *Numb* may be inactivated in a conditional way. Two different research groups inactivated *Numb* at E8.5 and at E9.5 to evaluate the role played by these two genes in neurogenesis (Petersen *et al*., 2002; Li *et al*., 2003). Subsequently DKO mice have been analyzed to understand the function of m*Numb* and m*Numblike* in development of mesodermal structures. At E8.5 both genes are expressed in notochord and in somites and DKO mice presented considerable alteration of these structures. Somites seemed to be decreased in size but not in number and were comparable to those observed in mutants *Numb*$^{-/-}$; notochord was partially or completely forked (fig. 26; Petersen *et al*., 2004; Petersen *et al*., 2006).

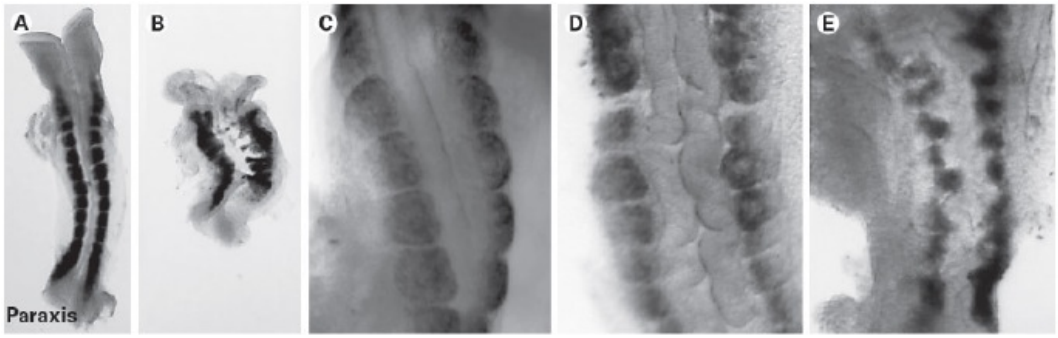

Fig. 26: Phenotypes of DKO mice. WISH conducted on embryos at E8.5 using a marker for somites. (A, C) control embryo; (B, E) DKO embryo; (D) Numb$^{-/-}$ embryo (adapted from Petersen *et al*., 2006).

Identification and expression pattern of *numb* in zebrafish

In zebrafish it has been identified a hortolog of m*Numb*, which encodes for a 680 aa protein showing the characteristic N-terminal PTB domain and a C-terminal PRR. The N-terminus displays a big identity with mice's (64%) while C-terminus is less conserved (fig. 27; Niikura *et* al., 2006; Reugels *et al*., 2006).

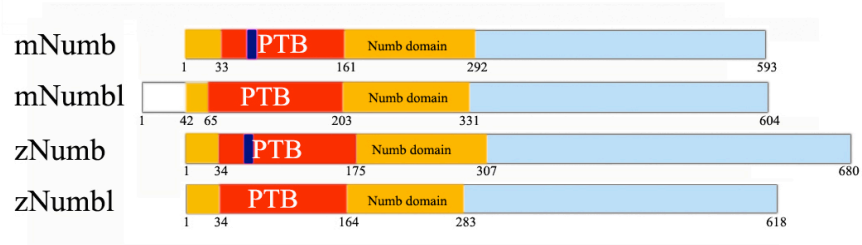

%ID aa	zNb	zNbl	mNb	mNbl
zNb	-	68%	59%	48%
zNbl	-	-	53%	57%

Fig. 27: Homologs of mouse Numb and Numblike have been identified and cloned in zebrafish. Peptide domains of both zNumb and zNumblike compared to murine. Table shows amino acid identity percentage.

Alternative splicing affects only PTB domain and generate two proteins of 680 aa and 669 aa; a 11 aa insert in PTB region distinguish between the isoforms (fig. 28; Reugels *et al*., 2006). This insert is responsible of the tethering of Numb to the cell membrane; thereby only the longer isoform may interact with the membrane while the smaller can't (Reugels *et al*., 2006).

Fig. 28: Splicing isoforms of zNumb. In zebrafish alternative splicing affect only PTB domain, generating two isoforms; the longer own the 11 aa insert and tether the membrane, while the shorter is cytoplasmic (adapted from Reugels *et al*., 2006).

Both transcripts have been detected by RT-PCR in all embryonic stages analyzed, since 64 cells stage to 5 dpf (Reugels *et al*., 2006); moreover RT-PCR assays conducted in our laboratory revealed that z*numb* is also expressed in ovary of adult females and in embryonic stages since 1 cell stage to 64 cells stage (fig.29).

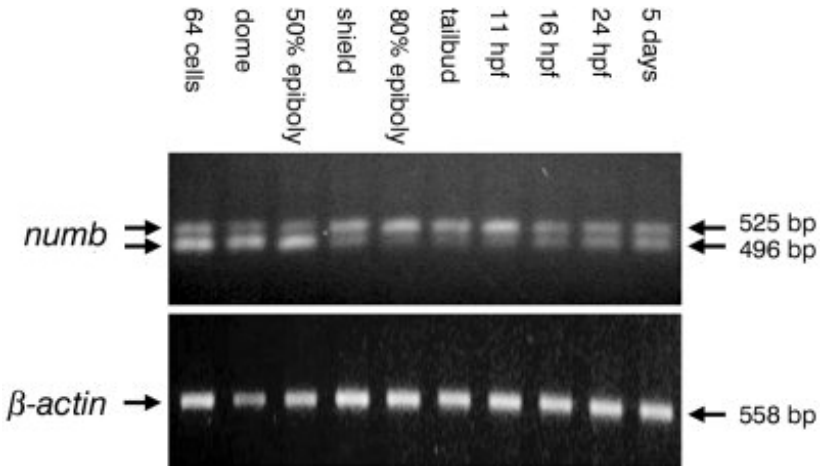

Fig. 29: Developmental expression of zebrafish isoforms of Numb. Total RNAs retro-transcribed and amplified by PCR with isoform-specific primer pairs. Both isoforms are expressed in all stages. A fragment of β-actin was amplified as a control (adapted from Reugels *et al*., 2006).

In order to continue and improve analysis of expression pattern, WISH have been conducted in embryos since 1-2 cells stage to 24 hpf. At early stages (1-2 cells - tail bud) the transcript was clearly ubiquitously expressed in the entire embryo. During somitogenesis the expression signal converged to the midline from the head to the tail region (fig. 30) and at later stages (18 somites - 24 hpf) z*numb* expression became restricted to the nervous system and in the eyes (fig. 30).

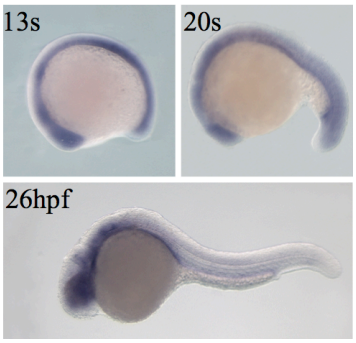

Fig. 30: *numb* expression by whole mount *in situ* hybridization. During somitogenesis (13 s and 20 s) a strong signal is found at the midline from the head to the tail region. At 24 hpf, its expression is restricted in the fore-, mid- and hindbrain and in the eyes. All the embryos are shown with head on the left.

Identification and expression pattern of *numblike* in zebrafish

numblike in zebrafish encode for a protein of 618 aa that exhibits the characteristic PTB domain. Otherwise it fails of SRR (peculiar of mNumb and mNumblike), of 41 N-terminal aa and of poly-glutamine repeats (characteristic of mNumblike; fig. 27, fig. 31). zNumblike show ≈53% aminoacidic identity with both mNumb and zNumb and 57% aminoacidic identity with mNumblike. Moreover it is a cytoplasmic protein because it doesn't present the 11 aa insert in PTB domain, necessary for the tethering of the protein with the plasma membrane (Niikura *et* al., 2006; Reugels *et al*., 2006).

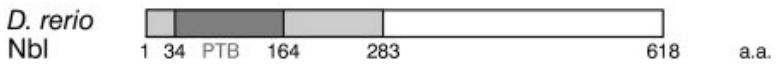

Fig. 31: Homolog of Numblike in zebrafish. In zebrafish there are no splicing events. The unique isoform is cytoplasmic, lacking of the 11 aa insert in the PTB domain (adapted from Reugels *et al*., 2006)

znumblike expression pattern has been analyzed during embryonic development and in different tissues from adult fish by RT-PCR and WISH.

RT-PCR revealed that mRNA is detectable in all the stages since 1-2 cells to 5 dpf, while in adult it is detectable in brain, eye, kidney, muscle, spleen, ovary and skin. It is not expressed in heart, liver, testis and gut.

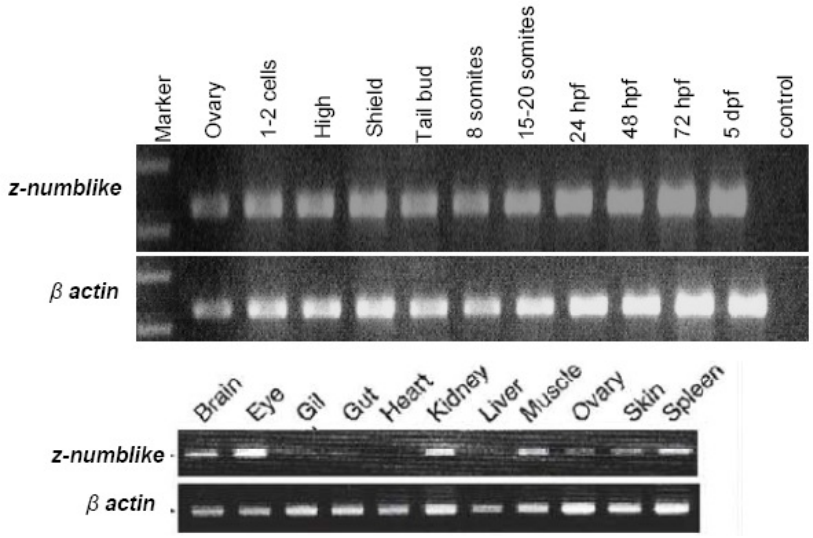

Fig. 32: Developmental expression of zebrafish *numblike*. Total RNAs retro-transcribed and amplified by PCR with specific primer pairs. z*numblike* is expressed in all stages. A fragment of β-actin was amplified as a control.

As previously observed in z*numb* expression pattern analysis, WISH showed that also z*numblike* is ubiquitously expressed during blastula and gastrula stages. Successively (13 somites, 15 somites and 20 somites) *numblike* mRNA was detectable in the central nervous system and in the somites (fig. 33). At 24-26 hpf its expression became restricted to the nervous system and in the eyes (fig.33).

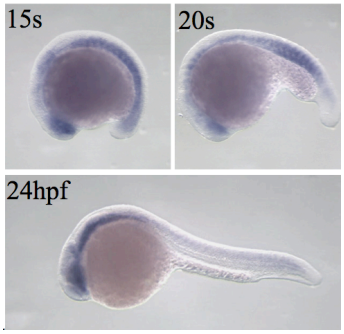

Fig. 33: *numblike* expression by whole mount *in situ* hybridization. During somitogenesis *numblike* mRNA is detectable in the central nervous system and in the somites. At 24-26 hpf, its expression becomes restricted to the nervous system and in the eyes. All the embryos are shown with head on the left.

Materials and Methods

MAINTENANCE OF FISH

Breeding fish were maintained at 28°C on a 14 hours light/ 10 hours dark cycle. They are bred in 3-5 liters tanks in three different systems (fig. 34).

Fig.24. One system where fish are maintained.

Embryos obtained from natural spawning were raised and maintained in an incubator at 28°C in fish water with 0.1% Methylene blue to prevent fungal growth in petri dishes, according to established techniques (Kimmel *et al*., 1995).

Beginning from 24 hpf, embryos were cultured in fish water containing 0.003% 1-phenyl-2-thiourea (PTU; Sigma-Aldrich corporation, St. Louis, MO, USA) to prevent pigmentation.

Stock solution for fish water: 34 g of Instant Ocean Sea Salt dissolved in 1 L of deionized water.

Fish water: 50 ml of stock solution in 10 L of deionized water.

The following lines were used:

Wild type lines:

- AB strain: obtained from the Wilson lab, University College London, London, United Kingdom.

Transgenic line:

- Tg(*fli1a*:EGFP)^{y1}: Enhanced Green Fluorescent Protein (EGFP) is expressed under the control of *fli1a* gene promoter in a wild type background (from the

Lawson lab, University of Massachusetts Medical School, Boston, MA, USA; Lawson and Weinstein, 2002a).

- Tg(*kdrl*:EGFP)^{S843}: EGFP is under the control of *kdrl* gene promoter in AB background (from the Stainier lab, University of California, San Francisco (UCSF), San Francisco, CA, USA; Jin *et al*., 2005).
- Tg(*gata1*:dsRed)^{sd2};Tg(*kdrl*:EGFP)^{S843}: dsRed is under control of *gata1* gene promoter, while EGFP is under control of *kdrl* gene promoter (from Massimo Santoro's lab, Molecular Biotechnology Center, University of Torino, Turin, Italy; Santoro *et al*., 2007).

MORPHOLINOS INJECTIONS

Three different antisense morpholinos were synthesized by Gene Tools LLC (Philomath, OR, USA):

*ve-ptp*MO, 5' AGGGCTCTGAAACACACACAAACAC 3'

*nb*MO 5' CACACAGCAAAACTTACTTTTTTAA 3'

*nbl*MO 5' CCCACTCTGAGGGTAGAAAAATTGA 3'

All of them are splice-blocking MOs designed on an intron/exon boundary. Respectively the target of *ve-ptp*MO is the intron 11/exon 12 boundary; the target of *nb*MO is the exon 4/intron 4; and the target of *nbl*MO is the intron 3/exon 4. As a control for unspecific effects, each experiment was performed in parallel with a std-ctrlMO (standard control oligo), with no target in zebrafish embryos, synthesized by Gene Tools LLC:

std-ctrlMO 5' CCTCTTACCTCAGTTACAATTTATA 3'

All morpholinos were diluted in Danieau Buffer (58 mM NaCl; o,7 mM KCl; 0,4 mM $MgSO_4.H_2O$; 0,6 mM $Ca(NO_3)_2$; 5 mM Hepes pH 7,2; Nasevicius and Ekker, 2000) at 2 mM and stored at -80°C.

The injected mixes were made up of:

- MOs at the desired concentrations, previously heated at 65°C for 5 min.
- 0.5 ml of rhodamine dextran (Molecular Probes).
- Danieau Buffer to reach the final volume of 5 ml

About 40 embryos was aligned on the edge of a slide that is placed in a Petri dish and were injected with 4 nl/embryo of mix at 1–4 cells stage; Rhodamine dextran was usually co-injected as a tracer.

Microinjection was carried out by using the Micromanipulator 5171 (Eppendorf, Hamburg, Germany) and the microinjector FemtoJet (Eppendorf).

After injection, embryos were raised in fish water at 28ºC and observed up to the stage of interest. For a better observation, the injected embryos were anaesthetized using 0.016% (1X) tricaine (Ethyl 3-aminobenzoate methanesulfonate salt, Sigma-Aldrich Corporation; Westerfield, 1995).

In vivo images were acquired by using a Leica MZ FLIII microscope (equipped with a Leica DCF 480 digital camera), provided of the LAS-Leica Application Suite V3 imaging software (Leica Microsystems GMBH, Wetzlar, Germany). Confocal images were acquired with a Leica TCS SP2 AOBS microscope (equipped with an Ar/Kr laser and the Leica LAS AF Lite software, Leica Microsystems GMBH).

After 24 hpf injected embryos were raised with PTU (1-phenil-2-thiourea, Sigma-Aldrich corporation) 1X at 28 hpf to inhibit the pigmentation and then fixed at the stage of interest in 4% PFA/PBS 1X, ON at 4°C.

- Stock PTU 10X: 0.015 g of powder in 50 ml of fish water.
- Stock Tricaine 0.4% (25X): 0.08 g of powder in 20 ml of mQ H_2O.
- PBS (Phosphate Buffered Saline) 10X: 180 g NaCl; 2 g KCl; 14,4 g $Na_2HPO_4 \cdot 2H_20$; 2,4 g KH_2PO_4 in 1l of distilled water (pH7.2-7.4).

Escalating doses of each MO were tested for phenotypic effects. For knockdown experiments, it were injected: 0.5 pmol/embryo of *ve-ptp*MO, 1.3 pmol/embryo of *nb*MO and 0.3 pmol/embryo of *nbl*MO.

DETECTION OF *nb* AND *nbl*MO EFFICIENCY BY RT-PCR (REVERSE TRANSCRIPTION-POLYMERASE CHAIN REACTION)

Reverse transcription.

RT-PCR was performed on total RNAs prepared from control embryos and *nb* and *nbl* morphants at 29 hpf using the RNAgents Total RNA Isolation System (Promega Corporation, Madison, WI, USA), treated with DNase I RNase free (Roche, Basel, Switzerland) to avoid possible contamination from genomic DNA and then reverse

transcribed using the ImProm-II Reverse Transcription System (Promega Corporation) and Random primers according to manufacturers' instructions.

PCR (polymerase chain reaction)

The cDNAs were then subjected to PCR amplification using GOTaq® DNA polymerase (Promega Corporation) following the manufacturer's instructions.

The following primers were used to determine the efficiency of *nbMO:*

SSFOR 5' CACCAGTGGCAGACCGATGAA 3' (Ta 61°C);

SSREV 5' ACCGCTCGCACAGCCTTCTTA 3' (Ta 61°C);

and of *nblMO:*

For nbl MOsplice 5' TCGGGCTGGTGGAGGTGGAT 3' (Ta 61°C);

Rev nbl MOsplice 5' CCGTCACGGCAGATGTAAGAG 3' (Ta 61°C).

Primers are synthesized by Invitrogen - Life Technologies (Carlsbad, CA, USA).

Reaction mixture (25 ml final volume):

- 5 ml of 5X reaction buffer
- 0.2 ml dNTPs 25 mM
- 0.125 ml GoTaq® DNA Polymerase (Promega Corporation)
- 5 ml cDNA
- 1.25 ml of both primers 20 mM
- 12.175 ml sterile H_2O

Cycles for amplification:

- 1st cycle:
  - 4 min at 95°C (denaturing)
- 2nd cycle up to 35th
  - 30 sec at 95°C (denaturing)
  - 30 sec at 61°C (annealing)
  - 1 min at 72°C (elongation)
- last cycle
  - 5 min at 72°C (final incubation)

Specific *b-actin* primers (Argenton *et al*., 2004) were used to check cDNA quality and possible genomic contamination.

Then the RT-PCR products were run on a 1% agarose gel, photographed on a trans illuminator and acquired with Epson 1200 scanner.

WHOLE-MOUNT *IN SITU* HYBRIDIZATION WISH

Whole-mount *in situ* hybridization (WISH) was performed using probes previously synthesized in Cotelli's Lab. The Table showed below display all the probes, the restriction enzymes, the vectors and the polymerases used for *in vitro* synthesis of the probes.

PROBE	VECTOR	ENZYME	RNA pol.
notch3	-	*Hind*III	T3
dll4	pBSKS^{+}	*Xho*I	T7
efnb2	pSK	*Sal*I	T7
ephB4	pSK	*Xba*I	T7
kdrl	pBSSK	*EcoR*I	T7
hey2	pCR2-TOPO	*Not*I	Sp6
flt4	pBS	*EcoR*I	T7
dab2	pBK-CMV	*Sol*I	T7
nr2f2	-	*EcoR*I	T7
sox18	pBSKS^{+}	*Sma*I	T7
cdh5	pCR4-TOPO	*Not*I	T3
myoD	-	*BamH*I	T7

Embryos at stage of interest, previously deprived of the chorions, was fixed in paraformaldehyde (PFA) 4% in PBS overnight at 4°C; subsequently they have been completely dehydrated through 25%, 50% and 75% MeOH/PBS solutions. Fixed embryos were stored at -20°C in 100% MeOH (Jowett and Lettice, 1994).

- Day 1

- Re-hydrate embryos through:

- 75% MeOH/25% PBS 1X (5 min at RT)
- 50% MeOH/50% PBS 1X (5 min at RT)
- 25% MeOH/75% PBS 1X (5 min at RT)

- 4 washes with PBT 1X (PBS 1X/Tween 20 1%; 5 min at RT each wash)

- Treat embryos in a Proteinase K solution (10 mg/ml in PBT) for: 10 min at RT for 24 hpf embryos and 12 min at RT for 29 hpf embryos
- Remove Proteinase K, brief wash in PBT and post-fix for 20 min at RT with PFA 4%/PBS to block the reaction
- 5 washes with PBT at RT, 5 min each wash
- Rinse with HM and incubate at 65°C for 2-5 hours.
- Denature the probe in HM (300 ng of probe in 400 ml) at 65°C for 5 min
- Hybridize incubating ON at 65°C with pre-denatured probe
    - Day 2
- Rinse with fresh HM.
- Wash for 15 min at 65°C with:
    - 75% HMw /25% SSC 2X
    - 50% HMw /50% SSC 2X
    - 25% HMw /75% SSC 2X
    - SSC 2X
- Wash twice for 30 min in SSC 0.1X at 65°C
- Wash for 10 min at RT with:
    - 75% SSC 0.1X /25% PBT
    - 50% SSC 0.1X /50% PBT
    - 25% SSC 0.1X /75% PBT
    - PBT
- Block in dark for at least 2 hours at RT in PBT/ 2% sheep serum/ 2 mg/ml BSA, gently shaking.
- Incubate in dark ON at 4°C in fresh PBT/ 2% sheep serum/ 2 mg/ml BSA containing 1:5000 antidig antibody conjugated with alkaline phosphatase (Roche), previously pre-absorbed for at least 2 hours at RT in PBT/ 2% sheep serum/ 2 mg/ml BSA containing zebrafish embryos homogenate.
    - Day 3
- Rinse with PBT at RT
- Wash 6 times for 15 min with PBT at RT
- Wash 3 times for 5 min with Stainig Buffer

- Incubate at RT in dark in Staining Solution, until the staining develops. To avoid the background due to endogenous alkaline phosphatases, Staining Buffer contain also 0.24mg/ml levamisole (Tetralevamisole, Sigma-Aldrich corporation).
- To stop the reaction rinse twice with PBT.
- Post-fix in PFA 4%/PBS for 30 min at RT
    - Solutions
- 10X PBS: 180 g NaCl; 2 g KCl; 14,4 g $Na_2HPO_4 \bullet 2H_20$; ; 2,4 g KH_2PO_4 in 1l of distilled water (pH7.2-7.4).
- PBT: PBS 1X + 1% Tween 20.
- 20X SSC: 3 M NaCl; 0.3 M $C_6H_5Na_3O_7 \bullet 2H_2O$ (sodium citrate) pH 7.0.
- HM (Hybridization mix): 50% formamide (Fluka, Sigma-Aldrich corporation); 5X SSC; 1M $C_6H_8O_7$ (citric acid) pH 6; 500 µg/ml Yeast RNA; 0.1% Tween 20; 50 µg/ml heparin.
- HMw (Hybridization mix wash): 50% formamide ; 5X SSC; 1M $C_6H_8O_7$ (citric acid) pH 6; 0.1% Tween 20.
- Staining Buffer: 100 mM NaCl; 100 mM Tris HCl pH 9.5; 50 mM $MgCl_2$; 0,1% Tween 20.
- Staining Solution: staining solution + BM Purple (diluted 1:2)

Images of stained embryos were taken with a Leica MZFLIII epifluorescence stereomicroscope equipped with a DFC 480 digital camera and Leica Application Suite LAS V3 imaging software.

MICROANGIOGRAPHY

Dechorionated tg(*fli1*:EGFP)^{y1} embryos at 2 dpf were anesthetized with tricaine (Sigma-Aldrich corporation) and located on a gel bed made of agarose; then Dextran-TMR (tetramethylrhodamine; molecular weight 70 kDa, Molecular Probes) have been injected. Dextran-TMR was dissolved in PBS at 25 mg/ml and microinjected into the sinus venosus or just ventro-posterior to the Sinus Venosus (Weinstein *et al.,* 1995).

Specimens were scanned using a Leica TCS SP2 AOBS microscope confocal microscope. For each sample, two images of the fluorescent tracer dye were collected,

10 min (t1) and 15 min (t2) after the dye injection. Pictures of the fluorescent vascular tree were also taken. The collected data were processed by ImageJ 1.41o: the pictures obtained at t1 were subtracted to the images obtained at t2 to evaluate changes of fluorescence occurred in 5 min for each injected embryo.

HISTOLOGICAL SECTIONS AND ELECTRON MICROSCOPY

Histological sections

Microinjected embryos were fixed, embedded in epoxy resin and sectioned.

- Fixation:

- Fix the samples at 4°C ON with a modified form of Karnovsky Fixative (Karnovsky, 1965), made up of 2.5% glutaraldehyde, 2% of paraformaldehyde and cacodilate buffer (sodium cacodilate in distilled water and chloridric acid) 0.1 M pH 7.4
- Rinse three times with cacodilate buffer 0.2 M pH 7.4 (5 min at RT)
- Wash in cacodilate buffer 0.2 M pH 7.4 at 4°C ON
- Post-fix in osmium tetroxide 2% in cacodilate buffer 0.1 M pH 7.4 (about 2-2.5 hours)
- Wash in cacodilate buffer 0.2 M pH 7.4

- Embedding:

- De-hydrate embryos through 35%-100% EtOH solutions
- Wash quickly in propylene oxide (5 min)
- Incubate for at least 3 hours at RT in a mix made up of 50% propylene oxide and 50% of epoxy resin (Epon 812- Araldite)
- Incubate in 100% epoxy resin (Epon 812- Araldite) at RT ON
- Embed embryos for 48hours at 68°C in 100% epoxy resin (Epon 812- Araldite)

Embedded samples were sectioned with a Reichter UltracutE ultra-microtome using glass blades. Semi-thin sections, 0.5-0.7 mm, were collected on SuperFrost slides (Bio Optica SpA, Milano, Italy), dried and rinsed with sodium metoxide, MeOH and EtOH, to remove the resin. Successively they were stained with gentian violet and basic

fuchsin and mounted with Eukitt (Bio Optica SpA). All slides were observed with a Leica DM6000 B microscope, equipped with a digital camera Leica DCF480 and provided of LAS-Leica Application Suite V3 imaging software (Leica Microsystems GMBH).

Electron microscopy

Microinjected embryos were fixed, embedded in epoxy resin and sectioned.

- Fixation:

- Fix the samples at 4°C ON with a modified form of Karnovsky Fixative (Karnovsky, 1965), made up of 2.5% glutaraldehyde, 2% of paraformaldehyde and cacodilate buffer (sodium cacodilate in distilled water and chloridric acid) 0.1 M pH 7.4
- Rinse three times with cacodilate buffer 0.2 M pH 7.4 (5 min at RT)
- Wash in cacodilate buffer 0.2 M pH 7.4 at 4°C ON
- Post-fix in osmium tetroxide 2% in cacodilate buffer 0.1 M pH 7.4 (about 2-2.5 hours)
- Wash in cacodilate buffer 0.2 M pH 7.4

- Embedding:

- De-hydrate embryos through 35%-50% EtOH solutions
- Incubate in dark at least 3 hours in 2% uranyl acetate solution (in 50% EtOH) gently shacked
- De-hydrate embryos through 50%-100% EtOH solutions
- Wash quickly in propylene oxide (5 min)
- Incubate for at least 3 hours at RT in a mix made up of 50% propylene oxide and 50% of epoxy resin (Epon 812- Araldite)
- Incubate in 100% epoxy resin (Epon 812- Araldite) at RT ON
- Embed embryos for 48hours at 68°C in 100% epoxy resin (Epon 812- Araldite)

Embedded samples were sectioned with a Reichter UltracutE ultra-microtome using diamond blades. Thin sections, about 80 nm, were collected on copper grid (thin mesh), stained with lead citrate (Reynolds, 1963) and coated with a thin carbon film using the carbon vacuum evaporator Emitech K400X. All the sections were observed and photographed using a transmission electron microscopy Jeol 100SX TEM. Plates were processed, and then acquired with an Epson Perfection 3710 scanner.

Statistical analysis

Statistical analysis was performed with Student's t-test or one-way ANOVA followed by Dunnett's post-test, when needed, using GraphPad PRISM version 5.0 (GraphPad, San Diego, CA, USA). A p value of <0.05 indicates a statistically significant effect.

Results

Functional characterizations of z*ve-ptp*, z*numb* and z*numblike* were conducted via loss-of-function assays, by microinjecting specifics morpholinos: *ve-ptp*MO, *nb*MO and *nbl*MO. In this work it has been microinjected for each morpholino previously tested doses. The dosage setting was performed on wild type embryos belonging to AB strain and the experimental doses were fixed to 0.5 pmol/embryo for *ve-ptp*MO, 1.3 pmol/embryo for *nb*MO and 0.3 pmol/embryo for *nbl*MO.

***ve-ptp* LOSS-OF-FUNCTION EXPERIMENTS**

*ve-ptp*MO is a splice-blocking morpholino designed on the intron 11/exon 12 boundary that cause the skipping of the 12th exon during splicing events. This exon encode for the FNIII domain closest to the cell membrane, so probably in morphants it is translated an altered isoform of zVe-ptp, lacking just this domain.

In order to demonstrate this alteration of splicing events were conducted RT-PCR experiments. Those assays performed on morphant's RNA showed the presence of two specific transcripts while control embryos displayed only one transcript for z*ve-ptp* mRNA. These data confirmed the presence of a non-physiological mRNA in embryo micro-injected with *ve-ptp*MO.

Transmission electron microscopy

As described before, consequently to the microinjection of *ve-ptp*MO embryos exhibited vascular defects ascribable to alteration of permeability caused to irregular conformation of endothelial junctional complexes. For instance morphants showed cephalic micro-haemorrhages and clots of erythrocytes in vessels.

With the aim to investigate the endothelial junction's structure and highlight eventual alterations it was conducted an ultra-structural analysis of endothelium of main axial vessels, through Transmission Electron Microscopy (TEM; fig.25).

Examining transverse sections collected from several areas, in trunk and tail region of different embryos microinjected with std-MO, it was detected a lot of junctions between endothelial cells (fig.25A, A'). Conversely, identify endothelial junctional complexes that surround DA and PCV/CV in morphants was quite difficult. The boundaries between cells usually lacked of junctions and only occasionally they showed few complexes of disorganized electrondense material (fig.25B, B').

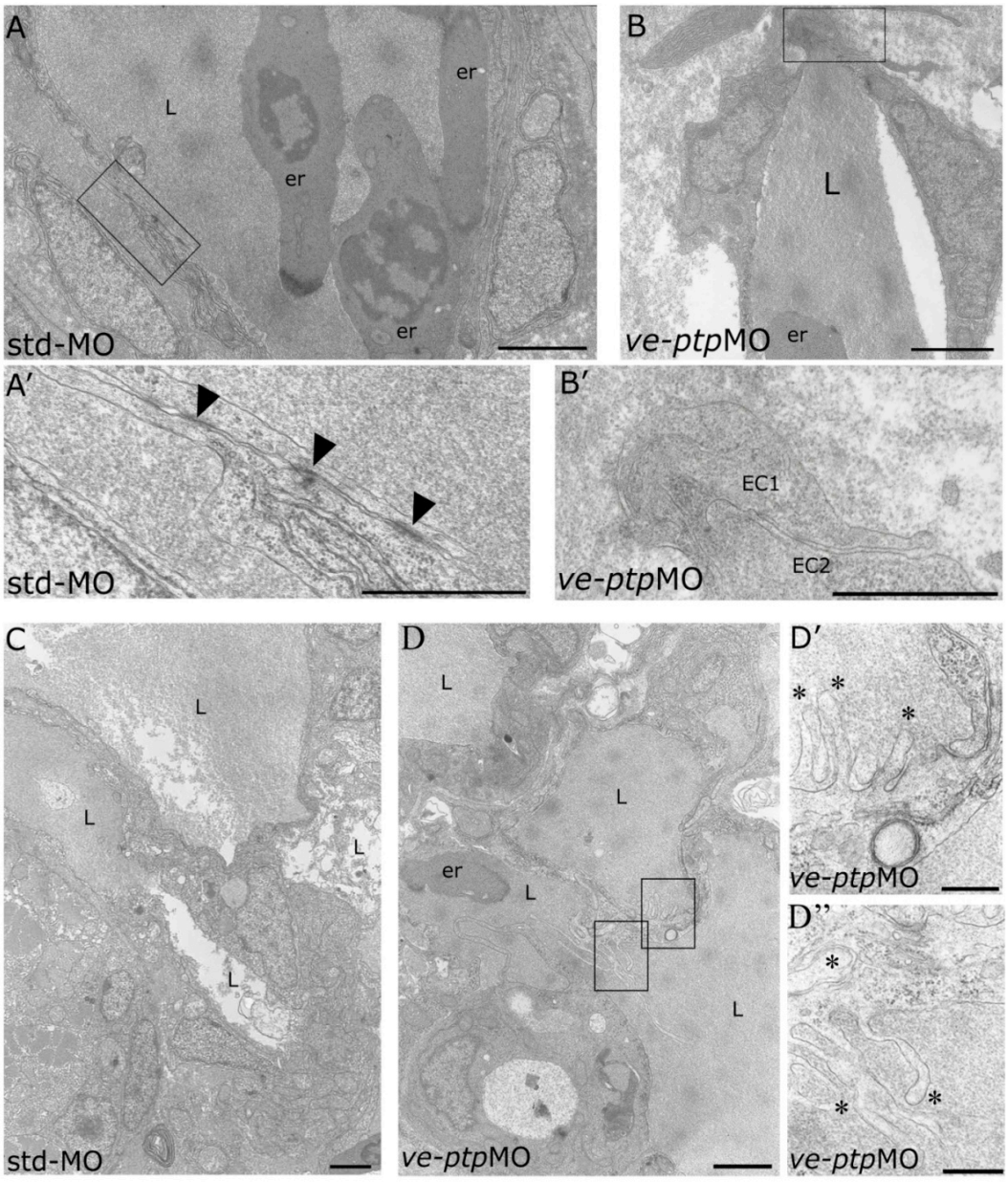

Fig.25. Ultra-structural analysis of endothelial junctions in control embryos (A, C) and morphants injected with *ve-ptp*MO (B, D). Transversal sections of embryos collected in trunk region (A, B); transversal sections of embryos collected in caudal region (C, D). (A', B', D', D") Higher magnification of the boxed areas. It is possible to observe the abundance of junctions (black arrowheads) between endothelial cells of control embryos (A, A') and their complete absence in morphants' endothelium (B, B'). In morphants' tail it was noted *filopodia* (asterisks; D, D', D"). er, eritrocytes; EC, endothelial cell; L, lumen of vessels. Black arrowheads, junctions; asterisks, *filopodia*. Bar: 2 μm in A, B, C and D; 1 μm in A', B',D' and D".

It was very interesting to note that in embryos microinjected with *ve-ptp*MO, endothelial cells of CV also exhibited alterations of the cell membrane. In fact these cells displayed digitiform membrane protrusions of the membrane, which were ascribable to *filopodia* (microspikes) and were completely absent in control sections (fig.25C-D").

These structures, quite crucial for a correct interaction between two cells membrane, may be related to an immature phase of junctions' development, in which cells contact their neighbours but they are not yet able to generate permanent junctions structures.

Statistical analysis of ultra-structural defects

To validate the data collected by TEM and to attribute them a quantitative meaning, it was conducted a thorough statistical analysis.

Because of the complexity of data collection via TEM, it was considered as "n" the single boundary between two different endothelial cells observed through electron microscopy, with the aim of obtaining a significative statistic. Moreover, several regions of different embryos (3 controls and 7 morphants) were examined to provide higher variability in this investigation.

So 112 boundaries were analysed from control embryos and 150 boundaries from morphants. Subsequently it was determined if the observed boundaries showed or not junctional complexes.

In controls 98 EC-EC boundaries exhibited at least one junctional complex (88.5%) and only 14 didn't displayed any complex (11.5%; fig.26). Contrariwise in morphants only 43 region showed adhesive complexes (29%), while 107 boundaries were lacking of junctions (71%). It is very interesting to note that in 29 examined region (20%) of embryos microinjected with *ve-ptp*MO, it were clearly identified the digitiform structures just described (*filopodia*; fig.26A, C). Overall morphants displayed a five-fold decrease in the ratio of number of endothelial junctional complexes with respect to controls, while the rate of junctions per boundary diminished from 1.24 to 0.48 from control to morphants.

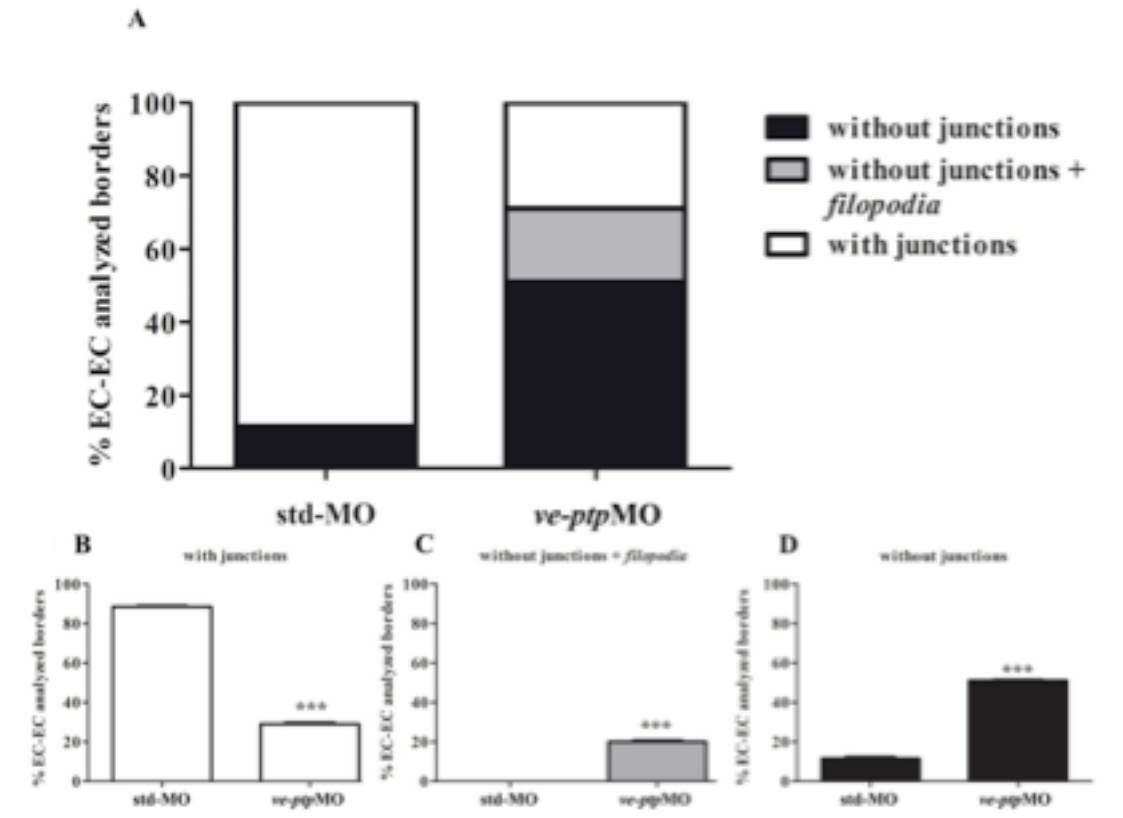

Fig.26. Quantitative analysis of % EC-EC borders. (A) Cumulative graph of the rate of EC-EC boundaries with any type of junctions (adherens and/or tight junctions), without junctions and without junctions but with *filopodia* in controls and in z*ve-ptp* morphants. Singles graphs of the data belonging to each class: with junctions (B), without junctions but with *filopodia* (C) and without junctions (D). The analysis was performed on the acquired images of trunk and tail regions. Three std-MO and seven z*ve-ptp* MOb injected embryos were analyzed. *** p<0.001 vs std-MO.

Microangiography assays.

With the purpose of supporting the working hypothesis, namely that the loss of function of Ve-ptp resulted in a change in vascular permeability, it have been conducted micro-angiography assays. Cause to the absence of considerable haemorrhages our goal was to demonstrate a change in permeability that would allows only the leakage of haematic fluid and not of blood cells.

So a fluorescent dye was injected in the cardiovascular system of control embryos and of morphants at the stage of 2 dpf. Micro-angiographed embryos were observed using a confocal microscope in two moments: 10 minutes after the microinjection of dye (t1) and 15 minutes after the microinjection of dye (t2). Successively each image obtained at t2 was compared to the corresponding image obtained at t1 to evaluate the dye leaked from the vessels in 5 min (fig.27).

Moreover, to further highlight an eventual extravasation of dye, endothelial transgenic line Tg(*fli1a*:EGFP)^{y1}, that express the green fluorescent protein EGFP in endothelial cells, was used to conduct this analysis and the images of dye and of vessels were added via imaging software (fig.27E-F).

The vast majority (62%) of micro-angiography experiments conducted on control embryos didn't show extravasation of dye (fig.27A, C, E) while morphants clearly exhibited a drastic increase of fluorescence outside from the vessels, indicative of dye extravasation (fig.27B, D, F). Must affected regions were the CV plexus and the DLAVs (fig.27F', F").

The statistical analysis indicate that only 38% (n=29) of control embryos showed dye extravasation, indicative of physiologic outflow, contrariwise 80% of morphants displayed this defect (n=32).

numb AND *numblike* LOSS-OF-FUNCTION EXPERIMENTS

In order to perform the functional characterization of the genes *numb* and *numblike*, two different morpholinos was microinjected separately: *nb*MO and *nbl*MO. *nb*MO was designed on the exon 4/intron 4 boundary and cause the skipping of the 4th exon during splicing events, without changing the sequence reading frame. This exon encodes for the characteristic sequence 11 aa long, responsible for the tethering of the protein to the cell membrane. The resulting altered protein might be a cytosolic form of Numb and the modified mRNA might coincide to one of the two physiological splicing isoform of the transcript. To demonstrate this hypothesis it was conducted an RT-PCR assay with specific primers, on cDNA retrotranscribed from total RNA extracted from 29 hpf embryos microinjected with std-ctrlMO and *nb*MO (fig.28). In control embryos it was clearly detected two bands while in morphants only a lower length band (fig.28A).

Successively this band was sequenced and it coincided (more than 99% identity) to the sequence of the transcript of cytosolic isoform of Numb. Basically, microinjection of *nb*MO altered the physiological balance between the two isoforms of Numb, towards cytoplasmic one.

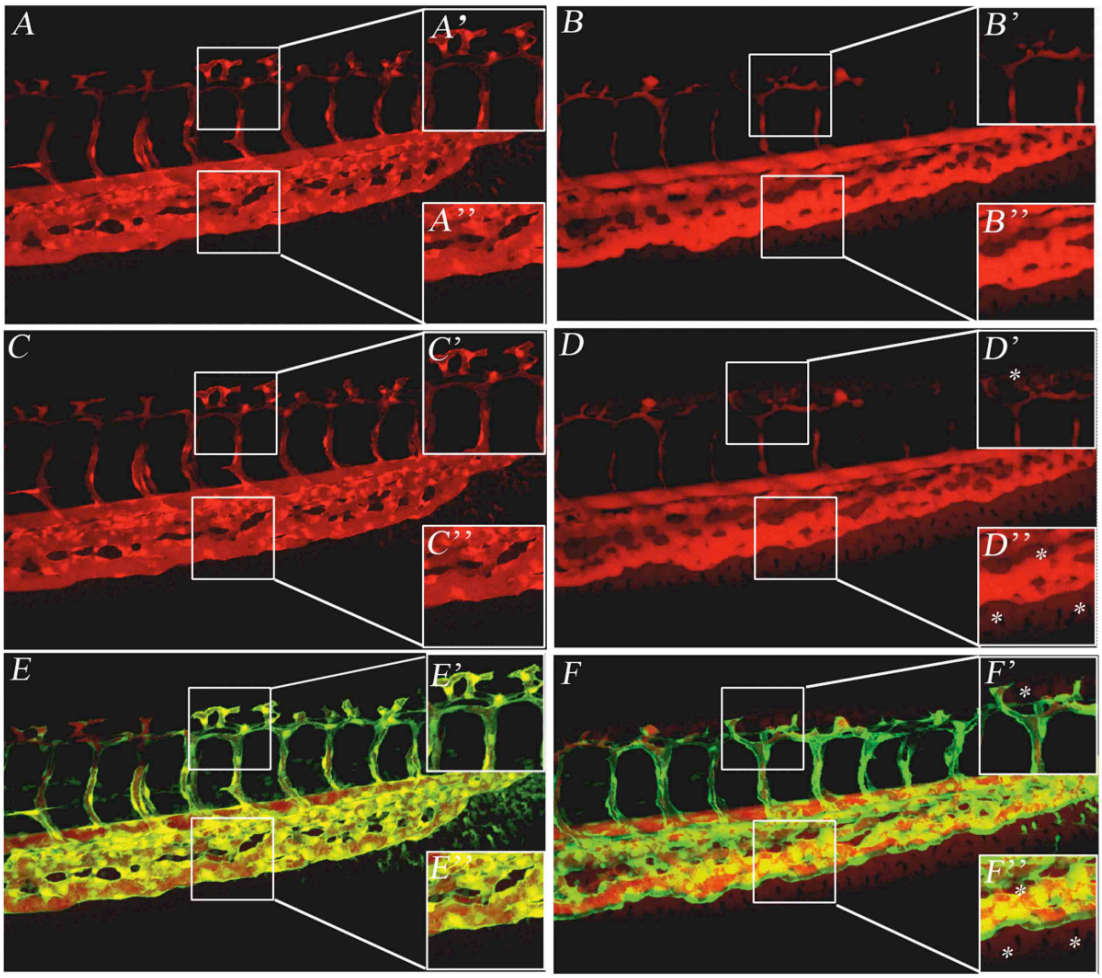

Fig.27. Micro-angiography assays performed on control embryos (A, C, E) and morphants microinjected with *ve-ptp*MO (B, D, F). Confocal microscopy images of the tail collected at t1 (10 min post-injection of the die; A and B) and at t2 (15 min post-injection of the die; C and D). (E and F) merger of vessels' picture and of circulating fluorescent die's picture; (A'-E") higher magnification of the boxed areas. Asterisks highlight the leakage of die from the vessels in the morphants.

*nbl*MO, designed on the intron 3/exon 4 boundary, was a splice-blocking morpholino, too. Its interaction with the *numblike* transcript caused the skipping of the 4th exon during splicing events, without altering the sequence reading frame. This exon encodes for a portion of the PTB domain. To clarify if *nbl*MO microinjection really may change splicing events generating a non-physiologic mRNA it was conducted a RT-PCR experiments with specific primers, on cDNA retrotranscribed from total RNA extracted from 29 hpf control embryos and from morphants (fig.28). Effectively RT-PCR performed on RNA extracted from embryos microinjected with *nbl*MO showed two different transcripts, one corresponding to the physiological mRNA and one shorter, probably corresponding to the non-physiologic *nbl* mRNA generated as a result of the micro-injection of the specific morpholino (fig.28B).

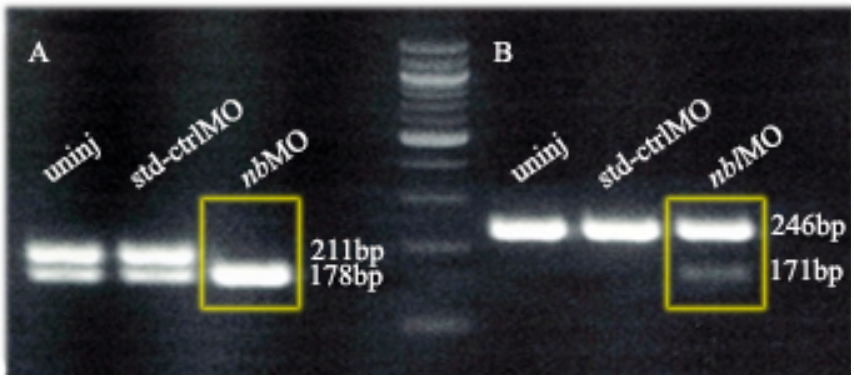

Fig.28. Qualitative RT-PCR analysis to test *nb*MO (A) and *nbl*MO (B) efficiency. The first and the second lanes of each panel show respectively amplified cDNA from uninjected embryos (uninj) and from embryos microinjected with std-ctrlMO. The third lanes of each panel show the amplified cDNA from morphants; *numb* morphants in A and *numblike* morphants in B. The central lane is the marker. In control embryos were seen two different bands for *numb* mRNA, and only one for *numblike* mRNA. Contrariwise *numb* morphants show only one band (178 bp), referred to the cytosolic isoform of Numb, while *numblike* morphants show two different bands (246 bp and 171 bp), referred to a physiologic and an altered form (shorter) of Numblike.

Phenotype of knocked down embryos

Microinjected embryos were observed *in vivo* at 2 dpf (fig.29). Embryos microinjected with *nb*MO and embryos microinjected with *nbl*MO showed evident defects if compared with control embryos. Sure enough morphants exhibited mild cerebral oedemas and yolk extensions thinner than controls. As a rule, morphants' body plans resulted unaffected (fig.29A, B, C).

Employing the transgenic line Tg(*gata1*:dsRed)^{sd2};Tg(*kdr*:EGFP)^{S843}, that express the red fluorescent protein dsRed in blood cells and the green fluorescent protein EGFP in endothelial cells, it was possible to observe *in vivo* vascular and circulatory defects. At the analysed stage both vasculogenesis and first intersegmental angiogenic event are already occurred. So in the trunk/tail region of a 2 dpf embryo is possible to distinguish two main axial vessels (DA and PCV/CV plexus) and a well organized series of ISVs. Embryos microinjected with *nb*MO and embryos microinjected with *nbl*MO showed a drastic reduction in dorsoventral size of CV plexus, if compared with control embryos (fig.29). This defect was detected analysing vessels structure (in green; fig.29D, E, F) and confirmed studying circulation (in red; fig.29 G, H, I). Blood flow examination has also allowed the characterization *in vivo* of a significant approach between the two main axial vessels in the trunk (fig.29 G, H, I). Honestly, despite neither circulation nor heartbeat were affected, blood flow observation has been very difficult, because morphants showed a reduction in number of erythrocytes. It is due to the fact that *numb* and *numblike* are involved in blood cells differentiation, as proved by previous studies (Bresciani *et al*., 2010).

Furthermore morphants displayed alterations of ISVs that lost their characteristic arrowhead shape and didn't seem to be still patent; nevertheless in this work the attention was focalized to the defects of main axial vessels.

All the decribed defects were detectable in both morphants but with different rate and severity. Sure enough embryos microinjected with *nb*MO displayed milder defects and a lower ratio of phenotypes (28%, n=495). Contrariwise embryos microinjected with *nbl*MO showed defects more pronounced than *numb* morphants and a higher ratio of phenotypes (64%, n=637).

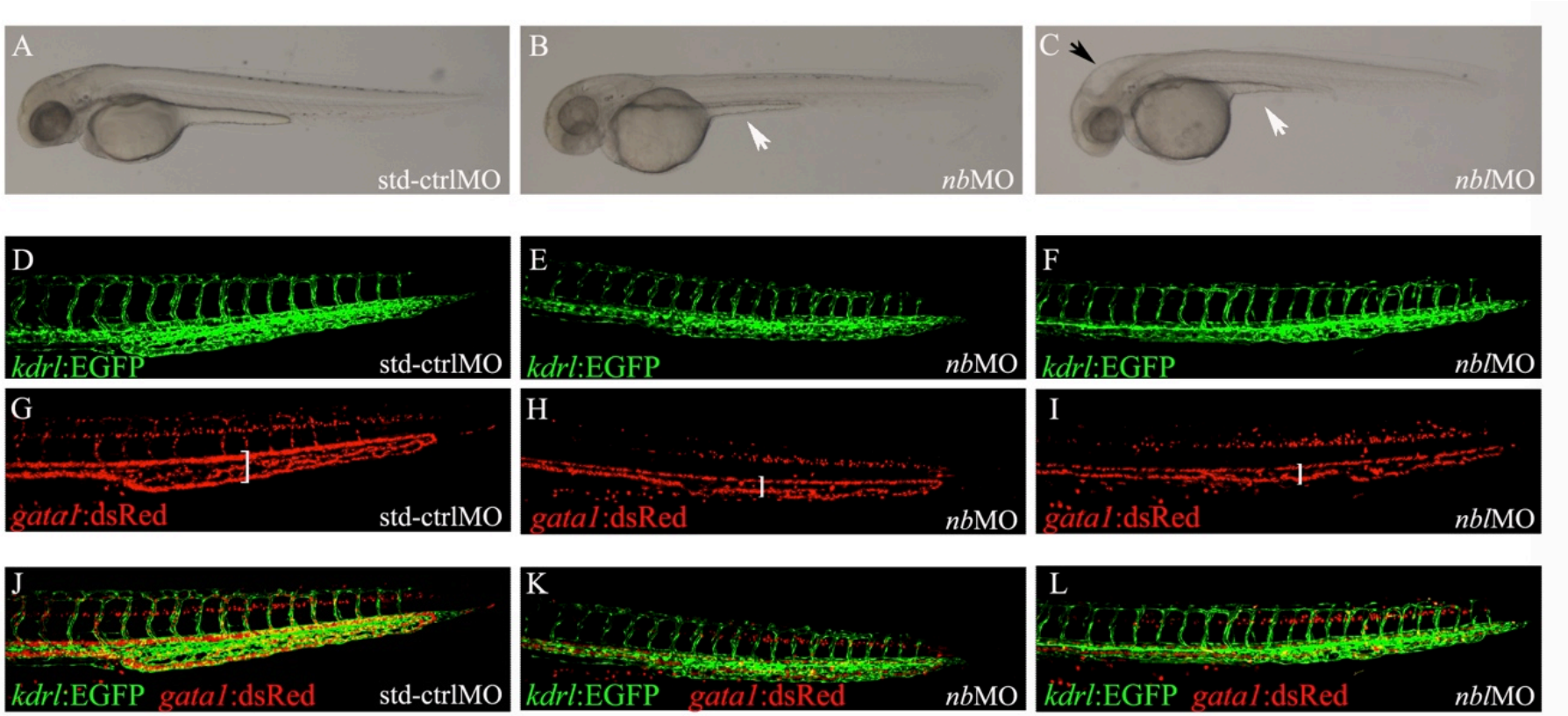

Fig.29. Phenotypes of *numb* (B, E, H and K) and *numblike* (C, F, I and L) morphants. Bright field pictures of 2 dpf whole mount embryos (A, B and C) and confocal microscopy analysis of trunk/tail region of 2 dpf Tg(*gata1*:dsRed)^{sd2};Tg(*kdrl*:EGFP)^{s843} embryos: detailed images of the vessels (EGFP; D, E and F); detailed images of the blood flow (dsRed; G, H and I); merging of EGFP and dsRed images (J, K and L). The body plan of morphants is substantially unaltered if compared with controls (A, D, G and J). Analysing bright field pictures, only the yolk extensions look thinner in morphants than in controls. On the contrary, confocal images show a drastic reduction in dorsoventral size of CV plexus and suggest an approach of main axial vessels. All the embryos are shown with the head on the left. White arrow, yolk extension; black arrow, cerebral oedema.

Histological analysis

To better characterize the defects of main axial vessels examined *in vivo* it was performed a histological investigation conducting semi-thin transverse sections of morphants' trunk and tail (fig.30).

Comparing sections obtained from the trunk of embryos microinjected with *nb*MO and *nbl*MO with sections obtained from the trunk of controls (fig.30, line I) it was observed that as a rule in morphants DA and PCV were not altered in shape or size, they were always luminized and they didn't display any evident defects of endothelium (fig.30A); in addition blood cells was detectable inside both main axial vessels. Transverse sections confirmed the approach of DA and PCV and permitted to evaluate the alteration of the distance between these two vessels (fig.30B, C). This distance was measured directly on the collected images of the sections, and then it was calculated the average distance for each embryo (1 control embryo, 2 *numb* morphants, 2 *numblike* morphants; almost 50 measuring per embryo). Comparing the data collected analyzing the transverse sections it was observed that *numb* morphants exhibited approximately 50% decrease of vessels distance, while *numblike* morphants showed about 80% decrease. Moreover vein lumina were larger in morphants than in controls (fig.30G).

In the tail of a 2 dpf embryo vascular tree is characterized by a single artery, the DA, and a vein organized in a complex plexus of vessels, the CV. In this plexus it is possible to identify a "preferential way" followed by red blood cells, corresponding to the most ventral vessel. Examining transverse section, these preferential vessels of the plexus are larger than the others and show the widest lumen (fig.30D). Morphants showed, as a rule, CVs with lumen wider than controls, and the DA and the most ventral vessel of CV closer than in embryos microinjected with std-ctrlMO (fig.30, line II). As for trunk sections, even in tail it was measured the distance between DA and the main vessel of CV, it was calculated the average and it was noted that *numb* morphants displayed approximately 30% decrease of width of the space between vessels, while *numblike* morphants exhibited about 90% decrease of the distance measured (1 control embryo, 2 *numb* morphants, 2 *numblike* morphants; almost 50 measuring per embryo; fig.30H).

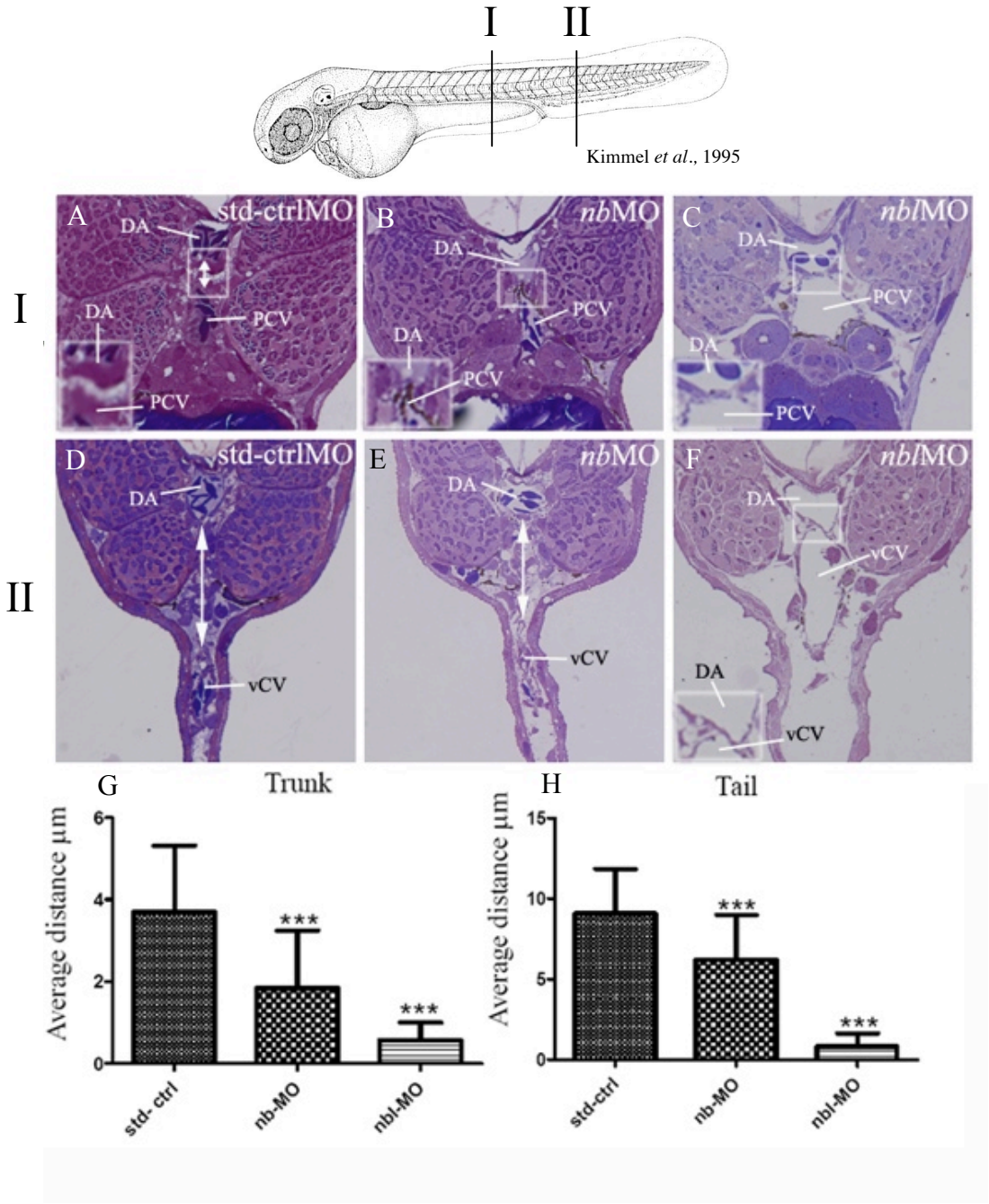

Fig.30. Morphological analysis of *numb* and *numblike* morphants. Transverse semi-thin plastic sections of 2 dpf embryos microinjected with std-ctrlMO (A, D), *nb*MO (B, E) and *nbl*MO (C, F); at the level of trunk (A, B and C) and tail (D, E and F) region. In the insets, higher magnifications of the space between the main axial vessels (boxed areas). Morphants sections show a drastic approach of the arterial and venous vessels (highlighted by inset and/or arrows), both in the trunk and in the tail; moreover *numblike* morphants exhibit a self-evident enlargement of the vein calibre. Erhitrocytes are detectable in the lumen of the vessels. Statistical analysis of vein-artery approach made measuring average of main axial vessels distance in trunk (G) and tail (H) region. The top image shows the section planes: I, trunk; II, tail. *** $p<0.001$ vs std-MO. DA, Dorsal Aorta; PCV, Posterior Cardinal Vein; vCV, most Ventral vessel of Caudal Vein; arrow, DA-PCV/DA-vCV distance.

Molecular analysis

The molecular analysis was conducted by WISH assays on 29 hpf embryos microinjected with std-ctrlMO, *nb*MO and *nbl*MO. The embryonic stage was selected considering that starting from 28/29 hpf the vessels begin to express different specific markers, in accordance with their arterial-venous identity.

- **Expression of Notch pathway markers**

With the aim of highlighting potential alterations in the expression of the major molecules involved in this signalling cascade it has been characterized the expression pattern of *notch3* and *dll4*.

- *notch3*

The gene *notch3* encodes for the vascular specific isoform of Notch. At 29 hpf this transcript is detectable, via WISH, in CNS and in DA (Lawson *et al*., 2001). Embryos microinjected with *nb*MO (n=60) and with *nbl*MO (n=58) exhibited a marked increase of hybridization signal (respectively 72% and 53% of embryos) if compared with control embryos (n=70; 92% of embryos with unaffected phenotype; fig.31A, C, E).

- *dll4*

The gene *dll4* encode for one of the Notch ligands expressed in vascular endothelium, Dll4 (Delta like ligand 4). Although it is not the preferential ligand of Notch3, previous data displayed that this receptor may interact with Dll4 protein, too (Hsiao *et al*., 2007; Indraccolo *et al*., 2009; Serafin *et al*., 2011). At 29 hpf *dll4* was expressed in ISVs and in DA (Leslie *et al*., 2007). Comparing hybridization signal in morphants (*nb*MO n=14; *nbl*MO n=13) and in control embryos (n=12), no evident alteration were detectable (fig.31B, D, F).

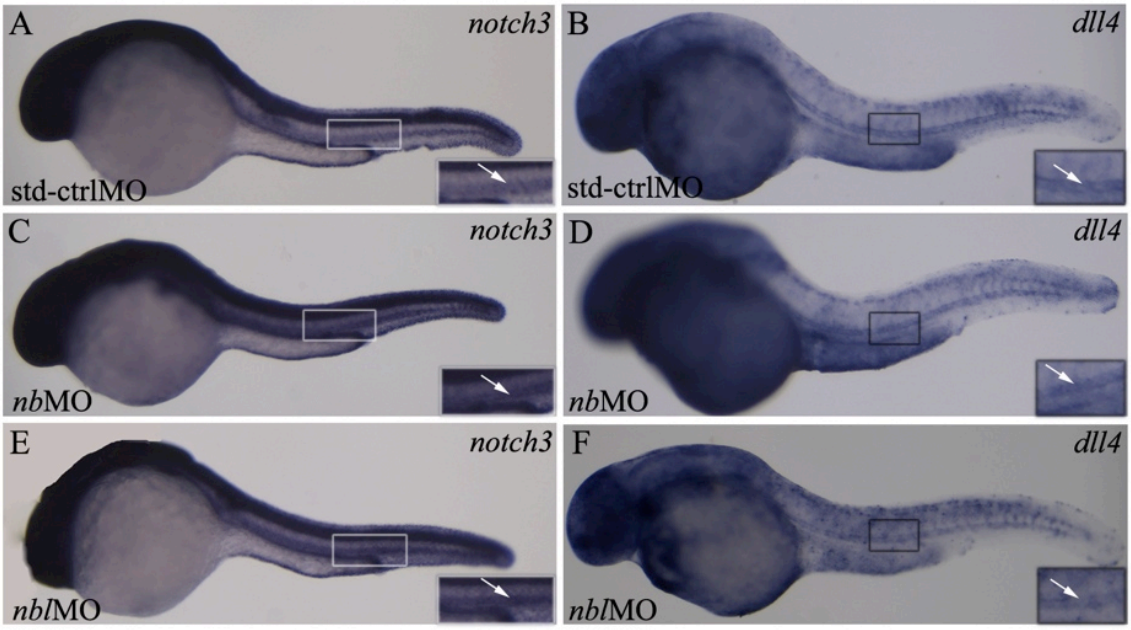

Fig.31. Expression of Notch pathway markers: *notch3* (A, C, E) and *dll4* (B, D, F). WISH on embryos at 29 hpf microinjected with std-ctrlMO (A, B), *nb*MO (C, D) and *nbl*MO (E, F). In the insets, higher magnification of the boxed areas. *notch3* hybridization signal increase in morphants if compared with control embryos. White arrow, hybridization signal in DA. All the embryos are shown with the head on the left.

- **Expression of Eph-ephrin signalling pathway markers**

As described thorough before, previous studies proved that Notch pathway plays a key role in arterial-venous differentiation of endothelial cells during embryonic development. In particular Notch may influence the consecutive expression of specific arterial or venous markers pertaining to Eph-ephrin signalling pathway (Wang *et* al., 1998; Lawson *et* al., 2001; Domenga *et al*., 2004).

The Ephrin ligand Efnb2 and Ephrin receptor EphB4 were identified in the late 1980's and they were linked to different physiological and pathophysiological processes like embryonic development, angiogenesis and tumorigenesis.

In order to characterize any alteration in expression pattern of these markers it has been conducted WISH assays with specific probes.

- *efnb2*

The gene *efnb2* encodes for a trans-membrane ligand, Efnb2 (Ephrin B2), and in 29 hpf embryos it is expressed in specific region of CNS and in DA (Adams *et al*., 1999).

Comparing data obtained from WISH conducted on controls (n=39) and on embryos microinjected with *nb*MO (n=64; fig32A) and with *nbl*MO (n=41), hybridization signal in the main arterial vessel of morphants resulted increased (29% and 72% of embryos), both in the trunk and in the tail (fig.32C, E). Nevertheless no ectopic expression has been detected. The probe is kindly provided by R. Patient.

- *ephB4*

The gene *ephB4* encodes for EphB4 (Ephrin B4 receptor) a trans-membrane tyrosine kinase receptor having a high affinity binding to Efnb2 (Adams *et al*., 1999). At 29 hpf it is specifically expressed in specialized region of CNS, in lateral line primordium, in PCV and in CV plexus.

Embryos microinjected with *nb*MO (n=82) and with *nbl*MO (n=74) and hybridized with the specific probe, kindly provided by R. Patient, showed a drastic reduction of the signal in main venous vessels (31% and 65% of embryos; fig.32D, F), particularly evident in CV plexus, if compared with embryos microinjected with std-ctrlMO (n=55; fig.32B).

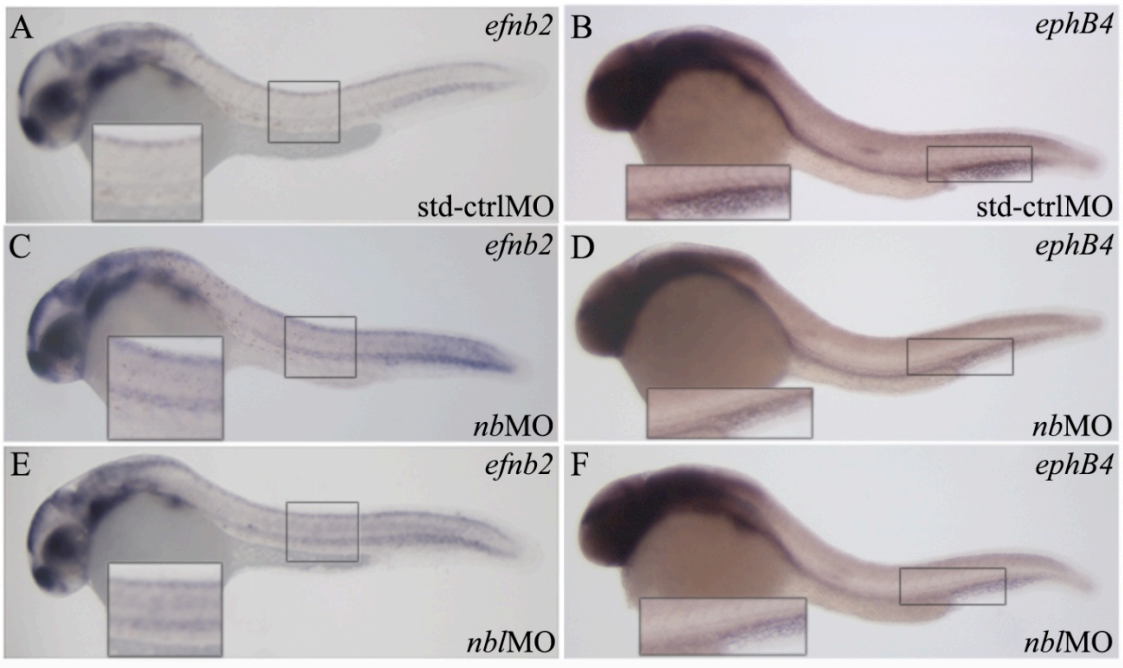

Fig.32. Expression of arteriovenous markers: *efnb2* (A, C, E) and *ephB4* (B, D, F). WISH on embryos at 29 hpf microinjected with std-ctrlMO (A, B), *nb*MO (C, D) and *nbl*MO (E, F). In the insets, higher magnification of the boxed areas. To note the increase of *efnb2* hybridization signal and the dicrease of *ephB4* in morphants. All the embryos are shown with the head on the left.

- **Expression of arterial-venous identity markers**

Alteration of *efnb2* and *EphB4* expression may have been related to a modification in arterial-venous identity acquisition of main axial vessels endothelium. In order to confirm that hypothesis were conducted WISH assays, to investigate expression patterns of arterial-venous identity markers involved in the Notch pathway.

- *kdrl*

The gene *kdrl* encodes for the protein Kdrl (Kinase insert domain receptor like), a tyrosine kinase receptor for Vegf (Holmes and Zachary, 2007). At 29 hpf the transcript is exclusively expressed in arterial vessels (Fouquet *et al*., 1997).

In *numb* and *numblike* morphants (n=14 and n=15 respectively; fig.33C, E) hybridization signal resulted considerably increased, if compared with embryos microinjected with std-ctrlMO (n=16; fig.33A).

- *hey2*

The gene *hey2* encodes for the protein Hey2 (Hairy/enhancer-of-split related with YRPW motif protein 2), a transcription factor that interact with a histone deacetylase complex. Notch signaling pathway induces the expression of this gene, although a very recent work demonstrate that *hey2* in zebrafish lays upstream of *notch* during haematopoiesis (Leimeister *et al*., 1999; Rowlinson and Gering, 2010). In embryos at 29 hpf the transcript is detectable in some specific area of CNS and in DA along its entire length, both in trunk and tail (Zhong *et al*., 2001).

Morphants microinjected with *nb*MO (n=50) and with *nbl*MO (n=45) showed a strong increment of the hybridization signal (respectively 31% and 57% of embryos; fig.33D, F), if compared with control embryos (n=61; 98% of embryos with unaffected phenotype; fig.33B). No ectopic signal was detected.

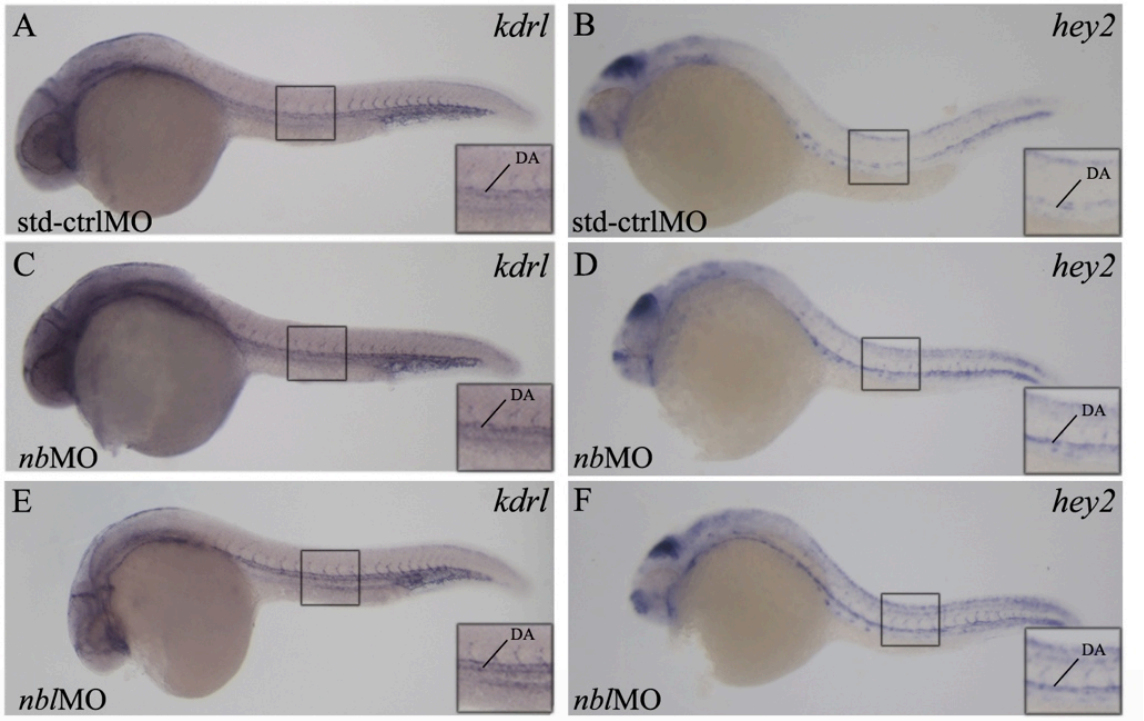

Fig.33. Expression of arterial-venous identity markers (I): *kdrl* (A, C, E) and *hey2* (B, D, F). WISH on embryos at 29 hpf microinjected with std-ctrlMO (A, B), *nb*MO (C, D) and *nbl*MO (E, F). In the insets, higher magnification of the boxed areas. An increase of hybridization signals in the arterial vessels was detected in morphants. All the embryos are shown with the head on the left. DA, Dorsal Aorta; PCV, posterior Cardinal Vein.

- *flt4*

The gene *flt4* encodes for the protein Flt4 (Fms-related tyrosine kinase 4), a tyrosine kinase receptor for VegfC and VegfD, involved in lymphangiogenesis and maintenance of the lymphatic endothelium (Petrova *et al*., 1999). At 29 hpf this gene is specifically expressed in venous vessels of head, trunk and tail (Thompson *et al*., 1998).

Comparing the hybridization signal observed in embryos microinjected with std-ctrlMO (n=31; fig.34A) with *numb* and *numblike* morphants (n=22 and n=43, respectively) it resulted that both microinjected embryos showed a drastic reduction in the expression of this venous marker (35% and 72% respectively; fig.34C, E).

- *dab2*

The gene *dab2* is exclusively expressed in venous endothelium and encodes for the protein Disabled homolog 2 (Dab2; Hocevar *et al*., 2003). At 29 hpf in control embryos it is expressed in venous vessels of head, trunk and tail (Song *et al*.,2004).

In *numb* and *numblike* morphants (n=66 and n=65 respectively) hybridization signals resulted unaltered (fig.34D, F), if compared with embryos microinjected with std-ctrlMO (n=110; fig.34B).

In the order 10% and 21% of samples exhibit a mild increase in the intensity of hybridization signal.

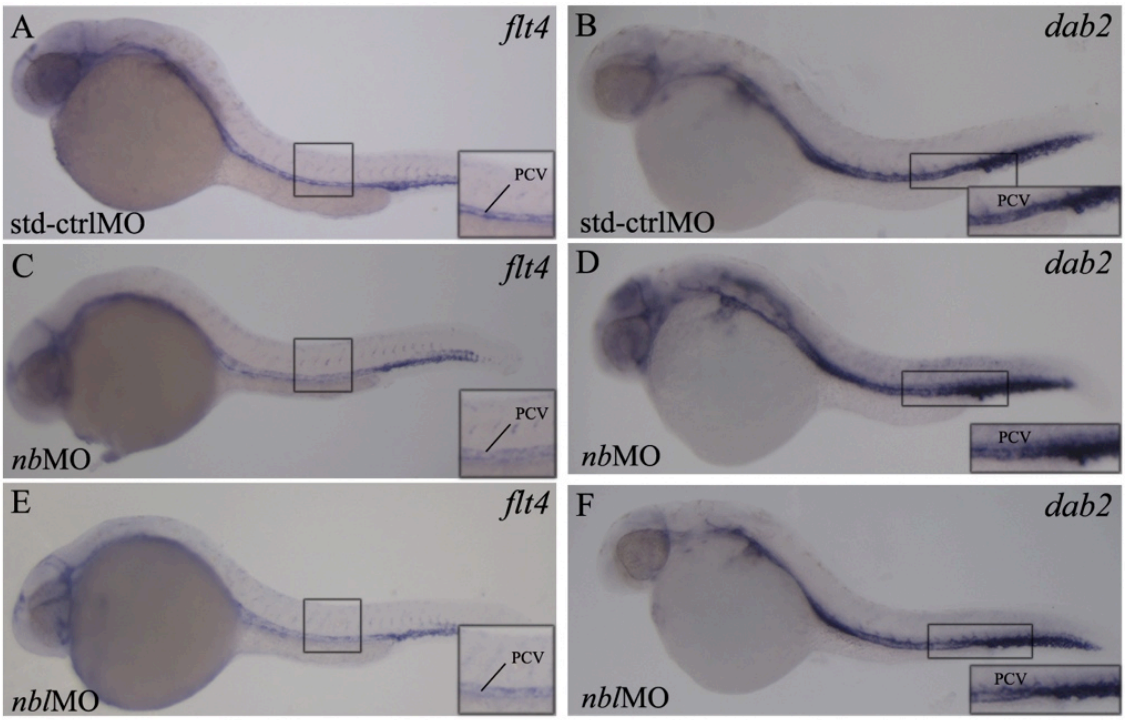

Fig.34. Expression of arterial-venous identity markers (II): flt4 (A, C, E) and dab2 (B, D, F). WISH on embryos at 29 hpf microinjected with std-ctrlMO (A, B), nbMO (C, D) and nblMO (E, F). In the insets, higher magnification of the boxed areas. A mild reduction of flt4 hybridization signal in the venous vessels was detected in morphants (C, E). All the embryos are shown with the head on the left. DA, Dorsal Aorta; PCV, posterior Cardinal Vein.

- *nr2f2*

nr2f2 encodes for the transcriptional factor Nr2f2 (nuclear receptor subfamily 2, group F, member 2) also known as COUP-TFII, which plays a critical role in controlling the development of a number of tissues and organs including heart, venous blood vessels, muscles and limbs (Pereira *et al*., 1999; Lee *et al*., 2004). In embryos at 29 hpf the transcript is detectable in some specific area of CNS, eyes, PCV and CV plexus (probe kindly provided by R. Wilkinson).

Morphants microinjected with *nb*MO (n=35) and with *nbl*MO (n=21) didn't show any alterations of the hybridization signal if compared with control embryos (n=41; fig.35A, C, E).

- *sox18*

The gene *sox18* encodes for the transcriptional factor Sox18 (SRY-related HMG-box 18) involved in the regulation of embryonic development and in the determination of the cell fate. In detail this protein plays a role in blood vessel and lymphatic vessels development (Garcìa-Ramirez *et al*., 2005; François *et al*., 2008). At 29 hpf the transcript is expressed in all vascular system (Cermenati *et al*.,2008).

In *numb* and *numblike* morphants (n=67 and n=56 respectively) hybridization signal resulted considerably reduced (33% and 78% of embryos; fig.35D, F) in both arterial and venous vessels, if compared with embryos microinjected with std-ctrlMO (n=49; 92% of embryos with unaffected phenotypes; fig.35B).

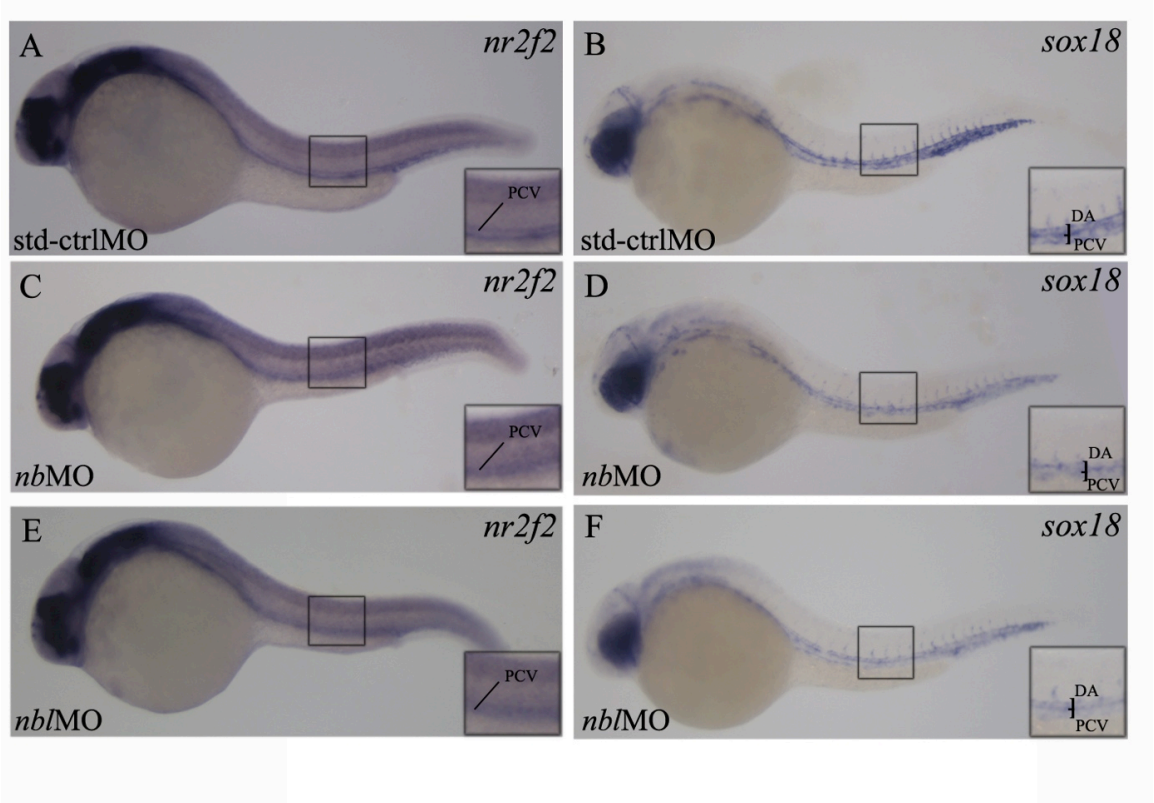

Fig.35. Expression of arterial-venous identity markers (III): *nr2f2* (A, C, E) and *sox18* (B, D, F). WISH on embryos at 29 hpf microinjected with std-ctrlMO (A, B), *nb*MO (C, D) and *nbl*MO (E, F). In the insets, higher magnification of the boxed areas. A strong reduction of *sox18* hybridization signal was detected in morphants (D, F). All the embryos are shown with the head on the left. DA, Dorsal Aorta; PCV, posterior Cardinal Vein.

As observed in previous experiments, alteration in embryos microinjected with *nbl*MO was, as a rule, stronger than in *numb* morphants both in percentage of embryos displaying the variation and in intensity of signal modification.

- **Expression of vascular and myogenic markers**

To demonstrate that the observed alterations of arterial-venous identity markers in *nb* and *nbl* morphants were not due to a drastic modification of the cardiovascular system or to a developmental delay it has been evaluated the expression of a vascular pan-endothelial marker and of a myogenic marker.

- *cdh5*

The vascular marker *cdh5* encodes for the protein Cdh5 also known as VE-cadherin, a junctional protein exclusively expressed in endothelial cells (Dejana, 2004). At 29 hpf *cdh5* is detectable via WISH in all embryonic vessels, both arterial that venous (Larson *et al*., 2004). Comparing morphants and control embryos it was not observed drastic a lteration of the expression pattern of *ve-cadherin* (fig.36A, C, E).

- *myoD*

The gene *myoD* encodes for MyoD, a transcription factor belonging to the protein family of myogenic regulatory factors (MRFs), which display a key role in regulating muscle differentiation. Moreover MyoD is one of the earliest markers of myogenic commitment (Emerson, 1993; Weintraub, 1993; Olson and Klein, 1998). *myoD* is expressed in all somites highlighting the number and consequently the developmental stage of embryo (Weinberg *et al*., 1996). WISH to detect *myoD* expression was conducted on embryos at 24hpf. Morphants microinjected with *nb*MO and with *nbl*MO was not affected by developmental delay, displaying the same number of somites if compared to controls (fig.36B, D, F). Moreover they didn't show any alteration of somites shape, further evidence that morphants body plan was correctly developed (fig.36B, D, F).

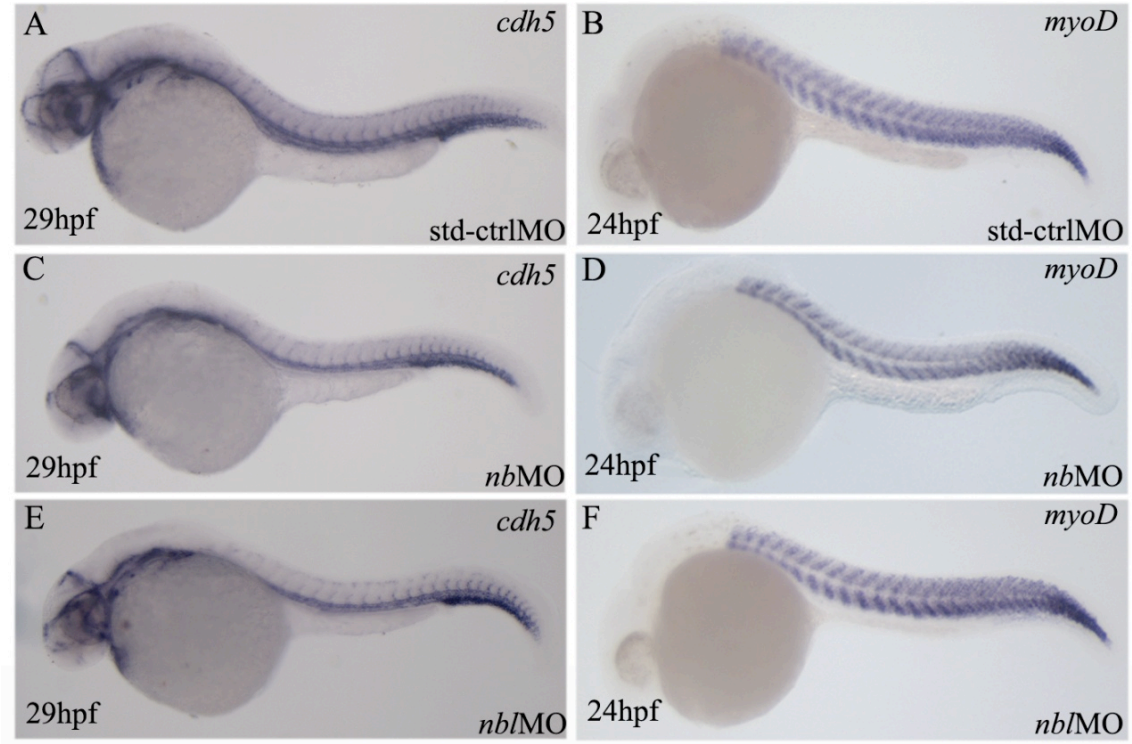

Fig.36. Expression of a vascular marker, *cdh5* (A, C, E), and a myogenic marker, *myoD* (B, D, F). WISH on embryos at 29 hpf, for the vascular marker, and 24 hpf, for the myogenic marker. The analysed embryos were microinjected with std-ctrlMO (A, B), *nb*MO (C, D) and *nbl*MO (E, F). Both the examined markers were basically unaltered, comparing control embryos and morphants. All the embryos are shown with the head on the left.

Double knockdown assays

To test the hypothesis that *numb* and *numblike* may play redundant roles in vascular development double knockdown assays have been conducted, simultaneously microinjecting both *nb*MO and *nbl*MO at low doses.

Low doses of morpholinos (0.65 rmol/embryo of *nb*MO and 0.15 rmol/embryo of *nbl*MO) injected separately (fig.37) caused morphologic alterations of the cardiovascular system at a lower rate if compared with embryos microinjected with higher doses (fig.37). In particular microinjection of low doses of *nb*MO caused the 21% of phenotypes (n=151) and microinjection of low doses of *nbl*MO caused the 26% of phenotypes (n=141). When low doses were coinjected in the same embryos, 63% (n=91) of the double morphants exhibited the characteristic approach of the two main axial vessels of the trunk and the typical reduction in dorsoventral size of CV plexus (fig.37).

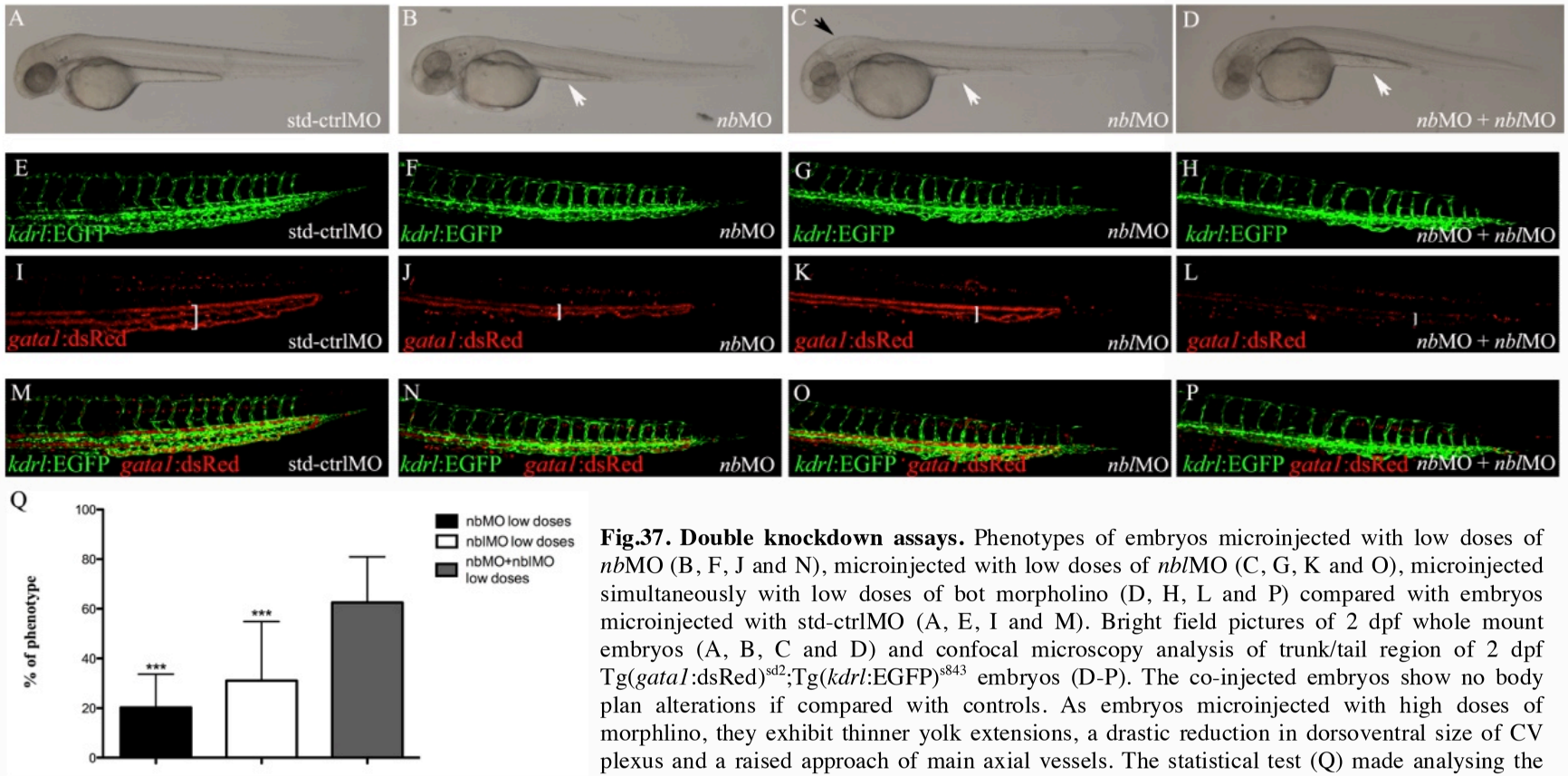

Fig.37. Double knockdown assays. Phenotypes of embryos microinjected with low doses of *nb*MO (B, F, J and N), microinjected with low doses of *nbl*MO (C, G, K and O), microinjected simultaneously with low doses of bot morpholino (D, H, L and P) compared with embryos microinjected with std-ctrlMO (A, E, I and M). Bright field pictures of 2 dpf whole mount embryos (A, B, C and D) and confocal microscopy analysis of trunk/tail region of 2 dpf Tg(*gata1*:dsRed)^{sd2};Tg(*kdrl*:EGFP)^{s843} embryos (D-P). The co-injected embryos show no body plan alterations if compared with controls. As embryos microinjected with high doses of morphlino, they exhibit thinner yolk extensions, a drastic reduction in dorsoventral size of CV plexus and a raised approach of main axial vessels. The statistical test (Q) made analysing the rate of phenotypes in the different groups indicate that the co-injection cause a noteworthy increase of vascular alteration. All the embryos are shown with the head on the left. White arrow, yolk extension; black arrow, cerebral oedema; . *** $p<0.001$ vs *nb*MO+*nbl*MO low doses.

Discussion

During Vertebrate embryogenesis one of the first apparatus to be formed is the cardio-vascular system. The cell lineages, which give rise to this system, originate from common mesodermal progenitors that subsequently differentiate in endothelial cells (Risau and Flamme, 1995; Vogeli *et al*., 2006), haematopoietic cells (Song *et al*., 2004), cardiomyocytes and endocardial cells (Lee *et al*., 1994).

Blood vessels network develops through two consecutive processes, vasculogenesis and angiogenesis (Risau, 1997; Roman and Weinstein, 2000). In the course of vasculogenesis angioblasts, the endothelial cells predecessors, aggregates to form *de novo* the primitive vascular plexus (Risau and Flamme, 1995). Afterwards, through sprouting, migration of endothelial cells and remodelling of pre-existing vessels, angiogenesis leads to the formation of a complex network of arteries and veins with different calibre. These processes are finely regulated by many angiogenic pathways and often linked to dissociation and formation of endothelial junctions (Risau, 1997; Roman and Weinstein, 2000).

The formation of a correct cardio-circulatory system has a crucial role during embryo development, cause to the essential functions of this apparatus. Sure enough blood vessels carry oxygen to tissues and take away catabolites and waste products. Moreover, vessels network serve as a way for transport of hormones, allowing communication between distant regions of the body.

In this work we focalized our attention on two processes, which play a crucial role during vascular development, the correct assembly of endothelial junctions and the acquisition of the arterial-venous identity of endothelial cells.

* * *

Cell-cell adhesion is critical for the development and maintenance of multicellular organisms. In the blood vessels the intactness of cell-cell adhesion is essential for a functional vascular system. The endothelial cells are one of the main cellular constituents of blood vessels, and one of their most important functions is to separate blood from underlying tissues (Stevens *et al*., 2000). Endothelial cells have complex junctional structures that are formed by transmembrane adhesive proteins that bind, with their cytoplasmic domain, to intracellular partners anchoring them to cytoskeletal filaments (Dejana, 2004). The correct link between these proteins and the cytoskeleton

is important for the junction stability and for the dynamic regulation of junction opening and closure (Schnittler, 1998; Dejana, 2004). A crucial concept is that cell–cell junctions are not only sites of attachment between endothelial cells, but they can also function as signalling structures that communicate cell position, limit growth and apoptosis, and regulate vascular homeostasis (Dejana, 2004). Therefore, any change in junctional organisation might have complex consequences, which could compromise the interaction between endothelium and blood elements or modify the normal architecture of the vessels wall (Dejana, 2004). The stability of many adhesion junctions is related with tyrosine phosphorylation level of the adhesion molecules and their associated components; usually high levels of phosphorylation promote the junction disassembly (Daniel and Reynolds, 1997). At adherens junction the adhesion between vascular endothelial cells is mediated by the transmembrane protein VE-cadherin, which through its extracellular domain physically interacts with Ve-ptp (Nawroth *et al*., 2002). Murine Ve-ptp is the first known receptor-type tyrosine phosphatase that is preferential expressed in endothelial cells (Fachinger *et al*., 1999; Bäumer *et al*., 2006). The analysis of mutant and null-mice phenotypes suggested that the deletion of m*Ve-ptp* causes severe cardiovascular defects and embryonic lethality from E10 stage for angiogenic and remodelling defects (Bäumer *et al*., 2006; Dominguez *et al*., 2007). In a previous work performed in our laboratory it was identified an homolog of mVe-ptp also in zebrafish. Through loss-of-function experiments it has been investigate the role of zVe-ptp, microinjecting a specific morpholino, *ve-ptp*MO; the microinjected embryos displayed *in vivo* cephalic haemorrhages and clots in the CV plexus and subsequent analysis of semi-thin plastic sections confirmed the described phenotypes. This characterisation strongly suggested an involvement of zVe-ptp in the maintenance of the cardiovascular system intactness and functionality. It has been supposed that leaks in the vessels wall could be related to a loss of adhesion at the level of the endothelial junctions, caused by an alteration of protein tyrosine phosphorylation level of adhesive molecules. Previous work had demonstrated that association between Ve-ptp and VE-cadherin regulate the phosphorylation level of the last one and that it is accompanied by the enhancement of the adhesive function of vascular cadherin itself (Nawroth *et al*., 2002). These data strongly suggest that Ve-ptp might influence VE-cadherin activity and, therefore, might play a crucial role in endothelial adherens junction stability. In

order to validate this hypothesis thorough ultrastructural analyses and micro-angiography assays were carried out.

With the aim of investigating the ultrastructure of blood vessels in trunk/tail region of morphants, we analyzed thin (about 80 nm thick) plastic sections of these anatomical districts by means of transmission electron microscopy (TEM). This analysis revealed a drastic reduction in number of adhesive structure and a generalized disorganization of endothelial AJs. Indeed only 29% of samples showed electron-dense structures located on the boundaries between ECs. Nevertheless, these structure was never organized as properly formed AJs, strongly suggesting that formation of these junctions has been severely affected, although not always prevented (71% of samples). This datum seems to indicate that the expression of adhesive proteins was not damaged, although might be an incorrect interaction between them.

The most striking feature of ECs in *ve-ptp* morphants at 2 dpf, in contrast to controls ECs at the same stage, is the presence of digitiform protrusions, referred to as *filopodia*, detected in 28% of affected EC-EC boundaries. These plasma-membrane extensions are transitional structures essential to initiate a cell-cell contact. When the cadherins of the neighbor cells establish stable bonds, the protrusions retire, AJs mature and the cell contact appears as a closed zipper (Vasioukhin *et al*., 2000; Brevier *et al*., 2008; Miyoshi and Takai, 2008). We speculate that endothelial AJs in morphants presented an immature structure in which VE-cadherins could be unable to contact each other in order to form the correct and mature adhesion complex, because of an altered phosphorylation level of junction members.

As previously described, vascular phenotypes caused by microinjection of *ve-ptp*MO seem to be related to loss of continuity between EC, which may alter permeability of endothelium.

In order to further investigate these defects in morphants we performed micro-angiography assays. In zebrafish this technique is usually used to visualise the entire vascular tree *in vivo* injecting fluorescent beads or fluorescent dye into the blood flow (Weinstein *et al*., 1995). In a recent work an alexafluor 555-labeled BSA was injected into the zebrafish blood flow at 2 dpf with the purpose to evaluate vessels permeability (Liu *et al*., 2007). By microangiography experiments, conducted on *ve-ptp*MO microinjected embryos, it was detected an increased extravasation of the dye out of the

CV plexus and of the DLAVs with respect to controls (80% vs 38% extravasation, respectively), confirming *in vivo* an increased vascular permeability due to the functional knockdown of *ve-ptp*. It is interesting to note that dye extravasation phenomena were noticed in body region characterized by angiogenesis and high rate of vascular remodelling, as previously remarked also for *in vivo* phenotypes. This observation completely fit with earlier data showing that this protein play a crucial role in angiogenesis (Bäumer *et al*., 2006; Dominguez *et al*., 2007).

In conclusion the obtained results confirm that zVe-ptp is involved in the zebrafish cardiovascular development. In particular it seems to play a key role in the modulation of vascular permeability and/or functionality and in the maturation and stability of endothelial AJs.

* * *

Arteries and veins are structurally different: the morphologic characteristics of their walls and the expression of specific receptors/ligands by their endothelium are the distinctive features that highlight the diversity between these vessels. For a long time experimental data demonstrate that arterial-venous identity acquisition was related to the direction of blood flow (Clark, 1918; Girard, 1973; Gonzales-Crussi, 1971). However, recent studies indicates that the identity of the endothelial cells that line arteries and veins is determined in the developing embryo, before circulation begins (Wang *et al*., 1998). The use of zebrafish as model system led to the identification of several signalling pathways that are responsible for arterial and venous differentiation of endothelial cells and demonstrated definitively that endothelial cell-fate decision is a critical step for normal blood vessels formation (Lawson and Weinstein, 2002).

Two early signalling pathways act determining arterial or venous specification of endothelial cells, SHH and Notch pathways (Smithers *et al*., 2000; Lawson *et al*., 2001; Villa *et al*., 2001). *Shh* is expressed in the notochord and induces the expression of *vegf* in the mesodermal tissues lying laterally (Lawson *et al*., 2002). The consequent activation of VEGF/VEGFR2 pathway determines the expression of *notch* in angioblasts positioned dorsally and the resulting expression of arterial-identity markers. Contrariwise the non-activation of Notch pathway in angioblasts located more ventrally allows the expression of venous-identity markers (Odenthal *et al*., 1996; Lawson *et al*.,

2002; Lawson and Weinstein, 2002).

Previous studies conducted on *D. melanogaster* and on mice showed that Notch signalling pathway may be regulated by Numb and Numblike, which interact directly with the protein Notch, recruiting Itch and leading to polyubiquitination and degradation of the NICD (McGill and McGlade, 2003; McGill *et al.,* 2009). Furthermore Numb may also control the intracellular trafficking of Notch, causing endocytosis and sequestration of full-length Notch or of the NICD. Therefore expression of Numb and Numblike produces the suppression of Notch function and may be involved in Notch pathway regulation also in vascular network formation (Knoblich, 2008; Gulino *et al*., 2010).

Numb and *Numblike* function in vascular development has been first analyzed in mice by characterization of mutant mice. *Numb*$^{-/-}$ mutant mice died before E11.5 stage because of defects in angiogenesis remodelling events of cranial capillaries and of intersomitic vessels (Zilian *et al*., 2001). Inversely *Numblike*$^{-/-}$ mutant mice didn't show any defect, nor embryonically nor in adult organisms (Petersen *et al*., 2002). All these data taken together suggest that m*Numb* play a crucial role in vascular development, especially during angiogenesis, while m*Numblike* hasn't any important function during the development of vascular system in mice.

In order to investigate the role of z*numb* and of z*numblike* during vascular development loss-of-function experiments have been performed, microinjecting two specific morpholinos, *nb*MO (1.3 pmol/embryo) and *nbl*MO (0.3 pmol/embryo), designed to block the maturation of transcripts and therefore the translation of Numb and Numblike in zebrafish. Interestingly both the knockdown of *numb* and of *numbl* resulted in an evident alteration of cardiovascular system, consisting in the approach of the main axial vessels in trunk and a reduction in size of CV plexus in tail. In particular *numb* morphants observed *in vivo* at 2 dpf showed the 28% of phenotypes while *numblike* morphants, at the same developmental stage, exhibited a higher ratio of phenotypes, 64% of affected embryos. Consecutive morphological investigation of plastic sections conducted on trunk and tail region confirmed the defects detected *in vivo*; moreover a statistical analysis of distance DA/PCV and DA/most ventral vessel of CV highlighted that the approach due to microinjection of *nbl*MO was stronger than that due to microinjection of *nb*MO; respectively 80% VS 50% of reduction degree in the trunk and

90% VS 30% in the tail. Intriguingly all these data seemed to suggest not only that both Numb and Numblike might be involved in zebrafish vascular development, contrary to what happens in mice (Petersen *et al*., 2002), but also that Numblike could play a role more important than that played by Numb.

Due to the interaction described from Numb/Numblike and Notch and their ability to antagonize it functions, the knockdown of the genes encoding for these two proteins could turns up the activation level of Notch and of its pathway. It's important to note that this may be possible only in those anatomical districts where *notch* is already expressed. Sure enough knockdown of z*numb* and z*numblike* didn't cause ectopic expression of *notch*; it exclusively stimulated Notch activation where it's physiologically expressed. Notch signalling pathway is crucial for vascular development and for the determination of arterial and venous identity of endothelial cells (Xue *et al*., 1999; Krebs *et al*., 2000; Thurston and Yancopoulos, 2001; Raya *et al*., 2003; Krebs *et al*., 2004). A common consequence of the incorrect identity acquisition of endothelial cells, related to an alteration of this pathway, is the non-physiological fusion of arteries and veins, called shunts (Lawson *et al*., 2001; Duarte *et al*., 2004; Krebs *et al*., 2004; You *et al*., 2005). So, we speculate that the observed phenotypes may be a milder version of shunts described in previous studies; we also hypothesize that in our morphants vessels move toward without completely fusing together, because of the alteration of Notch pathway.

With the aim of corroborating the idea that detected phenotypes were related to a wrong acquisition of arterial-venous identity, was carried out a thorough analysis of the expression pattern of specific vascular markers. Markers of Notch signalling pathway, *notch3* and *dll4* were considered first. These markers are specifically expressed in the developing vascular system, and encodes respectively for a Notch receptor isoform and a Notch ligand. In morphants the expression of *notch3* was increased, while the expression of *dll4* was unaltered. Previous works assessed and confirmed the presence of a positive feedback loop regulating *notch* expression (Cagan and Ready, 1989; Artavanis-Tsakonas *et al*. 1999, Del Monte *et al*., 2007). This regulating process might be responsible of the described increase of *notch* expression level, almost certainly caused to an over-activation of the protein Notch.

In a very short time we plan to validate these data using embryos of a Notch-inducible

transgenic line and performing rescue assays both microinjecting specific orthologue mRNA and treating morphants with specific substances which inactivate Notch pathway (DAPT; Geling *et al*., 2002).

Successively it has been considered markers of arterial-venous identity. As previously described, some studies indicates that angioblasts may be directed towards an arterial or venous destiny before blood vessels formation and before the onset of circulation (Lawson and Weinstein, 2002). Moreover previous studies about *notch* deletion and constitutive expression, performed in zebrafish *mib* mutants and in embryos in which NICD expression is ubiquitous, showed that *notch* expression decrease is followed by reduction of arterial specific markers (as *efnb2*) and increased of venous specific markers (as *flt4*); conversely intensification of *notch* expression results in diminution of venous markers (as *flt4*) and improve of arterial markers (as *grdl*; Lawson *et al*., 2001). In our experiments *numb* and *numblike* morphants showed an evident increasing in arterial markers expression (*efnb2*, *kdrl* and *hey2*) and a drastic reduction of venous markers expression (*ephB4* and *flt4*), strongly suggesting that the observed vascular defects were linked to over-activation of Notch. Interestingly other markers which lay upstream of *notch* (as *nr2f2*) or which are not involved in Notch pathway (as *dab2*) were unaltered in morphants, proving that alteration of arterial-venous identity was exclusively related to specific modification of Notch signalling pathway in developing vascular system.

In future we purpose to carry out real-time quantitative RT-PCR, with the aim to confirm and quantify the increase/decrease of the analysed vascular markers.

The subsequent analysis of a pan-endothelial vascular marker, *cdh5*, and a myogenic marker, *myoD*, excluded that the observed defects of vascular markers expression might be caused by severe alteration of body plan, to defects of vascular network structure or to a significant developmental delay. Sure enough both the vascular tree morphology and the number and the shape of somites of morphants were comparable with those of controls.

Mammalian Numb and Numblike proteins are believed to have overlapping functions, although distinct localization in the cell and specific expression pattern (Gulino *et al*., 2010). In fact Numblike is symmetrically distributed while, in contrast, Numb is asymmetrically localized to the apical membrane of dividing cells (Zhong *et al*., 1996).

Nevertheless *in vivo* studies revealed a redundant function for Numb and Numbl in mice (Petersen *et al*., 2002). Very recent studies confirmed it also in zebrafish (Bresciani *et al*., 2010). Numb and Numblike act as regulator proteins in many different developmental processes but their redundancy is not detectable in all of them. For example *numb* and *numblike* seem to play redundant role in haematopoiesis, both in mice (*in vitro* approach) and in zebrafish, and in neurogenesis (Petersen *et* al., 2002; Cheng *et al*., 2008; Bresciani *et al*., 2010). Conversely during mice vascular development Numb and Numblike play different roles, in particular m*Numb* plays a critical role in angiogenesis, while m*Numblike* appear dispensable (Zilian *et al*., 2001; Petersen *et al*., 2002).

The data showed in this work, strongly suggest that, conversely to what happen in mice, both z*numb* and z*numblike* play a critical function during arterial-venous differentiation of endothelial cells, although with different degrees. It raise a query about a potential interaction between zNumb and zNumblike. In order to assess this possibility, double knockdown assays were carried out, first injecting separately low doses (0.65 pmol/embryo of *nb*MO and 0.15 pmol/embryo of *nbl*MO) of the morpholinos and then co-injecting simultaneously both morpholinos together. As a result microinjecting separately the low doses of morpholinos, the ratio of phenotypes were lower than those obtained microinjecting separately the high doses of morpholinos (21% VS 28% for *numb* morphants and 26% VS 64% for *numblike* morphants). Intriguingly co-injecting both morpholinos together the ratio of phenotypes improve, reaching 63% of embryos exhibiting the described phenotypes. These data strongly assert that z*numb* and z*numblike* play a redundant, and probably synergic, role in vascular development.

In Vertebrates lymphatic system arise from pre-existing vessels. In zebrafish venous endothelial cells migrate from PCV to form venous InterSomitic Vessels (vISV) and Lymphatic Precursors Cells (LPCs). Subsequently LPCs first move along arterial InterSomitic Vessels (aISV) and then along myoseptum, towards the space between DA and PCV, where give rise to the Thoracic Duct (TD; Yaniv *et al*., 2006). Cause to the reduction of the space where the TD will develop and to the decrease of expression of venous markers, we speculated about a possible alteration of lymphangiogenesis due to knockdown of z*numb* and z*numblike*. In order to confirm this hypothesis it was assessed *sox18* expression. Recent works gave to this transcription factor a crucial role in

lymphatic development in mice, identifying it as an upstream regulator of *prox1*, which play a crucial for lymphatic development (Francois *et al*., 2008). Our experiments pointed out a drastic decrease of *sox18* expression level, suggesting a role for *numb* and *numblike* in lymphangiogenesis, and laying the foundation for a new and gripping research topic.

In conclusion these data prove that z*numb* and z*numblike* act in concert controlling the acquisition of arterial-venous identity and influencing the signalling pathway mediated by Notch.

Appendix

EMBRYONIC DEVELOPMENT OF ZEBRAFISH

The zebrafish eggs are small (400-500 μm), with a very large yolk mass. After the fertilization, several cytoplasmic rearrangements occur, and these events lead to the segregation of the cytoplasm to the animal pole, and the yolk mass to the vegetal pole. The segmentation (cleavage) is meroblastic and relative to the cytoplasm of the animal pole only. In this way, the formation of the "blastula" is observed. The blastula starts the gastrulation period, which is characterized by different cellular movements. Kimmel *et al*., (1995), distinguished the following developmental stages: zygote period (0-$^{3}/_{4}$ hpf), cleavage period ($^{3}/_{4}$-$2^{1}/_{4}$ hpf), blastula period ($2^{1}/_{4}$-$5^{1}/_{4}$ hpf), gastrula period ($5^{1}/_{4}$-10 hpf), segmentation period (10-24 hpf), pharingula period (24-48 hpf) and hatching period (48-72 hpf).

Zygote Period

The newly fertilized egg is in the zygote period until the first cleavage occurs, about 40 minutes after fertilization. The chorion swells and lifts away from the newly fertilized egg. Fertilization also activates cytoplasmic movements, easily evident within about 10 minutes. Nonyolky cytoplasm begins to stream toward the animal pole, segregating the blastodisc from the clearer yolk granule-rich vegetal cytoplasm. This segregation continues during early cleavage stages.

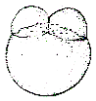

Cleavage Period

After the first cleavage the blastomeres divide at about 15-minute intervals. The cytoplasmic divisions are meroblastic; they only incompletely undercut the blastodisc, and the blastomeres, or a specific subset of them according to the stage, remain interconnected by cytoplasmic bridges. The six cleavages that comprise this period frequently occur at regular orientations and are synchronous. The cleavage period ends at 64-cell stage (2 hpf).

Blastula Period

We use the term blastula to refer to the period when the blastodisc begins to look ball-like, at the 128-cell stage, or eight zygotic cell cycle, and until the time of onset of gastrulation, about cycle 14. Important processes occur during this blastula period; the embryo enters midblastula transition (MBT), the yolk syncytial layer (YSL) forms, and epiboly begins. Epiboly continues during the gastrulation period. Three different phases can be observed.

-Early-blastula: the marginal blastomeres lie against the yolk cell and remain cytoplasmatically connected to it throughout cleavage. Beginning during cycle 10, the marginal cells undergo a collapse, releasing their cytoplasm and nuclei together into the immediately adjoining cytoplasm of the yolk cell and forming the Yolk Syncytial Layer (YSL). After the YSL forms, the enveloping layer cells (EVL) that were in the second blastodisc tier, now lie at the marginal position and they are nonsyncytial.
-Mid-blastula: the YSL nuclei continue to undergo mitotic divisions in the midblastula, but the nuclear divisions are unaccompanied by cytoplasmic ones, and the yolk remains uncleaved and syncytial. After about three cycles, and coinciding with the beginning of epiboly, the YSL divisions abruptly cease. The YSL nuclei now begin to enlarge, possibly meaning that they are actively transcribing RNA. The YSL, an organ unique to teleosts, may be extraembryonic, making no direct contribution to the body of the embryo. At first the YSL has the form of a narrow ring around the blastodisc edge, but soon it spreads underneath the blastodisc, forming a complete "internal" syncytium (I-YSL), that persists throughout embryogenesis. In this position, the I-YSL might be presumed to be playing a nutritive role. Another portion of it, the E-YSL, is transiently "external" to the blastodisc edge, and appears to be a major motor for epiboly.
-Late-blastula: epiboly beginning in the late blastula is the thinning and spreading of both the YSL and the blastodisc over the yolk cell. During the early stages of this morphogenetic movement the blastodisc thins considerably, changing from a high-piled cell mound to a cup-shaped cell multiplayer of nearly uniform thickness. This is accomplished by the streaming outward, toward the surface, of the deepest blastomeres. As they move, they mix fairly indiscriminately among more superficial cells along their way, except for the EVL and the marginal blastomeres. These nonmixing marginal blastomeres will give rise to the mesoderm, and suggest the existence of a pattern established during early development. At 30% epiboly stage, the proper blastoderm begins to develop: it is uniform and formed by the EVL monolayer and a deep cells multilayer (Deep Enveloping Layer, DEL).

Gastrula Period

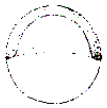

The beginning of ınvolutıon defines the onset of gastrulation, and, so far as we have been able to tell, this occurs at 50%-epiboly. As a consequence, within minutes of reaching 50%-epiboly a thickened marginal region termed the "germ ring" appears, nearly simultaneously all around the blastoderm rim. Convergence movements then, nearly as rapidly, produce a local accumulation of cells at one position along the germ ring, the so-called embryonic shield. During these events, epiboly temporarily arrests,

but after the shield forms, epiboly continues; the margin of the blastoderm advances around the yolk cell to cover it completely. The advance occurs at a nearly constant rate, over an additional 15% of the yolk cell each hour, and providing a useful staging index during most of gastrulation. Just as there was no blastocoele during the blastula period, there is no archenteron in the gastrula. Neither is there a blastopore; DEL cells involute at the blastoderm margin, which thus plays the role of the blastopore. Involution produces the germ ring by folding the blastoderm back upon itself. Hence, within the germ ring there are two germ layers: the upper, the epiblast, continues to feed cells into the lower, the hypoblast, throughout gastrulation. Between the two layers a fissure, termed "Brachet's cleft" is observed. Cells in the two layers are streaming in different directions. Except for the dorsal region, the epiblast cells generally stream toward the margin, and those reaching the margin move inward to enter the hypoblast. Then, as hypoblast cells, they stream away from the margin. The cells remaining in the epiblast when gastrulation ends correspond to the definitive ectoderm and will give rise to such tissues as epidermis, the central nervous system, neural crest, and sensory placodes. The hypoblast gives rise to derivatives classically ascribed to both the mesoderm and endoderm. At tail-bud stage (10 hpf), cell specifications processes are ending while cell differentiation mechanisms are turned on.

Segmentation Period

A wonderful variety of morphogenetic movements now occur, the somites develop, the rudiments of the primary organs become visible, the tail bud becomes more prominent and the embryo elongates. The AP and DV axes are unambiguous. The first cells differentiate morphologically, and the first body movements appear. Somites develop sequentially in the trunk and tail, and provide the most useful staging index. Anterior somites develop first and posterior ones last. Pronephric kidneys appear bilaterally deep to the third somite pair. The notochord differentiates, also in an AP sequence. Some of its cells vacuolate and swell to become the structural elements of this organ, and others later form a notochord sheath, an epithelial monolayer that surrounds the organ. Endoderm develops on only the dorsal side of the embryo, beneath the axial and paraxial mesoderm. The epiblast, now exclusively ectodermal, undergoes extensive morphogenesis during the segmentation period. As gastrulation ends, the primordium of the central nervous system, the neural plate, is already fairly well delineated, because of its prominent thickness. The anterior region where the brain will form is particularly thick. Formation of the neural tube then occurs by a process known as "secondary neurulation". Secondary neurulation contrasts with "primary" neurulation, the version in vertebrates where a hollow tube forms from the neural plate by an uplifting and meeting

together of neural folds. In teleosts the lumen of the neural tube, the neurocoele, forms by a late process of cavitation.

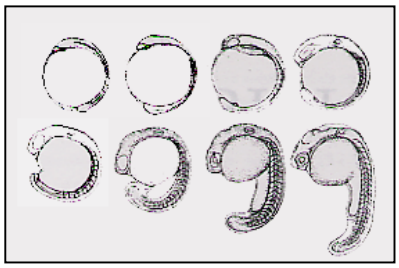

An intermediate and transient condensed primordium with no lumen, the neural keel, forms first. Because the times of neurulation and segmentation overlap so extensively the zebrafish does not have a distinct "neurula period" of development, such as occurs largely before segmentation in amphibian embryos.

Pharyngula Period

The pharyngula period (24-48 hpf) begins with the formation of the last somites (30/34 somites). At this time, the notochord is completely formed, and the brain is constituted by three lobes, which develop in an AP direction: forebrain, midbrain and hindbrain.

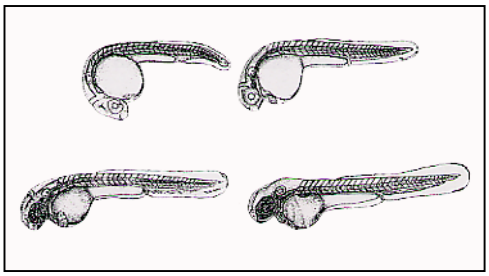

Hatching Period

During the last period, termed "hatching" (48-72 hpf), individuals within a single developing clutch hatch sporadically during the whole third day of development (at standard temperature), and occasionally later. At this time, we call these embryos "larvae"; morphogenesis of many organ rudiments is completing, and the embryo continues to grow at about the same rate.

References

- Adams R.H., Wilkinson G.A., Weiss C., Diella F., Gale N.W., Deutsch U., Risau W., Klein R. (1999). Roles of ephrinB ligands and EphB receptors in cardiovascular development: demarcation of arterial/venous domains, vascular morphogenesis, and sprouting angiogenesis. *Genes Dev*, **13**: 295-306.

- Amatruda J.F. and Zon L.I. (1999). Dissecting hematopoiesis and disease using the zebrafish. *Dev Biol*, **216**: 1-15.

- Androutsellis-Theotokis A., Leker R.R., Soldner F., Hoeppner D.J., Ravin R., Poser S.W., Rueger M.A., Bae S.K., Kittappa R., McKay R.D. (2006). Notch signalling regulates stem cell numbers in vitro and in vivo. *Nature*, **442**: 823-826.

- Argenton F., Giudici S., Deflorian G., Cimbro S., Cotelli F., Beltrame M. (2004) Ectopic expression and knockdown of a zebrafish sox21 reveal its role as a transcriptional repressor in early development. *Mech Dev* **121**, 131-142

- Artavanis-Tsakonas S., Rand M.D., Lake R.J. (1999). Notch signaling: cell fate control and signal integration in development. *Science*, **284**: 770-776.

- Bäumer S., Keller L., Holtmann A., Funke R., August B., Gamp A., Wolburg H., Wolburg-Buchholz K., Deutsch U. and Vestweber D. (2006). Vascular endothelial cell-specific phosphotyrosine phosphatase (VE-PTP) activity is required for blood vessel development. *Blood*, **107**: 4754-4762.

- Brady-Kalnay S.M. and Tonks N.K. (1995). Protein tyrosine phosphatases as adhesion receptors. *Curr Opin Cell Biol*, **7**: 650-657.

- Bray S. (1998). Notch signalling in Drosophila: three ways to use a pathway. *Semin Cell Dev Biol*, **9**: 591-597.

- Bresciani E., Confalonieri S., Cermenati S., Cimbro S., Foglia E., Beltrame M., Di Fiore P.P., Cotelli F. (2010). Zebrafish numb and numblike are involved in primitive erythrocyte differentiation. *PLoS One*, **5**: e14296.

- Brevier J., Montero D., Svitkina T., Riveline D. (2008). The asymmetric self-assembly mechanism of adherens junctions: a cellular push-pull unit. *Phys Biol*, **5**: 016005.

- Cagan R.L., Ready D.F. (1989). Notch is required for successive cell decisions in the developing Drosophila retina. *Genes Dev*, **3**: 1099-1112.

- Carmeliet P., Mackman N., Moons L., Luther T., Gressens P., Van Vlaenderen I., Demunck H., Kasper M., Breier G., Evrard P., Müller M., Risau W., Edgington T., Collen D. (1996). Role of tissue factor in embryonic blood vessel development. *Nature*, **383**: 73-75.

- Carra S., Foglia E., Cermenati S., Bresciani E., Lora Lamia C., Dejana E., Beltrame M., Cotelli F. Ve-ptp modulates vascular integrity by promoting adherens junctions maturation. *PLoS ONE*, manuscript under revision.

- Cayouette M. and Raff M. (2002). Asymmetric segregation of Numb: a mechanism for neural specification from Drosophila to mammals. *Nat Neurosci*, **5**: 1265-1269.

- Cermenati S., Moleri S., Cimbro S., Corti P., Del Giacco L., Amodeo R., Dejana E., Koopman P., Cotelli F., Beltrame M. Sox18 and Sox7 play redundant roles in vascular development. (2008) *Blood*, **111**: 2657-2666.

- Chan J., Bayliss P.E., Wood J.M., Roberts T.M. (2002). Dissection of angiogenic signaling in zebrafish using a chemical genetic approach. *Cancer Cell*, **1**: 257-267.

- Chen J.N., Haffter P., Odenthal J., Vogelsang E., Brand M., van Eeden F.J., Furutani-Seiki M., Granato M., Hammerschmidt M., Heisenberg C.P., Jiang Y.J., Kane D.A., Kelsh R.N., Mullins M.C., Nüsslein-Volhard C. (1996). Mutations affecting the cardiovascular system and other internal organs in zebrafish. *Development*, **123**: 293-302.

- Cheng S.H., Chan P.K., Wu R.S. (2001). The use of microangiography in detecting aberrant vasculature in zebrafish embryos exposed to cadmium. *Aquat Toxicol*, **52**: 61-71.

- Cheng X., Huber T.L., Chen V.C., Gadue P., Keller G.M. (2008). Numb mediates the interaction between Wnt and Notch to modulate primitive erythropoietic specification from the hemangioblast. *Development*, **135**: 3447-3458.

- Chin M.T., Maemura K., Fukumoto S., Jain M.K., Layne M.D., Watanabe M., Hsieh C.M., Lee M.E. (2000). Cardiovascular basic helix loop helix factor 1, a novel transcriptional repressor expressed preferentially in the developing and adult cardiovascular system. *J Biol Chem*, **275**: 6381-6387.

- Choi J., Mouillesseaux K., Wang Z., Fiji H.D., Kinderman S.S., Otto G.W., Geisler R., Kwon O., Chen J.N. (2011). Aplexone targets the HMG-CoA reductase pathway and differentially regulates arteriovenous angiogenesis. *Development*, **138**: 1173-1181.

- Clark E. R. (1918). Studies on the growth of blood vessels in the tail of the frog larvae. *Am J Anat*, **23**: 37–88

- Cleaver O. and Krieg P.A. (1998). VEGF mediates angioblast migration during development of the dorsal aorta in Xenopus. *Development*, **125**: 3905-3914.

- Corada M., Mariotti M., Thurston G., Smith K., Kunkel R., Brockhaus M., Lampugnani M.G., Martin-Padura I., Stoppacciaro A., Ruco L., McDonald D.M., Ward P.A., Dejana E. (1999). Vascular endothelial-cadherin is an important determinant of microvascular integrity in vivo. *Proc Natl Acad Sci U S A*, **96**: 9815-9820.

- Crosby C.V., Fleming P.A., Argraves W.S., Corada M., Zanetta L., Dejana E., Drake C.J. (2005). VE-cadherin is not required for the formation of nascent blood vessels but acts to prevent their disassembly. *Blood*, **105**: 2771-2776.

- Daniel J.M. and Reynolds A.B. (1997). Tyrosine phosphorylation and cadherin/catenin function. *Bioessays*, **19**: 883-891.

- Dejana E. (2004). Endothelial cell-cell junctions: happy together. *Nat Rev Mol Cell Biol,* **5**: 261-270.

- Dejana E., Lampugnani M.G., Martinez-Estrada O., Bazzoni G. (2000). The molecular organization of endothelial junctions and their functional role in vascular morphogenesis and permeability. *Int. J. Dev. Biol.*, **44**: 743-748.

- Del Monte G., Grego-Bessa J., González-Rajal A., Bolós V., De La Pompa J.L. (2007). Monitoring Notch1 activity in development: evidence for a feedback regulatory loop. *Dev Dyn*, **236**: 2594-2614.

- Dho S.E., French M.B., Woods S.A., McGlade C.J. (1999). Characterization of four mammalian numb protein isoforms. Identification of cytoplasmic and membrane-associated variants of the phosphotyrosine binding domain. *J Biol Chem*, **274**: 33097-33104.

- Di Marcotullio L., Ferretti E., Greco A., De Smaele E., Po A., Sico M.A., Alimandi M., Giannini G., Maroder M., Screpanti I., Gulino A. (2006). Numb is a suppressor of Hedgehog signalling and targets Gli1 for Itch-dependent ubiquitination. *Nat Cell Biol*, **8**: 1415-1423.

- Domenga V., Fardoux P., Lacombe P., Monet M., Maciazek J., Krebs L.T., Klonjkowski B., Berrou E., Mericskay M., Li Z., Tournier-Lasserve E., Gridley T., Joutel A. (2004). Notch3 is required for arterial identity and maturation of vascular smooth muscle cells. *Genes Dev*, **18**: 2730-2735.

- Dominguez M.G., Hughes V.C., Pan L., Simmons M., Daly C., Anderson K., Noguera-Troise I., Murphy A.J., Valenzuela D.M., Davis S., Thurston G., Yancopoulos G.D., Gale N.W. (2007). Vascular endothelial tyrosine phosphatase (VE-PTP)-null mice undergo vasculogenesis but die embryonically because of defects in angiogenesis. *Proc Natl Acad Sci U S A*, **104**: 3243-3248.

- Driever W. and Fishman M.C. (1996). The zebrafish: heritable disorders in transparent embryos. *J Clin Invest*, **97**: 1788-1794.

- Duarte A., Hirashima M., Benedito R., Trindade A., Diniz P., Bekman E., Costa L., Henrique D., Rossant J. (2004). Dosage-sensitive requirement for mouse Dll4 in artery development. *Genes Dev*, **18**: 2474-2478.

- Dunwoodie S.L., Henrique D., Harrison S.M., Beddington R.S. (1997). Mouse Dll3: a novel divergent Delta gene which may complement the function of other Delta homologues during early pattern formation in the mouse embryo. *Development*, **124**: 3065-3076.

- Ekker S.C. (2000). Morphants: a new systematic vertebrate functional genomics approach. *Yeast,* **17**: 302-306.

- Ellertsdóttir E., Lenard A., Blum Y., Krudewig A., Herwig L., Affolter M., Belting H.G. (2010). Vascular morphogenesis in the zebrafish embryo. *Dev Biol*, **341**: 56-65.

- Emerson C.P. Jr. (1993). Embryonic signals for skeletal myogenesis: arriving at the beginning. *Curr Opin Cell Biol*, **5**: 1057-1064.

- Fachinger G., Deutsch U., Risau W. (1999). Functional interaction of vascular endothelial-protein-tyrosine phosphatase with the angiopoietin receptor Tie-2. *Oncogene*, **18**: 5948-5953.

- Fauman E.B., Cogswell J.P., Lovejoy B., Rocque W.J., Holmes W., Montana V.G., Piwnica-Worms H., Rink M.J., Saper M.A. (1998). Crystal structure of the catalytic domain of the human cell cycle control phosphatase, Cdc25A. *Cell*, **93**: 617-625.

- Ferrara N., Carver-Moore K., Chen H., Dowd M., Lu L., O'Shea K.S., Powell-Braxton L., Hillan K.J., Moore M.W. (1996). Heterozygous embryonic lethality induced by targeted inactivation of the VEGF gene. *Nature*, **380**: 439-442.

- Fouquet B., Weinstein B.M., Serluca F.C., Fishman M.C. (1997). Vessel patterning in the embryo of the zebrafish: guidance by notochord. *Dev Biol*, **183**: 37-48.

- François M., Caprini A., Hosking B., Orsenigo F., Wilhelm D., Browne C., Paavonen K., Karnezis T., Shayan R., Downes M., Davidson T., Tutt D., Cheah K.S., Stacker S.A., Muscat G.E., Achen M.G., Dejana E., Koopman P. (2008). Sox18 induces development of the lymphatic vasculature in mice. *Nature*, **456**: 643-647.

- García-Ramírez M., Martínez-González J., Juan-Babot J.O., Rodríguez C., Badimon L. (2005). Transcription factor SOX18 is expressed in human coronary atherosclerotic lesions and regulates DNA synthesis and vascular cell growth. *Arterioscler Thromb Vasc Biol*, **25**: 2398-2403.

- Geling A., Steiner H., Willem M., Bally-Cuif L., Haass C. (2002). A gamma-secretase inhibitor blocks Notch signaling in vivo and causes a severe neurogenic phenotype in zebrafish. *EMBO Rep* **3**: 688–694.

- Gering M., Rodaway A.R., Göttgens B., Patient R.K., Green A.R. (1998). The SCL gene specifies haemangioblast development from early mesoderm. *EMBO J*, **17**: 4029-4045.

- Girard H. (1973). Arterial pressure in the chick embryo. *Am J Physiol*, **224**: 454–460.

- Gonzales-Crussi F. (1971). Vasculogenesis in the chick embryo. An ultrastructural study. *Am J Anat*, **130**: 441–460.

- Gotsch U., Borges E., Bosse R., Böggemeyer E., Simon M., Mossmann H., Vestweber D. (1997). VE-cadherin antibody accelerates neutrophil recruitment in vivo. *J Cell Sci*, **110**: 583-588.

- Greenwald I. (1998). LIN-12/Notch signaling: lessons from worms and flies. *Genes Dev*, **12**: 1751-1762.

- Guan K.L. and Dixon J.E. (1991). Evidence for protein-tyrosine-phosphatase catalysis proceeding via a cysteine-phosphate intermediate. *J Biol Chem*, **266**: 17026-17030.

- Gulino A., Di Marcotullio L., Screpanti I. (2010). The multiple functions of Numb. *Exp Cell Res*, **316**: 900-906.

- Guo M., Jan L.Y., Jan Y.N. (1996). Control of daughter cell fates during asymmetric division: interaction of Numb and Notch. *Neuron* **17**: 27-41.

- Habeck H., Odenthal J., Walderich B., Maischein H., Schulte-Merker S. (2002). Analysis of a zebrafish VEGF receptor mutant reveals specific disruption of angiogenesis. *Curr Biol*, **12**: 1405-1412.

- Haffter P., Granato M., Brand M., Mullins M.C., Hammerschmidt M., Kane D.A., Odenthal J., van Eeden F.J., Jiang Y.J., Heisenberg C.P., Kelsh R.N., Furutani-Seiki M., Vogelsang E., Beuchle D., Schach U., Fabian C., Nüsslein-Volhard C. (1996). The identification of genes with unique and essential functions in the development of the zebrafish, Danio rerio. *Development*, **123**: 1-36.

- Hanahan D. (1997). Signaling vascular morphogenesis and maintenance. *Science*, **277**:48-50.

- Herbert S.P., Huisken J., Kim T.N., Feldman M.E., Houseman B.T., Wang R.A., Shokat K.M., Stainier D.Y. (2009). Arterial-venous segregation by selective cell sprouting: an alternative mode of blood vessel formation. *Science*, **326**: 294-298.

- Hocevar B.A., Mou F., Rennolds J.L., Morris S.M., Cooper J.A., Howe P.H. (2003). Regulation of the Wnt signaling pathway by disabled-2 (Dab2). *EMBO J*, **22**: 3084-3094.

- Holder N. and Xu Q. (1999). Microinjection of DNA, RNA, and protein into the fertilized zebrafish egg for analysis of gene function. *Methods Mol Biol*, **97**: 487-490.

- Holmes D.I. and Zachary I.C. (2008). Vascular endothelial growth factor regulates stanniocalcin-1 expression via neuropilin-1-dependent regulation of KDR and synergism with fibroblast growth factor-2. *Cell Signal*, **20**: 569-579.

- Hsiao C.D., You M.S., Guh Y.J., Ma M., Jiang Y.J., Hwang P.P. (2007). A positive regulatory loop between foxi3a and foxi3b is essential for specification and differentiation of zebrafish epidermal ionocytes. *PLoS One*, **2**: e302.

- Indraccolo S., Minuzzo S., Masiero M., Pusceddu I., Persano L., Moserle L., Reboldi A., Favaro E., Mecarozzi M., Di Mario G., Screpanti I., Ponzoni M., Doglioni C., Amadori A. (2009). Cross-talk between tumor and endothelial cells involving the Notch3-Dll4 interaction marks escape from tumor dormancy. *Cancer Res*, **69**: 1314-1323.

- Isogai S., Horiguchi M., Weinstein B.M. (2001). The vascular anatomy of the developing zebrafish: an atlas of embryonic and early larval development. *Dev Biol*, **230**: 278-301.

- Isogai S., Lawson N.D., Torrealday S., Horiguchi M., Weinstein B.M. (2003). Angiogenic network formation in the developing vertebrate trunk. *Development*, **130**: 5281-5290.

- Jen W.C., Wettstein D., Turner D., Chitnis A., Kintner C. (1997). The Notch ligand, X-Delta-2, mediates segmentation of the paraxial mesoderm in Xenopus embryos. *Development*, **124**: 1169-1178.

- Jiang J. and Hui C.C. (2008). Hedgehog signaling in development and cancer. *Dev Cell*, **15**: 801-812.

- Jiang Y.J., Brand M., Heisenberg C.P., Beuchle D., Furutani-Seiki M., Kelsh R.N., Warga R.M., Granato M., Haffter P., Hammerschmidt M., Kane D.A., Mullins M.C., Odenthal J., van Eeden F.J., Nüsslein-Volhard C. (1996). Mutations affecting neurogenesis and brain morphology in the zebrafish, Danio rerio. *Development*, **123**: 205-216.

- Jin S.W., Beis D., Mitchell T., Chen J.N., Stainier D.Y. (2005). Cellular and molecular analyses of vascular tube and lumen formation in zebrafish. *Development*, **132**: 5199-5209.

- Jin S.W., Beis D., Mitchell T., Chen J.N., Stainier D.Y. (2005). Cellular and molecular analyses of vascular tube and lumen formation in zebrafish. *Development*, **132**: 5199-5209.

- Jowett T. (1999). Transgenic zebrafish. *Methods Mol Biol*, **97**: 461-486.

- Jowett T. and Lettice L. (1994). Whole-mount in situ hybridizations on zebrafish embryos using a mixture of digoxigenin- and fluorescein-labelled probes. *Trends Genet*, **10**: 73-74.

- Karnovsky M.J. (1965). A formaldehyde-glutaraldehyde fixative of high osmolarity for use in electron microscopy. *J. Cell Biol*, **27**: 137A.

- Kataoka H., Ochi M., Enomoto K., Yamaguchi A. (2000). Cloning and embryonic expression patterns of the zebrafish Runt domain genes, runxa and runxb. *Mech Dev*, **98**: 139-143.

- Keele K.D. (1957). Movement of the Heart and Blood in Animals: An Anatomical Essay. *Med Hist*, **1**: 371–372.

- Kidd K.R. and Weinstein B.M. (2003). Fishing for novel angiogenic therapies. *Br J Pharmacol*,**140**: 585-594.

- Kidd S., Kelley M.R., Young M.W. (1986). Sequence of the notch locus of Drosophila melanogaster: relationship of the encoded protein to mammalian clotting and growth factors. *Mol Cell Biol*, **6**: 3094-3108.

- Kimmel C.B., Ballard W.W., Kimmel S.R., Ullmann B., Schilling T.F. (1995). Stages of embryonic development of the zebrafish. *Dev Dyn* **203**: 253-310

- Knoblich J.A. (2008). Mechanisms of asymmetric stem cell division. *Cell*, **132**: 583-597.

- Kole R. and Sazani P. (2001). Antisense effects in the cell nucleus: modification of splicing. *Curr Opin Mol Ther*, **3**: 229-234.

- Kozlowski D.J. and Weinberg E.S. (2000). Photoactivatable (caged) fluorescein as a cell tracer for fate mapping in the zebrafish embryo. *Methods Mol Biol*, **135**: 349-355.

- Krebs L.T., Shutter J.R., Tanigaki K., Honjo T., Stark K.L., Gridley T. (2004). Haploinsufficient lethality and formation of arteriovenous malformations in Notch pathway mutants. *Genes Dev*, **18**: 2469-2473.

- Krebs L.T., Xue Y., Norton C.R., Shutter J.R., Maguire M., Sundberg J.P., Gallahan D., Closson V., Kitajewski J., Callahan R., Smith G.H., Stark K.L., Gridley T. (2000). Notch signalling is essential for vascular morphogenesis in mice. *Genes Dev* **14**: 1343-1352.

- Krueger N.X., Streuli M., Saito H. (1990). Structural diversity and evolution of human receptor-like protein tyrosine phosphatases. *EMBO J*, **9**: 3241-3252.

- Kuramochi S., Matsuda S., Matsuda Y., Saitoh T., Ohsugi M. and Yamamoto T. (1996). Molecular cloning and characterization of Byp, a murine receptor-type tyrosine phosphatase similar to human DEP-1. *FEBS Lett*, **378**: 7-14.

- Lampugnani M.G., Resnati M., Raiteri M., Pigott R., Pisacane A., Houen G., Ruco L.P., Dejana E. (1992). A novel endothelial-specific membrane protein is a marker of cell-cell contacts. *J Cell Biol*, **118**: 1511-1522.

- Lardelli M., Dahlstrand J., Lendahl U. (1994). The novel Notch homologue mouse Notch 3 lacks specific epidermal growth factor-repeats and is expressed in proliferating neuroepithelium. *Mech Dev*, **46**: 123-136.

- Larson J.D., Wadman S.A., Chen E., Kerley L., Clark K.J., Eide M., Lippert S., Nasevicius A., Ekker S.C., Hackett P.B., Essner J.J. (2004). Expression of VE-cadherin in zebrafish embryos: a new tool to evaluate vascular development. *Dev Dyn*, **231**: 204-213.

- Lawson N.D. and Weinstein B.M. (2002). Arteries and veins: making a difference with zebrafish. *Nat Rev Genet*, **3**: 674-682.

- Lawson N.D. and Weinstein B.M. (2002a). In vivo imaging of embryonic vascular development using transgenic zebrafish. *Dev Biol*, **248**: 307-318.

- Lawson N.D., Scheer N., Pham V.N., Kim C.H., Chitnis A.B., Campos-Ortega J.A. and Weinstein B.M. (2001). Notch signaling is required for arterial-venous differentiation during embryonic vascular development. *Development*, **128**: 3675-3683.

- Lawson N.D., Vogel A.M., Weinstein B.M. (2002). sonic hedgehog and vascular endothelial growth factor act upstream of the Notch pathway during arterial endothelial differentiation. *Dev Cell*, **3**: 127-136.

- Lee C.T., Li L., Takamoto N., Martin J.F., Demayo F.J., Tsai M.J., Tsai S.Y. (2004). The nuclear orphan receptor COUP-TFII is required for limb and skeletal muscle development. *Mol Cell Biol*, **24**: 10835-10843

- Lee R.K., Stainier D.Y., Weinstein B.M., Fishman M.C. (1994). Cardiovascular development in the zebrafish. II. Endocardial progenitors are sequestered within the heart field. *Development*, **120**: 3361-3366.

- Leslie J.D., Ariza-McNaughton L., Bermange A.L., McAdow R., Johnson S.L., Lewis J. (2007). Endothelial signalling by the Notch ligand Delta-like 4 restricts angiogenesis. *Development*, **134**: 839-844.

- Liang D., Xu X., Chin A.J., Balasubramaniyan N.V., Teo M.A., Lam T.J., Weinberg E.S., Ge R. (1998). Cloning and characterization of vascular endothelial growth factor (VEGF) from zebrafish, Danio rerio. *Biochim Biophys Acta*, **1397**: 14-20.

- Liao E.C., Paw B.H., Oates A.C., Pratt S.J., Postlethwait J.H., Zon L.I. (1998). SCL/Tal-1 transcription factor acts downstream of cloche to specify hematopoietic and vascular progenitors in zebrafish. *Genes Dev*, **12**: 621-626.

- Liao W., Bisgrove B.W., Sawyer H., Hug B., Bell B., Peters K., Grunwald D.J. and Stainier D.Y. (1997). The zebrafish gene cloche acts upstream of a flk-1 homologue to regulate endothelial cell differentiation. *Development*, **124**: 381-389.

- Lin F.J., Tsai M.J., Tsai S.Y. (2007). Artery and vein formation: a tug of war between different forces. *EMBO Rep*, **8**: 920-924.

- Lindsell C.E., Shawber C.J., Boulter J., Weinmaster G. (1995). Jagged: a mammalian ligand that activates Notch1. *Cell*, **80**: 909-917.

- Liu J., Fraser S.D., Faloon P.W., Rollins E.L., Berg J.V., Olivera S.S., Laliberte A.L, Chen J.N, Serluca F.C. and Childs S.J. (2007). A betaPix–Pak2a signaling pathway regulates cerebral vascular stability in zebrafish. *P Natl Acad Sci USA* , **104**: 13990–13995.

- Luo B., Aster J.C., Hasserjian R.P., Kuo F., Sklar J. (1997). Isolation and functional analysis of a cDNA for human Jagged2, a gene encoding a ligand for the Notch1 receptor. *Mol Cell Biol*, **17**: 6057-6067.

- Lyons M.S., Bell B., Stainier D., Peters K.G. (1998). Isolation of the zebrafish homologues for the tie-1 and tie-2 endothelium-specific receptor tyrosine kinases. *Dev Dyn*, **212**: 133-140.

- McGill M.A. and McGlade C.J. (2003). Mammalian numb proteins promote Notch1 receptor ubiquitination and degradation of the Notch1 intracellular domain. *J Biol Chem*, **278**: 23196-23203.

- McGill M.A., Dho S.E., Weinmaster G., McGlade C.J. (2009). Numb regulates post-endocytic trafficking and degradation of Notch1. *J Biol Chem*, **284**: 26427-26438.

- Millauer B., Wizigmann-Voos S., Schnürch H., Martinez R., Møller N.P., Risau W. and Ullrich A. (1993). High affinity VEGF binding and developmental expression suggest Flk-1 as a major regulator of vasculogenesis and angiogenesis. *Cell*, **72**: 835-846.

- Miyoshi J., Takai Y. (2008). Structural and functional associations of apical junctions with cytoskeleton. *Biochim Biophys Acta*, **1778**: 670-691.

- Mizuno T., Shinya M. and Takeda H. (1999). Cell and tissue transplantation in zebrafish embryos. *Methods Mol Biol*, **127**: 15-28.

- Nasevicius A. and Ekker S.C. (2000). Effective targeted gene 'knockdown' in zebrafish. *Nat Genet*, **26**: 216-220.

- Nawroth R., Poell G., Ranft A., Kloep S., Samulowitz U., Fachinger G., Golding M., Shima D.T., Deutsch U. and Vestweber D. (2002). VE-PTP and VE-cadherin ectodomains interact to facilitate regulation of phosphorylation and cell contacts. *Embo J*, **21**: 4885-4895.

- Niikura Y., Tabata Y., Tajima A., Inoue I., Arai K., Watanabe S. (2006). Zebrafish Numb homologue: phylogenetic evolution and involvement in regulation of left-right asymmetry. *Mech Dev* **123**: 407-414.

- Odenthal J., Haffter P., Vogelsang E., Brand M., van Eeden F.J., Furutani-Seiki M., Granato M., Hammerschmidt M., Heisenberg C.P., Jiang Y.J., Kane D.A., Kelsh R.N., Mullins M.C., Warga R.M., Allende M.L., Weinberg E.S., Nüsslein-Volhard C. (1996), Mutations affecting the formation of the notochord in the zebrafish, Danio rerio. *Development,* **123**: 103-115.

- Oleinikov A.V., Zhao J., Makker S.P. (2000). Cytosolic adaptor protein Dab2 is an intracellular ligand of endocytic receptor gp600/megalin. *Biochem J*, **347**: 613-621.

- Olson E.N. and Klein W.H. (1998). Muscle minus myoD. *Dev Biol*, **202**: 153-156.

- Ong C.T., Cheng H.T., Chang L.W., Ohtsuka T., Kageyama R., Stormo G.D., Kopan R. (2006). Target selectivity of vertebrate notch proteins. Collaboration between discrete domains and CSL-binding site architecture determines activation probability. *J Biol Chem*, **281**: 5106-5119.

- Pereira F.A., Qiu Y., Zhou G., Tsai M.J., Tsai S.Y. (1999). The orphan nuclear receptor COUP-TFII is required for angiogenesis and heart development. *Genes Dev*, **13**: 1037-1049.

- Petersen P.H., Tang H., Zou K., Zhong W. (2006). The enigma of the numb-Notch relationship during mammalian embryogenesis. *Dev Neurosci*, **28**: 156-168.

- Petersen P.H., Zou K., Hwang J.K., Jan Y.N., Zhong W. (2002). Progenitor cell maintenance requires numb and numblike during mouse neurogenesis. *Nature*, **419**: 929-934.

- Petersen P.H., Zou K., Krauss S., Zhong W. (2004). Continuing role for mouse Numb and Numbl in maintaining progenitor cells during cortical neurogenesis. *Nat Neurosci*, **7**: 803-811.

- Petrova T.V., Makinen T., Alitalo K. (1999). Signaling via vascular endothelial growth factor receptors. *Exp Cell Res*, **253**: 117-130.

- Pham V.N., Roman B.L., Weinstein B.M. (2001). Isolation and expression analysis of three zebrafish angiopoietin genes. *Dev Dyn*, **221**: 470-474.

- Raya A., Kawakami Y., Rodriguez-Esteban C., Buscher D., Koth C.M., Itoh T., Morita M., Raya R.M., Dubova I., Bessa J.G., de la Pompa J.L., Izpisua Belmonte J.C. (2003). Notch activity induces Nodal expression and mediates the establishment of left-right asymmetry in vertebrate embryos. *Genes Dev*, **17**: 1213-1218.

- Reifers F., Walsh E.C., Léger S., Stainier D.Y. and Brand M. (2000). Induction and differentiation of the zebrafish heart requires fibroblast growth factor 8 (fgf8/acerebellar). *Development*, **127**: 225-235.

- Reugels A.M., Boggetti B., Scheer N., Campos-Ortega J.A. (2006). Asymmetric localization of Numb:EGFP in dividing neuroepithelial cells during neurulation in Danio rerio. *Dev Dyn*, **235**: 934-948.

- Reynolds E.S. (1963). The use of lead citrate at high pH as an electron-opaque stain in electron microscopy. *J Cell Biol*, **17**: 208-212.

- Rhyu M.S., Jan L.Y., Jan Y.N. (1994). Asymmetric distribution of numb protein during division of the sensory organ precursor cell confers distinct fates to daughter cells. *Cell* **76**: 477-491.

- Risau W. (1997). Mechanisms of angiogenesis. *Nature*, **386**: 671-674.

- Risau W. and Flamme I. (1995). Vasculogenesis. *Annu Rev Cell Dev Biol*, **11**: 73-91.

- Roman B.L. and Weinstein B.M. (2000). Building the vertebrate vasculature: research is going swimmingly. *Bioessays*, **22**: 882-893.

- Rowlinson J.M., Gering M. (2010). Hey2 acts upstream of Notch in hematopoietic stem cell specification in zebrafish embryos. *Blood*, **116**: 2046-2056.

- Santolini E., Puri C., Salcini A.E., Gagliani M.C., Pelicci P.G., Tacchetti C., Di Fiore P.P. (2000). Numb is an endocytic protein. *J Cell Biol*, **151**: 1345-1352.

- Santoro M.M., Samuel T., Mitchell T., Reed J.C., Stainier D.Y. (2007). Birc2 (clap1) regulates endothelial cell integrity and blood vessel homeostasis. *Nat Genet*, **39**: 1397-1402.

- Schnittler H.J. (1998). Structural and functional aspects of intercellular junctions in vascular endothelium. *Basic Res Cardiol*, **93**: 30–39.

- Serafin V., Persano L., Moserle L., Esposito G., Ghisi M., Curtarello M., Bonanno L., Masiero M., Ribatti D., Stürzl M., Naschberger E., Croner R.S., Jubb A.M., Harris A.L., Koeppen H., Amadori A., Indraccolo S. (2011). Notch3 signalling promotes tumour growth in colorectal cancer. *J Pathol*, **224**: 448-460.

- Shimojo H., Ohtsuka T., Kageyama R. (2011). Dynamic expression of notch signaling genes in neural stem/progenitor cells. *Front Neurosci*, **5**: 78.

- Shutter J.R., Scully S., Fan W., Richards W.G., Kitajewski J., Deblandre G.A., Kintner C.R., Stark K.L. (2000). Dll4, a novel Notch ligand expressed in arterial endothelium. *Genes Dev*, **14**: 1313-1318.

- Smithers L., Haddon C., Jiang Y.J., Lewis J. (2000). Sequence and embryonic expression of deltaC in the zebrafish. *Mech Dev*, **90**: 119-123.

- Song H.D., Sun X.J., Deng M., Zhang G.W., Zhou Y., Wu X.Y., Sheng Y., Chen Y., Ruan Z., Jiang C.L., Fan H.Y., Zon L.I., Kanki J.P., Liu T.X., Look A.T., Chen Z. (2004). Hematopoietic gene expression profile in zebrafish kidney marrow. *Proc Natl Acad Sci USA*, **101**: 16240-16245.

- Spana E.P., Kopczynski C., Goodman C.S., Doe C.Q. (1995). Asymmetric localization of numb autonomously determines sibling neuron identity in the Drosophila CNS. *Development* **121**: 3489-3494.

- Stainier D.Y. (2001). Zebrafish genetics and vertebrate heart formation. *Nat Rev Genet*, **2**: 39-48.

- Stainier D.Y., Fouquet B., Chen J.N., Warren K.S., Weinstein B.M., Meiler S.E., Mohideen M.A., Neuhauss S.C., Solnica-Krezel L., Schier A.F., Zwartkruis F., Stemple D.L., Malicki J., Driever W., Fishman MC. (1996). Mutations affecting the formation and function of the cardiovascular system in the zebrafish embryo. *Development*, **123**: 285-292.

- Stainier D.Y., Lee R.K., Fishman M.C. (1993). Cardiovascular development in the zebrafish. I. Myocardial fate map and heart tube formation. *Development*, **119**: 31-40.

- Stevens T., Garcia J.G., Shasby D.M., Bhattacharya J. and Malik A.B. (2000). Mechanisms regulating endothelial cell barrier function. *Am J Physiol Lung Cell Mol Physiol*, **279**: L419-L422.

- Sumanas S. and Lin S. (2004). Zebrafish as a model system for drug target screening and validation. *Drug Discov Today*, **3**: 89-96.

- Swift M.R. and Weinstein B.M. (2009). Arterial-venous specification during development. *Circ Res*, **104**: 576-588.

- Thisse C. and Zon L.I. (2002). Organogenesis-heart and blood formation from the zebrafish point of view. *Science*, **295**: 457-462.

- Thompson M.A., Ransom D.G., Pratt S.J., MacLennan H., Kieran M.W., Detrich H.W. 3rd, Vail B., Huber T.L., Paw B., Brownlie A.J., Oates A.C., Fritz A., Gates M.A., Amores A., Bahary N., Talbot W.S., Her H., Beier D.R., Postlethwait J.H., Zon L.I. (1998). The cloche and spadetail genes differentially affect hematopoiesis and vasculogenesis. *Dev Biol*, **197**: 248-269.

- Thurston G. and Yancopoulos G. D. (2001). Gridlock in the blood. *Nature*, **414**: 163-164.

- Tonks N.K. and Neel B.G. (2001). Combinatorial control of the specificity of protein tyrosine phosphatases. *Curr Opin Cell Biol*, **13**: 182-195.

- Tonks N.K., Diltz C.D., Fischer E.H. (1988). Purification of the major protein-tyrosine-phosphatases of human placenta. *J Biol Chem*, **263**: 6722-6730.

- Torres-Vázquez J., Gitler A.D., Fraser S.D., Berk J.D., Van N. Pham, Fishman M.C., Childs S., Epstein J.A., Weinstein B.M. (2004). Semaphorin-plexin signaling guides patterning of the developing vasculature. *Dev Cell*, **7**: 117-123.

- Ullrich A. and Schlessinger J. (1990). Signal transduction by receptors with tyrosine kinase activity. *Cell*, **61**: 203-212.

- Uyttendaele H., Marazzi G., Wu G., Yan Q., Sassoon D., Kitajewski J. (1996). Notch4/int-3, a mammary proto-oncogene, is an endothelial cell-specific mammalian Notch gene. *Development*, **122**: 2251-2259.

- Vasioukhin V., Bauer C., Yin M., Fuchs E. (2000). Directed actin polymerization is the driving force for epithelial cell-cell adhesion. *Cell*, **100**: 209-219.

- Verdi J.M., Schmandt R., Bashirullah A., Jacob S., Salvino R., Craig C.G., Program A.E., Lipshitz H.D., McGlade C.J. (1996). Mammalian NUMB is an evolutionarily conserved signalling adapter protein that specifies cell fate. *Curr Biol* **6**: 1134-1145.

- Vestweber D. (2000). Molecular mechanisms that control endothelial cell contacts. *J. Pathol.*, **190**: 281-291.

- Villa N., Walker L., Lindsell C.E., Gasson J., Iruela-Arispe M.L., Weinmaster G. (2001). Vascular expression of Notch pathway receptors and ligands is restricted to arterial vessels. *Mech Dev*, **108**: 161-164.

- Vogel A.M. and Weinstein B.M. (2000). Studying vascular development in the zebrafish. *Trends Cardiovasc Med*, **10**: 352-360.

- Vogeli K.M., Jin S.W., Martin G.R., Stainier D.Y. (2006). A common progenitor for haematopoietic and endothelial lineages in the zebrafish gastrula. *Nature*, **443**: 337-339.

- Wakamatsu Y., Maynard T.M., Jones S.U., Weston J.A. (1999). NUMB localizes in the basal cortex of mitotic avian neuroepithelial cells and modulates neuronal differentiation by binding to NOTCH-1. *Neuron*, **23**: 71-81.

- Wang H.U., Chen Z.F., Anderson D.J. (1998). Molecular distinction and angiogenic interaction between embryonic arteries and veins revealed by ephrin-B2 and its receptor Eph-B4. *Cell*, **93**: 741-753.

- Weinberg E.S., Allende M.L., Kelly C.S., Abdelhamid A., Murakami T., Andermann P., Doerre O.G., Grunwald D.J., Riggleman B. (1996). Developmental regulation of zebrafish MyoD in wild-type, no tail and spadetail embryos. *Development*, **122**: 271-280.

- Weinmaster G. (1997). The ins and outs of notch signaling. *Mol Cell Neurosci*, **9**: 91-102.

- Weinmaster G., Roberts V.J., Lemke G. (1991). A homolog of Drosophila Notch expressed during mammalian development. *Development*, **113**: 199-205.

- Weinmaster G., Roberts V.J., Lemke G. (1992). Notch2: a second mammalian Notch gene. *Development*, **116**: 931-941.

- Weinstein B.M. (2002). Plumbing the mysteries of vascular development using the zebrafish. *Semin Cell Dev Biol*, **13**: 515-522.

- Weinstein B.M., Stemple D.L., Driever W. and Fishman M.C. (1995). Gridlock, a localized heritable vascular patterning defect in the zebrafish. *Nat Med*, **1**: 1143-1147.

- Weintraub H. (1993). The MyoD family and myogenesis: redundancy, networks, and thresholds. *Cell,* **75**: 1241-1244.

- Westerfield M. (1995). The Zebrafish Book. A Guide for the Laboratory Use of Zebrafish (Danio rerio), 3rd Edition. Eugene, OR, University of Oregon Press,385 (Book).

- Wilson A., Ardiet D.L., Saner C., Vilain N., Beermann F., Aguet M., Macdonald H.R., Zilian O. (2007). Normal hemopoiesis and lymphopoiesis in the combined absence of numb and numblike. *J Immunol*, **178**: 6746-6751.

- Xue Y., Gao X., Lindsell C.E., Norton C.R., Chang B., Hicks C., Gendron-Maguire M., Rand E.B., Weinmaster G., Gridley T. (1999). Embryonic lethality and vascular defects in mice lacking the Notch ligand Jagged1. *Hum Mol Genet*, **8**:723-730.

- Yaniv K., Isogai S., Castranova D., Dye L., Hitomi J., Weinstein B.M.(2006). Live imaging of lymphatic development in the zebrafish. *Nat Med*, **12**: 711-716.

- You L.R., Lin F.J., Lee C.T., DeMayo F.J., Tsai M.J., Tsai S.Y. (2005). Suppression of Notch signalling by the COUP-TFII transcription factor regulates vein identity. *Nature*, **435**: 98-104.

- Yuvaniyama J., Denu J.M., Dixon J.E. and Saper M.A. (1996). Crystal structure of the dual specificity protein phosphatase VHR. *Science*, **272**: 1328-1331.

- Zhong T.P., Childs S., Leu J.P. and Fishman M.C. (2001). Gridlock signalling pathway fashions the first embryonic artery. *Nature*, **414**: 216-220.

- Zhong W., Feder J.N., Jiang M.M., Jan L.Y., Jan Y.N. (1996). Asymmetric localization of a mammalian numb homolog during mouse cortical neurogenesis. *Neuron* **17**: 43-53.

- Zhong W., Jiang M.M., Schonemann M.D., Meneses J.J., Pedersen R.A., Jan L.Y., Jan Y.N. (2000). Mouse numb is an essential gene involved in cortical neurogenesis. *Proc Natl Acad Sci U S A*, **97**: 6844-6849.

- Zhong W., Jiang M.M., Weinmaster G., Jan L.Y., Jan Y.N. (1997). Differential expression of mammalian Numb, Numblike and Notch1 suggests distinct roles during mouse cortical neurogenesis. *Development* **124**: 1887-1897.

- Zilian O., Saner C., Hagedorn L., Lee H.Y., Säuberli E., Suter U., Sommer L., Aguet M. (2001). Multiple roles of mouse Numb in tuning developmental cell fates. *Curr Biol*, **11**: 494-501.